AIAA TEAM SPACE TRANSPORTATION DESIGN COMPETITION

# PROJECT HITCHHIKER

## PROPOSAL FOR THE DESIGN OF A MARS SAMPLE RETURN SYSTEM

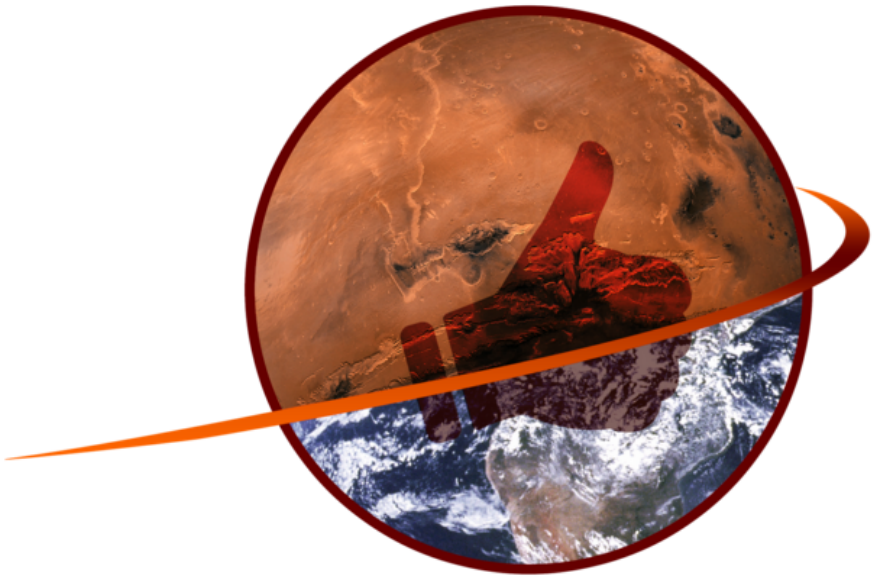


*Submitted by:*

Team MARVIN

| | | | |
|---|---|---|---|
| Loren Clark | Patrick Clark | Anthony Gaudino | Dylan Greene |
| Jacob Katuin | Diane Kjelby | Grant Roth | Sean Ryan |

*Faculty Advisor:*

Dr. Kevin Shinpaugh

Virginia Polytechnic Institute and State University
Department of Aerospace and Ocean Engineering

215 Randolph Hall
460 Old Turner Street
Blacksburg VA, 24060


May 16, 2016

# Table of Contents

# List of Figures

# List of Tables

# List of Abbreviations

| | |
|---|---|
| AD&CS | Attitude Determination and Control Subsystem |
| AHP | Analytic Hierarchy Process |
| ASTRG | Advanced Stirling Radioisotope Thermoelectric Generator |
| BOL | Beginning of Life |
| C&DHS | Command and Data Handling Subsystem |
| CEA | Chemical Equilibrium with Applications |
| COTS | Commerical Off The Shelf |
| DCIU | Digital Control Interface Unit |
| DT&E | Development, Testing and Evaluation |
| DGB | Disc Gap Band |
| EDL | Entry Descent and Landing |
| EEV | Earth Entry Vehicle |
| EOL | End of Life |
| EPS | Electrical Power Subsystem |
| ERV | Earth Return Vehicle |
| GN&CS | Guidance, Navigation and Control Subsystem |
| HTPB | Hydroxl-Terminated Polybutadiene |
| IAD | Inflatable Aerodynamic Decelerator |
| ISPP | In-Situ Propellant Production |
| ISRU | In-Situ Resource Utilization |
| ITV | Interplanetary Transfer Vehicle |
| LIDAR | Light Detection and Ranging |
| LOX | Liquid Oxygen |
| MAV | Mars Ascent Vehicle |
| MOLA | Mars Orbiter Laser Altimeter |
| MMRTG | Multi-Mission Radioisotope Thermoelectric Generator |
| MIT | Minimum Impulse Thruster |
| MRO | Mars Reconaissance Orbiter |
| MLI | Multi-Layer Insulation |
| MSL | Mars Science Laboratory |
| MSRS | Mars Sample Return System |
| NGAVGS | Next Generation Advanced Video Guidance Sensor |
| NSTAR | NASA Solar Electric Propulsion Technology |
| OS | Orbiting Sample |
| PBAN | Polybutadiene Acryolonitrile |
| PPU | Power Processing Unit |
| RFP | Request for Proposal |
| RP-1 | Rocket Propellant-1 or Refined Pretroleum-1 |
| RTG | Radioisotope Thermoelectric Generator |
| SRP | Supersonic Retro Propulsion |
| STK | Systems Tool Kit |
| TCS | Thermal Control Subsystem |
| TRL | Technology Readiness Level |
| TRN | Terrain Relative Navigation |
| TT&CS | Telemetry, Tracking, and Command Subsystem |
| TWTA | Travelling Wave Tube Amplifier |
| UTTR | Utah Testing and Training Range |
| VSD | Value System Design |

# List of Symbols

| | |
|---|---|
| $A$ | Area |
| $A_{Mars}$ | Albedo of Mars's Surface |
| $C_D$ | Drag Coefficient |
| $\Delta V$ | Change in Velocity |
| $D$ | Distance from the Sun |
| $\eta$ | Efficiency |
| $\overline{F}_{tot}$ | Total Average Solar Insolation on Martian Surface |
| $H$ | Half Day Length Measured in Radians |
| $H_0$ | Solar Irradiance |
| $H_{sun}$ | Power Density of the Sun |
| $I_{sp}$ | Specific Impulse |
| $\mu_{sun}$ | Standard Gravitational Parameter of the Sun |
| $\mu_{SZA}$ | Solar Zenith Angle |
| $NNIF$ | Normalized Net Irradiance Function |
| $P$ | Power |
| $r$ | Distance from Mars to the Sun |
| $\overline{r}$ | Average Distance from Mars to the Sun |
| $r_{Departure}$ | Average Radius of Departure Orbit |
| $r_{Destination}$ | Average Radius of Destination Orbit |
| $R_{sun}$ | Radius of the Sun |
| $S_0$ | Average Solar Insolation Hitting Top of Martian Atmosphere |
| $\tau$ | Optical Depth |
| $\theta_{Hohmann}$ | Hohmann Angle |
| $TOF_{Hohmann}$ | Hohmann Time of Flight |

# Preface: Project Management

This project serves as both an AIAA competition paper and undergraduate senior design capstone project. As such, the team was subjected to scheduling and deadlines imposed by both the RFP stakeholder and the senior design course. Basic project tools and an organized team structure were created in order to effectively manage work throughout the timeline of the project. The first product of this effort brought together the required deliverables, key deadlines, estimates of required work effort, and a fundamental understanding of the engineering design process in order to establish the project's key phases of development: conceptual mission design, preliminary vehicle design, and detailed mission design. Preliminary work was centered on conceptual mission design, whereas later work was dedicated to the preliminary vehicle design and detailed mission design that serves as the primary focus of this report.

In order to manage the broad technical scope of the project, the team is organized into two primary subteams: the Interplanetary Team and the Mars Team. Each team is responsible for design decisions made in mission elements that are relevant to their respective grouping. The Interplanetary Team handles the Earth launch, interplanetary travel, and Earth return elements of the mission while the Mars Team handles Mars entry, descent, and landing, Mars surface operations, and Mars surface ascent elements of the mission. The intent was to form teams around two highly coupled design domains, thereby maximizing the amount of relevant information exchange and work efficiency within each environment. This environment fostered each team member to specialize and develop expertise in their respective domains.

Throughout the spring semester the team held three weekly meetings, each with a different purpose and structure. Both sub-teams would meet separately once a week to discuss, present, or produce material relevant to their domain. The next meeting was held with all team members to present weekly updates to the team's faculty advisor. These meetings also served for teammates to provide updates, feedback, and guidance to the rest of the team in preparation for the final weekly meeting. The final weekly team meeting focused on making key design decisions, coordinating schedules, and taking care of administrative tasks.

Several times during the semester the team had the opportunity to present and receive feedback from aerospace professionals in academia and the industry. Audiences included faculty and graduate students through the Center for Space Science and Engineering Research at Virginia Tech as well as engineers from Orbital-ATK. In February, the team was able to visit the Orbital-ATK satellite manufacturing facility in Dulles, VA to learn more about real-world spacecraft design and manufacturing. Feedback from these experiences offered critical insight into the industry standard methods to approach technical problems.

**Figure 1:** Organization chart and division of team resources.

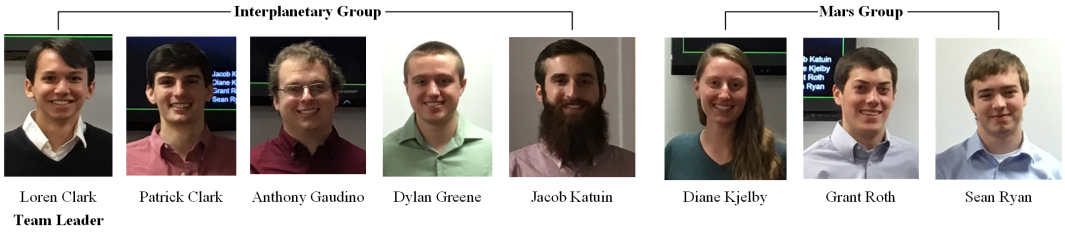


Loren Clark
AIAA Member No: #489166

Jacob Katuin
AIAA Member No: #455067

Patrick Clark
AIAA Member No: #462991

Diane Kjelby
AIAA Member No: #446766

Anthony Gaudino
AIAA Member No: #644762

Grant Roth
AIAA Member No: #644890

Dylan Greene
AIAA Member No: #510405

Sean Ryan
AIAA Member No: #644615

Dr. Kevin Shinpaugh
Faculty Advisor

AIAA Member No: #25807

# Executive Summary

## 0.1 Background

The objective of the Mars Sample Return (MSR) mission is to collect soil samples from the surface of Mars and return the collected sample cache to Earth. While the comprehensive MSR mission concept includes the design and operation of a rover that will gather and cache the samples on the surface of Mars, the Mars Sample Return System (MSRS) proposed herein focuses only on the mission architecture, concepts, and vehicles involved with transporting the sample cache from the surface of Mars to Earth. This proposal is in direct response to the MSR Request for Proposal (RFP) sponsored by the American Institute of Aeronautics and Astronautics(AIAA) Space Transportation Technical Committee (STTC).

Per the constraints imposed by RFP, the proposed MSRS operates within the assumption that NASA will deliver the sample caching rover to Mars in February 2021 and that the rover will remain operable until February 2023. Furthermore, the RFP has constrained the design space such that the MSRS must land a vehicle within 5 km of the NASA rover and that a minimum 50-day surface stay is required within the aforementioned 2 year window for successful sample transfer from the rover. Lastly, internal constraints were imposed by the team that require the sample to be returned to Earth by 2030, and that the overall mission must cost below that of the Mars Science Laboratory (MSL) mission. Development and operations for the MSRS will require significant coordination with NASA for mission success, and it is anticipated that NASA will lead the effort for all elements of the MSR mission.

## 0.2 Mission Concepts

Three primary architectures were considered for the basis of a mission design. Their differentiating features complemented architectural-level design trades including the number of Earth launches, the fuel-type and return payload of the Mars Ascent Vehicle (MAV), the propulsion system of Interplanetary Transfer Vehicle, and the final destination of the Earth return vehicle. These architectures were evaluated with respect to a developed value system design (VSD) which weighted the impact of design decisions on reducing chance of mission failure (0.591), reducing mission cost (0.336) and reducing mission duration (0.073).

These trades led to a final MSRS concept that features six key technologies: an NSTAR-powered ion electric interplanetary vehicle propulsion system, a Mars Entry Descent and Landing (EDL) system derived and augmented from the MSL program, a Mars lander vehicle with contamination control systems to ensure Back Planetary Protection (BPP), a two-stage solid motor Mars Ascent Vehicle, a JPL derived on-orbit sample rendezvous and capture system, and a NASA Langley (LaRC) derived direct Earth Entry Vehicle (EEV). At Earth, all six components are assembled as a part of the ITV.

The MSRS will launch from Earth on an Atlas V-541 in June 2020 and after performing a series of maneuvers, arrive at Mars in October 2021. Upon close Mars approach, the ITV will maneuver to perform a precision release the EDL system

in January 2022, and then the ITV will maneuver to a stable 300 km parking orbit by August 2022. In that time, the EDL system will deliver the lander and MAV system to the Martian surface within 5 km of the rover's present position by February 2022. This provides a one year window until the rover reaches its end of life for the rover to transfer the sample to the lander's retrieval system. In the transfer, the 3 kg, 15 cm by 15 cm sample cache will be encased in an Orbiting Sample (OS) system after passing through a series of heat-sealed membranes and other cross contamination prevention systems. The OS, complete with solar panels, sensors, and a radio beacon, serves as a payload that will be delivered to a 300 km rendezvous orbit by the MAV in March 2023. The ITV will locate, maneuver, and rendezvous with the OS using the radio beacon and on-board LIDAR systems. The return trajectory begins immediately after successful capture and transfer to the EEV with a spiral maneuver from Mars parking orbit to escape, followed by a transfer burn that places the ITV on an intercept trajectory with Earth. The phasing between Earth and Mars requires an orbit around the Sun and time for corrections that will enable accurate Earth entry. In August 2025, the ITV will detach its EEV, burning up in Earth's atmosphere while the EEV lands within the Utah Testing and Training Range.

## 0.3 Key Risks and Projected Cost

Considering the four-year development testing and evaluation (DT&E) schedule before launch, the primary risk associated with this mission stems from the BPP contamination control systems onboard the lander, the MAV solid motors, and guidance systems. Both lander BPP systems and MAV motor and guidance systems are at Technology Readiness Levels (TRL) of 4 or lower. If the BPP lander systems cannot be verified, or MAV motor development is delayed, then sample retrieval with this proposed system would be likely hindered. Failure to fully develop these systems could lead to consequences such as missing the desired launch window or requiring different procedures to breaking the chain of contact between Earth and Mars. At worst, developmental delays in these systems could invalidate the effectiveness of this design for this MSR mission. The primary risk reduction strategy includes adopting commercial-off-the-shelf (COTS) or components of TRL 6 or greater for the remainder of the MSRS, but only to the extent that the resultant increased system integration times do not threaten the overall DT&E schedule.

A cost estimating relationship (CER) for this mission was developed by using historical data on development and operations costs of previous Mars missions. Relevant missions which bound project cost include the OSIRIS-REx asteroid sample return mission on the lower bound and the Mars Science Laboratory Mission on the upper bound. These upper and lower bounds were established by comparing the complexity and required technology development of these systems as compared with the one outlined in this paper. Using this CER and a NASA Decadal Survey recommended 50 percent reserve for DT&E and 25 percent reserve for operations, the projected MSRS cost is approximately $1.61 billion of which $1.38 billion comprises DT&E expenses and the $229 million comprises operating phase expenses assuming MSRS work begins in May of 2016.

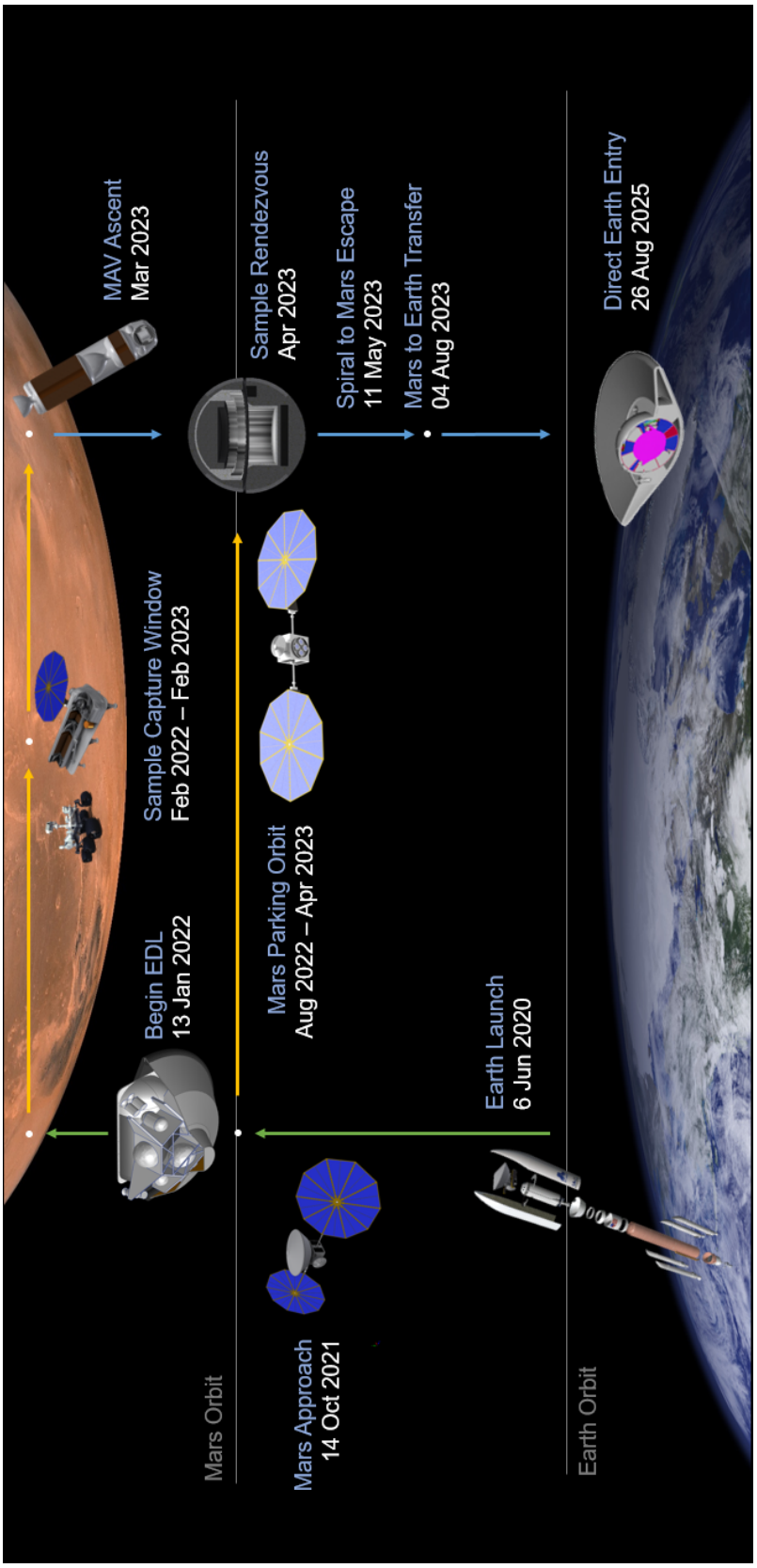


**Figure 2:** Visualization of the complete mission architecture. Arrows depict the direction the mission progresses as time passes, and vehicle models are included at the relevant dates.

# 1 Introduction and Problem Definition

## 1.1 Motivation and Background

The Mars Sample Return Mission was conceived in order to develop a deeper understanding of the geologic and climatic history of the planet through in-depth analysis of Martian regolith with methods currently only available on Earth. The mission presents a valuable opportunity to reveal information regarding the history of the solar system, predictions about the nature of extrasolar planets, and the continuing search for life in the universe. Furthermore, a sample return mission lays the groundwork for future human missions to Mars, currently planned for the mid 2030s, by expanding knowledge of the Martian surface environment and developing critical technology [1].

In current and past missions to Mars, the depth to which regolith has be studied has been limited by the instrumentation aboard rovers and by observation from orbiting satellites. While the scientific equipment carried aboard these rovers is sophisticated, it is far surpassed by the ability on Earth to perform extensive, high-quality analysis using state-of-the-art laboratory equipment and world class personnel. Designers must trade the costs of increasing scope (adaptability) with the quality and depth of study, or risk developing a mission that quickly becomes prohibitively expensive. The most recent rover sent to Mars was the Curiosity rover which landed in 2012. The rover cost $2.5 billion for capabilities which included spectroscopy, broad spectrum radiation analysis, and the detection of organics [2]. In contrast to Mars Science Laboratory (MSL), NASA's Stardust mission is an example of a sample return mission which returned dust from comets to Earth in January of 2006 [3]. The cost of this mission was $200 million, demonstrating that sample retrieval can be performed without incurring prohibitive cost. Compared to the cost of the curiosity rover, scientific analysis on earth is marginal, providing this mission the potential to offer scientific gains and cost reduction from a MSL sized mission.

Two proposals of note have been made recently to perform mars sample return missions. The first is the Red Dragon proposal out of NASA Ames. This proposal uses a modified Dragon capsule to land on the surface of mars using supersonic retro propulsion. The entire earth return vehicle (ERV) then launches from the surface of Mars, and returns to Earth. Due to the direct launch from earth the ERV is contaminated and enters a lunar trailing orbit so that it can be picked up and returned to earth by a separate system. The other alternative is a concept out of JPL which proposes two separate launches. The first launch lands the MAV on the surface of mars and the other sends the return vehicle. The sample then is launched into orbit where it is picked up by the second launch vehicle and returned to earth. The sample is then returned to Earth on a parachute-less EEV which enters directly and used foam to absorb the impact. Our design process will consider elements of both systems.

## 1.2 Problem Definition

In 2011, a survey completed by planetary scientists of the National Research Council identified caching of Martian samples for future return to Earth as the top-priority large mission for the 2013 - 2022 decade. In 2014, NASA announced plans for a new robotic science rover expected to launch in 2020 that will be capable of caching rock and soil samples. The American Institute of Aeronautics and Astronautics (AIAA) Space Transportation Technical Committee (STTC) has released a request for proposal (RFP) for a Mars Sample Return Mission that involves the samples collected by the Mars 2020 Rover. The overarching objective of the proposed mission is to retrieve a sample container from the Mars 2020 Rover during the rover's operational period and return the container back to Earth. This section defines the project scope with regard to the requested deliverables, as well as the needs, alterables, and constraints of the mission design. Additionally, this section discusses how the mission architecture was divided into relevant elements and the extent to which the elements are interdependent.

## 1.3 Project Scope

The mission solution space, the envelope of all possible Mars sample return mission solutions, is bounded by the required deliverables stated in the RFP and by reasoned, self-imposed constraints for items not explicitly discussed in the RFP. Per the RFP, developing a Mars sample return mission entails an overall concept of operations to retrieve the sample on Mars and return the sample to Earth. This overall concept of operations will include a mission architecture, timeline, and budget, as well as detailed design work for interplanetary transfer vehicles (ITV), the systems that will retrieve the sample from the rover, and the Mars Ascent Vehicle (MAV). For this mission, detailed design work entails performance analysis and sizing calculations for all critical subsystems. Higher-level analysis will be required to select, but not necessarily design, systems to launch vehicles from Earth, systems to perform EDL onto the Martian surface, and systems for returning the sample back to Earth. Detailed design work for ITVs include spacecraft propulsion, power, avionics, communication, and bus structures. This work is also extended to include the number and configuration of vehicles, their launch and operational schedule, and all required orbits and trajectories. With respect to the sample retrieval system, the detailed design work is specific to how to how the surface vehicle will interact with the rover and safely store the sample with the MAV. While the rover's logistics must be considered, any design of the rover's systems is beyond the scope this project. For the MAV, detailed design work primarily encompasses propulsion and trajectory design. Additional detailed design work must also be performed for any fuel production systems which includes fuel production power systems.

The overall mission start date is 2015 when mission planning and system analysis begins, but no explicit mission end date is stated in the RFP. Thus, a self-imposed mission end date of 2030 is established. It is important to note that the mission end date corresponds to the moment when the Mars sample has successfully returned to Earth's surface or when the sample return system transfers the sample over to the ISS. The rationale behind a mission end date of 2030 is that, as part of NASA's Journey to Mars timeline, manned missions to Mars will ramp up in the mid 2030's [1]. If the mission ends at the latest possible date

of 2030, then time will still remain for any scientific findings to be incorporated into NASA's mid 2030's manned missions. A 2030 mission end date was also relaxed enough that potentially superior technological solutions would not be ruled infeasible due to time required to develop or utilize novel technologies. Thus, the mission end date of 2030 helps to maximize the value of the Mars sample return mission.

Additionally, no explicit bounds on project budget exist, but the mission budget will remain on the order of magnitude of previous missions to Mars. The budget will likely exceed the cost of missions such as Osiris-Rex, but will have an upper bound budget that is similar to MSL, due to the need for technology development in multiple arenas on a tightly constrained timeline in order to accomplish a set of novel feats. As an example, mission budgets on orders of magnitude greater than $2.5 billion are outside of the mission scope [3].

## 1.4 Needs, Alterables and Constraints

A table of high-level mission needs, alterables, and constraints (NAC) was developed as a succinct way to encapsulate the critical parameters for the proposed Mars Sample Return Mission. These critical parameters are shown in Table 1.1 and are derived chiefly from the RFP and preliminary investigation into the mission architecture. Following the overarching mission objective, the primary need is to collect a container of Martian samples of from the Mars 2020 rover and return the samples to Earth. The eight alterables in the NAC table do not encompass all of the mission alterables - only those which drive the mission design on an architectural level. Among the most important of the alterables are the configuration of the ITVs and their propulsion systems. The ITV configuration refers to not only how many distinct ITVs the mission will require, but also the schedule at which the ITVs will perform maneuvers such as leaving Earth and Mars. The ITV propulsion system is an important driver for ITV performance, and therefore the overall performance of the sample return mission. One overall mission constraint is that the sample return system must rendezvous with the rover by a latest possible date of December 2022. This constraint is due to the rover's anticipated landing date of February 2020 and the rover's nominal operational lifespan of two years [4]. Key constraints on sample retrieval system design include that a single 3 kg, 15 cm diameter, 15 cm tall cylindrical sample be collected, and that the rover can only place the sample a maximum of 2 m off the Martian surface [4]. An additional detailed design constraint is that the Planetary Protection Provisions for Robotic Extraterrestrial Missions, NPR 8020.12D must be followed in order to prevent cross-contamination of Earth and Mars [3]. A final key constraint is that the sample return system must be able to accommodate whichever landing site the rover mission requires.

**Table 1.1:** Overarching mission needs, alterables and constraints. The listed alterables are those which impact the mission architecture.

| Category | Element |
|---|---|
| *Needs* | Retrieve a scientific sample from a rover on the Martian surface and return the sample to Earth |
| *Alterables* | Interplanetary transfer vehicle (ITV) configuration<br>ITV primary propulsion method<br>Earth-Mars and Earth-Mars ITV trajectories<br>Mars EDL method<br>Sample retrieval method at Mars<br>Mars ascent vehicle (MAV) fuel and payload<br>Mission timeline<br>Sample capture method at Earth |
| *Constraints* | Ready for sample retrieval between 2/2020 and 12/2022<br>Land within 5 km of rover location<br>Remain on Mars surface at least 50 Earth days during sample retrieval<br>Accommodate rover's ability to place sample at maximum 2 m height above Martian surface<br>Adhere to planetary protection procedures outlined in NPR 8020.12D<br>Sample must return to Earth by 2030 |

# 2 Value System Design

Value System Design (VSD) is a fundamental part of the systems engineering design process and can be used to systematically evaluate how well a design is aligned to its mission requirements [6]. This is done by first defining overarching design objectives, which can be qualitative or quantitative, set forth either by the stakeholder or design requirements. Qualitative objectives are ideally given quantitative metrics. These objectives are then compared to each other in a pairwise manner using the Analytic Hierarchy Process (AHP), which provides relative numeric weightings for each objective. The result is value system that can be used to evaluate and compare different architectural level design options with a numeric score.

## 2.1 Design Objectives

Across the six mission segments minimization of cost, chance of mission failure, and total mission duration were chosen as the driving design objectives. These are shown in Figure 2.1, along with their corresponding measures of effectiveness.

### 2.1.1 Cost

Since there is no constraint on cost set forth by the RFP, a self-imposed constraint was set to keep the cost on the order of past missions to Mars ensuring that the mission was overall realistic. Cost is primarily driven by the research and development, production and operational cost of technology and is measured in current US dollars. The production and operational costs can be estimated by studying past missions to Mars. However, in the absence of being able to obtain a direct estimation of the development cost in dollars, the technology readiness level (TRL) can be used. The TRL can be used as a scale to infer the cost of developing a technology to a desired readiness level for use on the mission. The reality of the Mars Sample Return Mission is that there are elements of the mission that have never been attempted before and therefore may incur added costs to prove reliability.

### 2.1.2 Chance of Mission Failure

Considerations that pertain to chance of the mission failure include the flight history of the particular technology or components, how robust the system is withstanding a range of extreme operating environments, and the overall complexity of the system.

A Mars sample return mission requires systems that must be able to withstand several extreme environments of both interplanetary space and the Martian surface. Interplanetary space requires radiation hardened and thermally managed electronics and hardware. On Mars, the system must be able to withstand at least 50 days on the planet's surface at any of the chosen landing locations, whose environmental conditions vary significantly with location and time of the year. In cases where a long surface stay is desired, in-situ resource utilization (ISRU) may be desired which means the system's environmental tolerances

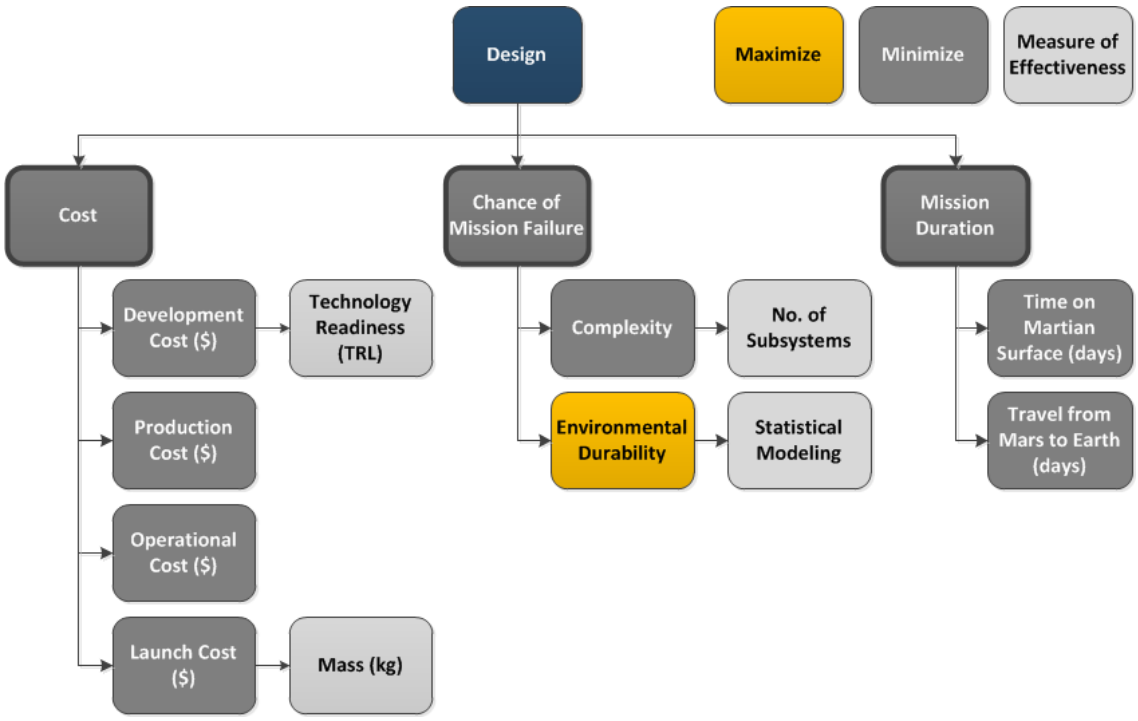


**Figure 2.1:** Objective Hierarchy Diagram showing how each of the three mission objective feed into the final design and what qualitative metric are used to classify and measure them.

would need to be more robust in order to reduce chance of fuel production failure. Furthermore, a complicated fuel production system would have higher chance of being damaged or failing with long exposure to the Martian surface.

### 2.1.3 Mission Duration

Mission duration becomes an effective way of evaluating different architectures if it can be associated with value. It was determined that the value of earlier sample return is that there is a greater potential for scientific return as analysis can begin earlier on Earth. Hence, why minimizing the duration of the mission is of importance in the mission objectives and one of the few performance measures for the system.

Per the RFP, the sample retrieval must be performed between February 2020, when the rover arrives, and December 2022, 50 days before the rover's end-of-life. This establishes the lower bound for the MSR mission duration, whereas the upper bound is set by the self-imposed constraint to return before January 1, 2030. In order to maximize the amount of time for development, designs will tend to arrive at the latest possible date and the total mission duration will become largely a function of the return timeline from the Martian surface. Thus, the duration of the mission varies only in the time spent on the Martian surface and the interplanetary travel time between Mars and Earth.

**Table 2.1:** The final weighted results of the AHP analysis showing the importance of each objective to the mission architecture.

| Objective: | Weighting: |
|---|---|
| Cost | 0.336 |
| Chance of Mission Failure | 0.591 |
| Mission Duration | 0.073 |

## 2.2 Analytic Hierarchy Process (AHP)

The AHP is a decision making tool in which the objectives of the design are compared in a pairwise manner. The results of the AHP analysis were used to form normalized weightings for each of the respective mission design objectives. These weightings are shown in Table 2.1. Minimizing the chance of mission failure was by far the dominant objective, followed by minimizing the cost of the mission and then by duration of the mission. It is also important to note that although mission cost is not the highest design objective, it is something to be cautious of to prevent designing an excessively expensive system would likely not be chosen for funding.

## 2.3 Summary

Developed through Value System Design, the design objectives deemed most important to the whole mission across all of the mission segments were the minimization of cost, chance of mission failure, and the mission duration. The result of the AHP on these design objectives found that minimizing the chance of mission failure was predominantly the driving objective, followed by minimizing the mission duration and lastly cost. While cost of the mission is not a heavily-weighted factor in evaluating mission architectures, further consideration is required for architectures that are prohibitively expensive.

# 3 Mission Architecture

## 3.1 Assessment of Three Candidate Architectures

This section will address the three primary architectures that were considered as the design basis for a Mars sample return mission. Each features key architectural-level design trades including the number of Earth launches, the fuel-type and return payload of the Mars Ascent Vehicle (MAV), the propulsion system of Interplanetary Transfer Vehicle, and the final destination of the Earth return vehicle. These architectures were evaluated using the developed value system design (VSD) which weighted the impact of design decisions on reducing chance of mission failure (0.591), reducing mission cost (0.336) and reducing mission duration (0.073).

The first architecture uses a single interplanetary transfer that contains an EDL vehicle assembly, an on-orbit sample capture system, and Earth entry vehicle (EEV). Upon arriving at Mars, the ITV separates into an EDL vehicle assembly and orbiter vehicle. The EDL vehicle assembly will land the sample retrieval system and Mars ascent vehicle near the rover, while the orbiter will stabilize into a low Mars parking orbit. The ITV has an electric propulsion system used on both the outgoing and return transfers, looking for mass and cost savings from highly mass-efficient thrusters. The EDL system will use heritage systems due to its relatively small mass, and sample retrieval system will make use of a tilt mechanism in order to accommodate the rover's reach while still enabling a vertical rocket launch. MAV tilt has benefits of minimizing risk due to the capture method's passive and simplistic nature. Having the captured sample launch from Mars and be captured by the orbiter through on-orbit rendezvous in Mars orbit, this design presents a relatively small MAV compared to one that launches directly back to earth. Storable fuel is necessary based on the mission length and fact that ISRU/ISPP is not feasible for a MAV of this scale. Once the orbiter performs on-orbit rendezvous and capture, it will maneuver to a return trajectory back at Earth. Since the orbiter has not been contaminated by Mars it can burn up in the Earth's atmosphere while allowing direct Earth entry using an EEV to transfer the sample directly to Earth's surface.

The second architecture also features a single ITV, however it serves all of the roles as outgoing ITV, EDL vehicle, sample capture vehicle, MAV, and interplanetary return vehicle. This vehicle is inherently much more massive compared to other options because it must return a larger payload from the surface of Mars back to Earth, therefore a chemical propulsion is required in order to achieve proper accelerations and flight times. The large mass at Mars EDL also means supersonic retropropulsion is necessary to transfer the MAV to the surface. Since the MAV will serve as the return ITV, the size and mass will increase, necessitating the use of a robotic arm to retrieve the sample. Lastly, to avoid contamination from Martian dust on the Earth Return Vehicle, this architecture would require rendezvous with the ISS, or similar on-orbit station, to return the sample to Earth.

The third and final architecture is a synthesis of the first two architectures and is generally the most complex of the the three. Similar to the first mission architecture, a Mars orbiter and lander will be used for rendezvous and return, however the

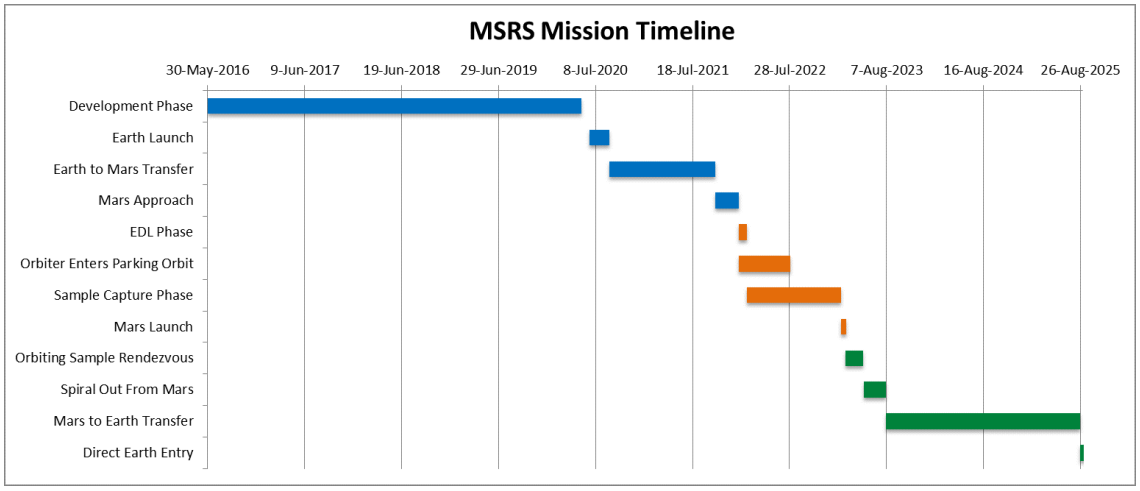


**Figure 3.1:** Gantt Chart depicting the complete mission timeline. Segments in blue represent the journey to Mars, segments in orange represent the mission stages occurring at Mars, and segments in green represent the return from Mars to Earth.

vehicles will not travel together on their transit from Earth to Mars. Instead, the lander will travel to Mars first using a chemical thrust propulsion system in order to complete a timely transfer from Earth to Mars. Similar to the first mission architecture, EDL will be selected based upon the lander's mass, and MAV tilt will be used to retrieve the sample. The orbiter vehicle, unconstrained by the required land date, will feature electric propulsion and take a slower but more efficient trajectory to Mars. Like the first architecture, the MAV will then launch with a payload containing only the sample, which with then rendezvous with the orbiter. The orbiter will return the sample to Earth using electric propulsion, meaning a longer relative return flight but increased fuel and mass efficiency. Upon return to Earth, the orbiter would perform a direct Earth entry to deliver the sample to Earth's surface. By separating the vehicles and choosing electric propulsion, this mission architecture provides the greatest opportunity to explore creative interplanetary trajectory solutions, as well as mass efficient vehicle designs.

## 3.2 Selected Mission Architecture

Of the three mission architecture candidates considered, the first mission architecture was selected as the design for this Mars sample return mission. The goal of this section is to provide an overview of the mission architecture that was chosen to return the sample. Each element of this mission architecture will be examined in chronological order with the goal of describing the most important pieces in each element. Figure 3.1 shows the complete mission timeline.

### 3.2.1 Development Phase

This mission will be scheduled to launch in the near future, so final system developments must begin as soon as possible. For this reason, development is slated to begin in May 2016 and continue for the next four years. Development will be completed by May 2020, which gives enough time to meet the allocated launch window. Meeting this launch window is a crucial part of the mission as it is necessary to arrive at Mars before the deadline set by the Mars rover end of life.

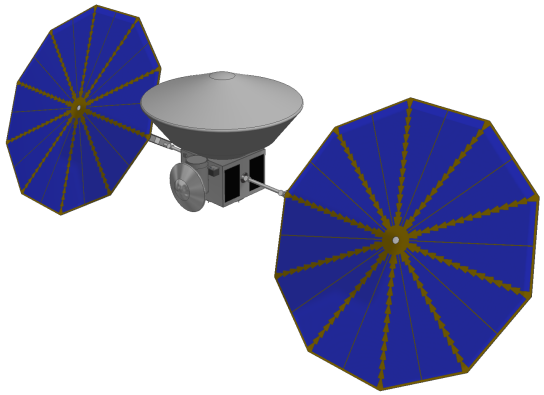

**Figure 3.2:** CAD Model showing a view of the interplanetary transfer vehicle. This vehicle serves to as a transport to deliver the mission payload to Mars, and upon completion of the Mars segment it will also serve as the return vehicle to bring the sample back to Earth.

### 3.2.2 Earth Launch

The mission begins with an Earth launch from Cape Canaveral, Florida on June 14, 2020. An Atlas V 541 with a Centaur upper stage will be used as the launch vehicle. This vehicle was chosen due to its reliability, cost, and ability to provide the C3 capabilities necessary to complete the orbital transfer to Mars in a timely manner [5] [6]. This segment of the mission will conclude when the Centaur upper stage detaches from the Interplanetary Transfer Vehicle (ITV), starting it on its trajectory toward Mars.

### 3.2.3 Earth to Mars Transfer

At this point in the mission, the ITV has completely separated from the launch vehicle and is now operating independently. The primary purpose of ITV is to transport the lander to Mars to collect the sample, and then serve as the return vehicle to deliver the sample back to Earth. The ITV requires the use of a primary propulsion system in order to successfully complete the transfer, and for that an electric propulsion system consisting of three NASA Solar Electric Propulsion Technology (NSTAR) ion electric thrusters. These thrusters have a high ISP and low power requirement, allowing for a very mass efficient transfer and overall low ITV mass [7]. The thrusters and other ITV subsystems will be powered by two Orbital ATK UltraFlex solar arrays [19], which can extend from a folded configuration to allow the ITV to be compact enough to fit inside the launch vehicle fairing. Powered propulsion will begin on August 30, 2020 and continue for most of the duration to Mars.

### 3.2.4 Mars Approach

The ITV is scheduled to begin Mars approach on October 14, 2021. The most important part of this segment is the separation of the ITV into two separate vehicles, an orbiter and a lander segment. After using the thrusters to slow the ITV sufficiently, the ITV will pass close to Mars so it can detach the lander. This maneuver will occur on January 13, 2022, officially beginning the Entry, Descent, and Landing (EDL) segment. Simultaneously, the orbiter segment of the ITV will continue its spiral

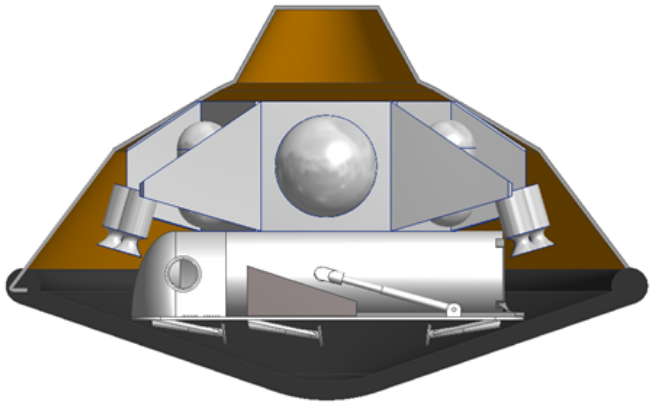

**Figure 3.3:** EDL model depicting an interior view of the Mars descent vehicle. This vehicle combines heritage components with innovative navigation equipment to achieve the required mission parameters.

trajectory around Mars in order to enter into a stable 300 km parking orbit by August 1, 2022. The orbiter will remain in this orbit until the Mars ground segment of the mission is completed.

### 3.2.5 Entry, Descent and Landing Phase

At this point in the mission, the Mars rover will already be waiting on the surface of Mars, having landed in February 2022. The rover has a lifespan of two years, so the lander is scheduled to arrive during the middle of its lifespan. As per the design requirements the lander must land within 5 km of the rover, and this is accomplished using bank angle navigation and error reduction maneuvers during the powered descent phase. A supersonic disc-gap band parachute was chosen as the main means of deceleration due to accuracy and mass constraints. Once successfully landed, the Mars Ascent Vehicle (MAV) will be deployed to allow for sample capture.

### 3.2.6 Sample Capture Phase

This phase begins as soon as the MAV is deployed on the Martian surface, and this is where the schedule allows a great deal of room to account for errors. The rover will survive until February 2023, which gives ample time to meet the mission requirement of allowing for 50 days on the Mars surface for sample capture. Since the rover arm can only reach a height of 2 meters above the surface of Mars, the MAV has been developed so that it lies on its side until ready to tilt up for the Mars Launch phase. This is also where chain of contact with Mars will be broken to avoid contamination from the sample. The MAV contains an Earth clean environment inside the aperture which is where the sample will be placed before transport to Mars orbit. Setting up the MAV in this manner allows the rover to easily transfer control of the sample while meeting all design requirements with time to spare.

### 3.2.7 Mars Launch

With the sample secured within the Earth clean environment on the MAV, the Mars launch phase will be ready to commence. Accounting for any delays, the MAV will launch by March 2023. The MAV uses a two-stage solid rocket in order to propel the sample into a 300 km circular parking orbit around Mars. Once there, the sample will separate from the MAV, remaining inside the spherical Earth clean environment. At this point the orbiting sample is primed for the next phase of the mission.

### 3.2.8 Orbiting Sample Rendezvous

This phase is scheduled to begin in March 2023. When the orbiting sample enters stable Mars orbit it will have no navigation equipment of its own, so it is the job of the orbiter to rendezvous with and retrieve the sample. For this purpose, the orbiter will be equipped with a LIDAR system which will be able to detect the sample container. Once located, the orbiter will complete a rendezvous maneuver to capture the sample and transfer to container to the Earth Entry Vehicle (EEV), where it will remain for the duration of the mission. At the conclusion of this phase, the sample will be safely secured aboard the orbiter, which will serve as the ITV for Mars to Earth transfer segment.

### 3.2.9 Mars to Earth Transfer

Based on planetary positions and the chosen propulsion system, this phase should begin May 11, 2023 with a spiral out from Mars. Because the ITV is still using NSTAR ion electric propulsion, this spiral will take almost three months and result in a Mars escape on August 4, 2023. Once the ITV escapes Mars influence, it will begin the transfer back to Earth, using the NSTAR thrusters to burn for most of the trajectory. In order to save mass on the return journey, this trajectory involves a full orbit around the Sun, and therefore the ITV will not return to Earth until August 26, 2025. There are no defined time constraints on the end of the mission, but this return time is still well within the self-imposed constraint to return by 2030.

### 3.2.10 Direct Earth Entry

The final phase of the mission will occur on August 26, 2025 when the EEV performs a direct entry onto Earth's surface. Because the chain of contact was broken on Mars, this maneuver poses no contamination risk. After separating with the EEV, the ITV will burn up in Earth's atmosphere while the EEV travels toward its landing site in the Utah Test and Training Range. The EEV is a parachute-less design; it is built using impact-absorbing carbon foam which has been proven to be able to easily absorb the forces of the landing. EEV impact marks a safe return of the sample to Earth's surface, and an end to the mission.

### 3.2.11 Mission Architecture Summary

Figure 2 shows a visual summary of the complete final mission architecture. This serves as a simplified representation of all stages previously discussed. The presented architecture is optimal due to its low risk and cost, as well as a mission

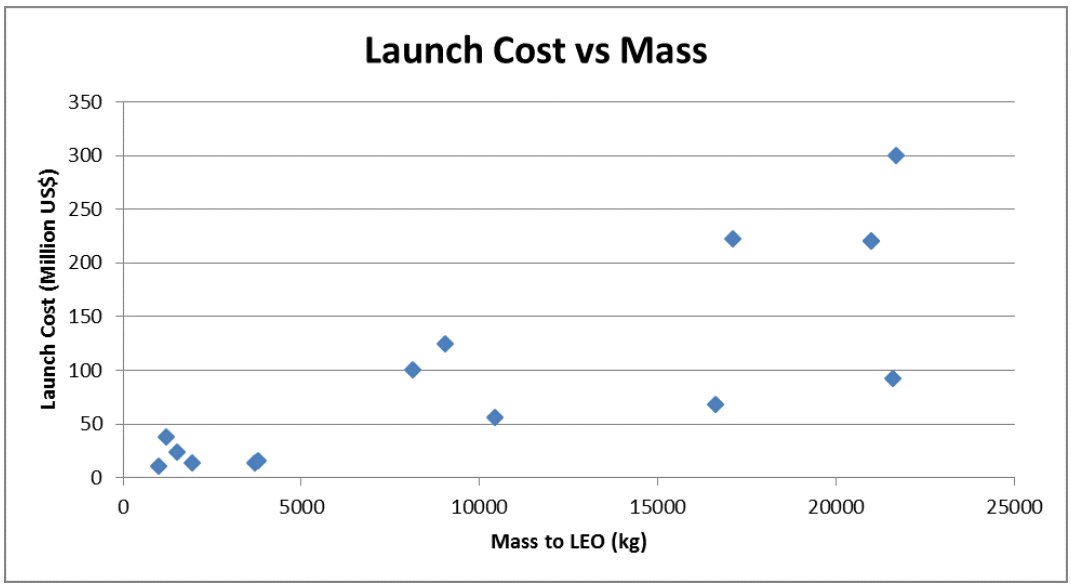


**Figure 3.4:** Plot comparing the total cost launching different vehicles with the amount of mass they are able to bring to Low Earth Orbit (LEO).

duration within the bounds of the stated requirements. Using this architecture, the mission can be completed successfully while optimizing the values laid out in the VSD section.

## 3.3 Key Trades

There were several key decision points that influenced the overall direction of the mission architecture design. In order to make these decisions the benefits of each were weighed with a focus on Value System Design. Overall each decision seeks to minimize risk, cost, and mission duration.

### 3.3.1 Number of Earth Launches

As mentioned in the discussion of the third proposed architecture, two separate Earth launches were considered as a possible way to reduce total mission mass and extend the mission timeline. The first would contain an ITV with only the lander segment attached, and the second would be a much smaller launch containing only the return vehicle. This architecture would offer several advantages in that the ITV for the return journey would be much less massive and the second launch would occur at a later date, allowing for more development time.

Upon further examination, however, this architecture was found undesirable due to two main factors, added complexity and added cost. Analyzing Earth launch costs led to data suggesting that two separate launches would always result in a higher total cost for the mission unless both vehicles could be drastically reduced in mass, because launch vehicles become more cost efficient as launch mass increases as shown in Figure 3.7. Such reductions were not possible while still maintaining full mission capability, so total cost could not be reduced using this separation. Added complexity proved to be another issue

as developing two separate vehicles would mean almost double the amount of total subsystems, leaving much more risk of failure when considering both vehicles. Mission duration would also not see any notable improvement using this architecture, so this was not a factor in rating this choice. Overall, the added cost and complexity made it clear that a single Earth launch was optimal for this mission. [8]

### 3.3.2 Decision to Perform Mars Orbit Rendezvous

Another key decision point was the choice between option one of performing a rendezvous with the sample in Mars orbit and option two of landing the entire return ITV on the Martian surface. Originally the second option was considered because it represented less overall risk, since it eliminated the complex rendezvous maneuver in Mars orbit. Additionally, having a single vehicle throughout the entirety of the mission eliminates a great deal of complexity as it would no longer be necessary to monitor multiple systems at once.

The key factor in analyzing this decision was comparing the weight of the cost saving of the rendezvous option with the risk and complexity reduction of the large MAV option. Analyzing mass costs first, the NASA Red Dragon proposal [9] provided data showing that the mass of the MAV payload would increase from 30 kg to 500 kg. This would in turn increase the total mass of the MAV to over 1000 kg due to the fuel and size increase necessary to transfer this payload to Mars orbit. In addition, in order to transfer this much more massive MAV to the surface, the Mars EDL segment would require a much more massive deceleration system. This added EDL mass would both increase the launch cost at Earth and affect the ability of the lander to maintain the necessary 5 km accuracy requirement. Additionally, launching the Mars to Earth ITV from the Martian surface would result in the entire surface of the ITV becoming contaminated. This means direct descent upon returning to Earth would no longer be possible due to contamination concerns. Instead, the ITV would have to dock with the International Space Station (ISS) or a similar orbiting station in order to drop off the sample, and this type of maneuver adds a great deal of necessary mass and cost.

Next it was necessary to consider just how much risk would be added by undertaking a rendezvous in Martian orbit. Research showed that there has already been significant development time but into this type of maneuver, and it had previously been successfully performed in simulated environments aboard the Orbital Express vehicle. These tests showed that an orbiting sample could be captured by using a Light Detection and Ranging (LIDAR) system to locate the sample and an orbiting sample transfer tube to grasp the sample container. As of now the TRL of the necessary equipment is a 5, so it is very likely that it will be ready to implement on well before the mission start date [44]. In conclusion, performing an orbital rendezvous increases risk slightly but decreases mass by a factor of 5. Therefore, in accordance with the relative weightings defined in VSD, the decision was made to proceed with the plan to perform a rendezvous in Mars orbit.

### 3.3.3 Sample Retrieval Decision

The choice between performing a rendezvous maneuver to deliver the sample container to an orbiting station or performing an Earth landing to deliver the sample directly to Earth's surface also required consideration. There were several considerations

involved with analyzing this decision, including cost comparisons, inherent risk, and contamination concerns.

First each decision was analyzed with respect to mass, which corresponds to total mission cost due to Earth launch considerations. Looking first at a direct Earth landing, this option has been successfully completed in the past at the conclusion of the Stardust mission [48]. Using this mission and other mission concepts tested by the NASA Langley Research Center (LaRC) [52] as a baseline, the conclusion is that this method represents a very small increase in total system mass due to the EEV requiring no complex instruments or equipment. Conversely, performing on orbit station rendezvous requires a much larger additional mass due to the necessary addition of guidance systems, communication equipment, and maneuvering capabilities. Docking with the ISS requires a human rated vehicle, and preliminary estimates point to an extra mass cost greater than 500 kg in order to provide this capability to the ITV. In order to provide this capability the ITV would either need to carry all this mass throughout the entire journey, or there would need to be a separate launch that would deliver the necessary equipment to the ITV upon its return to Earth orbit. Either option would result in a much greater cost than that associated with a direct Earth landing.

Next it was necessary to compare the risk associated with each option. Direct Earth entry has some inherent risks such as missing the designated landing site or failure to deploy the deceleration system, but these risks can be greatly reduced by using a passive EEV. This means that the EEV uses no parachutes and instead absorbs the force of landing using resistant materials and a high drag structure design. Such a system has been proven successfully, so incorporating a similar system into this mission would result in minimal risk from a direct Earth entry. An orbit station rendezvous would also involve very minimal risk, even less so than direct entry due to the frequency and success rate of Earth orbit rendezvous maneuvers. However, the risk of both options is small enough that this should not be a deciding factor in this trade.

Contamination concerns were the last important factor in this trade, and this involves the need to ensure that no material from Mars is directly exposed to Earth. For this reason, any vehicle that has landed on the Martian surface cannot perform a direct Earth entry, meaning this option cannot be chosen if the return ITV launches directly from the Mars surface. However, direct Earth entry can still be performed without risk of contamination if the chain of contact with Mars is broken through use of a Mars orbit rendezvous maneuver. The orbit station option does not have these same contamination issues, so it can be chosen regardless of complementary mission architecture. In conclusion, direct Earth entry is the most desirable sample retrieval method due to drastically lower mass and similar risk, and therefore contamination concerns drive the overall architecture towards including a Mars rendezvous segment.

### 3.3.4 MAV Fuel: ISRU or ISPP vs. Storable

Investigations were performed to determine whether performing in situ resource utilization (ISRU) to produce the fuel for the MAV would offer net savings to the system. While these do offer savings in terms of fuel mass, it was found that the additional equipment and power required caused significant mass penalties. Using storable solid fuel was found to be more mass efficient than the ISRU options considered. Details of this trade will be discussed in Section 7.

**Table 3.1:** It is shown here that given mission values prioritizing mass over time of flight penalties, electric propulsion is desirable in comparison to chemical propulsion methods due to the mass savings observed during a simplified trajectory analysis. This analysis is completed using approximate mass values for the spacecraft and these values do not reflect final system mass values. [10]

| Thruster Configuration | Orbiter Dry Mass (kg) | Flight Time (days) | dV Required (km/s) | Total Wet Orbiter + Payload Mass (kg) | Flight Time Compared to Chemical | Mass Compared to Chemical |
|---|---|---|---|---|---|---|
| JPL Chemical | 659.40 | 258.80 | 2.60 | 2038.18 | 100.00% | 100.00% |
| NSTAR x 1 | 599.36 | 775.83 | 4.85 | 915.61 | 299.78% | 44.92% |
| NSTAR x 2 | 676.81 | 389.76 | 3.71 | 993.06 | 150.60% | 48.72% |
| NSTAR x 3 | 754.27 | 337.77 | 3.27 | 1070.52 | 130.52% | 52.52% |
| NSTAR x 4 | 831.73 | 318.72 | 3.15 | 1147.98 | 123.15% | 56.32% |
| NSTAR x 5 | 909.19 | 308.28 | 3.09 | 1225.44 | 119.12% | 60.12% |
| NEXT x 1 | 708.13 | 351.03 | 3.38 | 1024.38 | 135.64% | 50.26% |
| NEXT x 2 | 894.35 | 306.27 | 3.08 | 1210.60 | 118.34% | 59.40% |
| NEXT x 3 | 1080.58 | 294.19 | 3.02 | 1396.83 | 113.67% | 68.53% |
| NEXT x 4 | 1266.81 | 288.53 | 3.00 | 1583.06 | 111.49% | 77.67% |
| NEXT x 5 | 1453.04 | 285.24 | 2.99 | 1769.29 | 110.21% | 86.81% |

### 3.3.5 Electric vs. Chemical Propulsion

Planetary missions in the past have been completed with chemical systems. There are several aspects of planetary missions that are much easier to perform with impulsive thrust than with constant thrust, not to mention the time of flight benefits associated with travelling at a high constant velocity throughout the duration of the journey. However, for certain missions, using higher $I_{sp}$ electric propulsion systems can result in large mass savings. In order to investigate if the MSRS mission design was capable of seeing mass savings benefits by using an electric propulsion system instead of a traditional chemical propulsion system, a baseline chemical propulsion system was identified as JPL's Planetary Science Decadal Survey for a Mars Sample Return Orbiter Mission [10]. For the purposes of the return journey to Earth, JPL's system is very similar to the MSRS mission. The simplifying assumptions in the electric system testing are that Mars and Earth are in circular, coplanar orbits. These are significant assumptions but are acceptable to determine orders of magnitude or factors difference between time of flight and mass of the two systems.

In order to get values for the electric propulsion system's time of flight and mass, a low thrust trajectory was used [11]. For the sake of comparison, it was desirable to have the constant thrust spacecraft be able to achieve a trajectory similar to a Hohmann transfer in a single pass rather than a spiral. This meant that time of flight was similar enough to the chemical system to compare the masses without including time as a significant trade. The results of the analysis using a dry orbiter mass equivalent to the chemical system with the propulsion system replaced are shown in Table 3.1.

With increases in time of flight on the order of 20 to 30 percent, mass savings on the order of 40 to 50 percent can be achieved. Because the mass savings are more valuable than the time of flight penalties, the team used this analysis as the basis to decide to use electric propulsion and further explore the design space in order to find the best solution available. Subsequent analyses included searching for an optimal $I_{sp}$ and varying the number and kinds of thrusters to increase the thrust capability and create the opportunity to perform a wider array of maneuvers. As is presented in Section 4.1, the proposed MSRS ITV design is significantly less massive than JPL's wet orbiter mass of 2038 kg, validating the decision to pursue electric propulsion methods [10].

### 3.3.6 Key Trades Summary

Figure 3.8 depicts a summary of key architectural decision points. Any of the paths shown on the flowchart would have resulted in a viable mission architecture, but the chosen path leads to the optimal architecture when analyzing trades in accordance with VSD. After finalizing these decision points, the final mission architecture was developed in accordance with the aforementioned trades.

## 3.4 Critical Technology Development and Mission Risk

Three of the more significant risks to the development of this system are contained within the martian ground systems. These are the motors and guidance on the MAV, and the contamination area on the lander. The rocket motors used on this design are not legacy parts and will require a significant effort to design. While they do not require the development of new technology, the system as a whole will need to be developed. Additionally, the MAV position and orientation determination system would be relatively novel. These systems on earth rely on infrastructure that is not in place on mars. It is for this reason that this system would require a new design, or the development of martian infrastructure such as a martian gps system. For the lander the planetary protection procedures and mechanisms are the areas where most of the development has to focus. The system must break the chain of contact and prevent recontamination of the system. Failing to do so would have consequences further down the mission timeline. Risk comes from the fact that these systems are just concepts with low TRL's that would require time to develop fully.

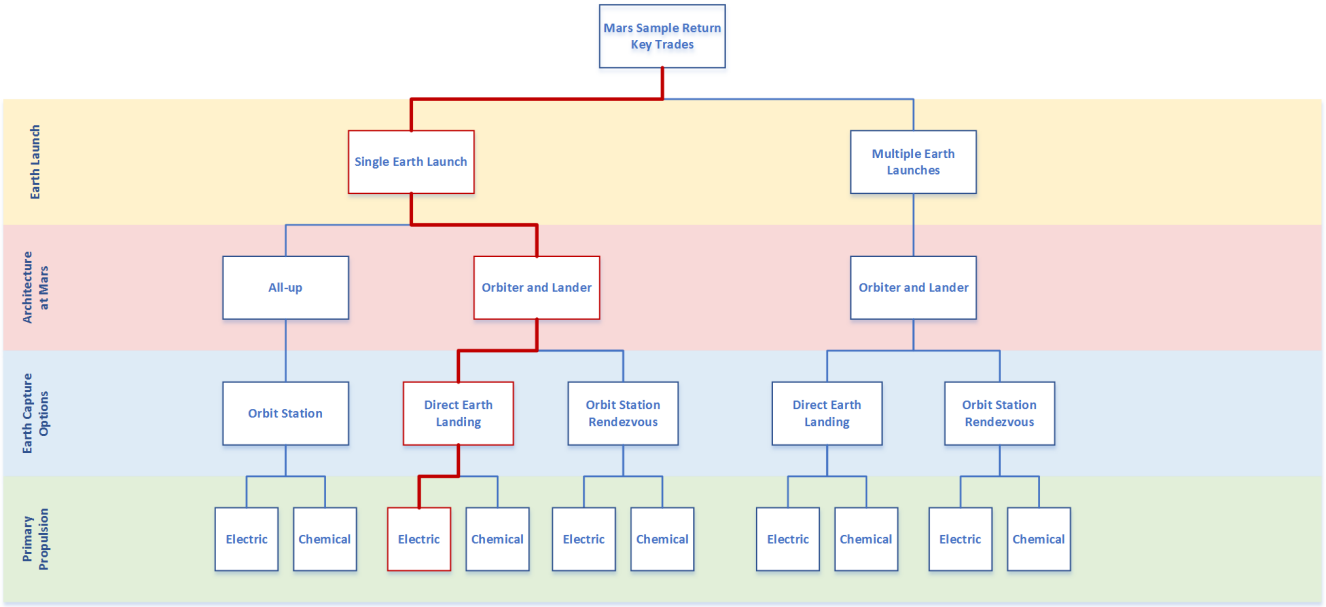


**Figure 3.5:** Flowchart depicting the key architectural decision points analyzed during the mission development phase of design. The red line highlights the chosen path.

# 4 Trajectories

The decision for an electric interplanetary propulsion system requires a shift from conventional route planning to Mars with an emphasis on providing the same capability while working within the limitations of small acceleration. The key challenge for low-thrust trajectory design is planning finite maneuvers that must span long durations compared to the impulsive burn durations of high-thrust chemical propulsion systems. The loss in efficiency where maneuvers cannot be completed at their optimal point in time and space is offset by a significantly greater overall propulsion system efficiency. Low-thrust trajectory design at the scale and complexity of a Mars sample return mission presents an opportunity that is equally challenging as it is novel. The following section details the preliminary analysis, mission modeling, and a multidisciplinary attention to the design of unique, low-thrust trajectories that enable the use of solar electric propulsion for a Mars sample return mission.

## 4.1 Elements of Trajectory Design

The proposed architecture poses an interplanetary vehicle schedule in multiple configurations and environmental conditions throughout the span of the mission. Therefore, it was important to identify key segments of the Mars sample return mission that would foster meaningful preliminary analysis and decision decisions within a defined, workable scope. This process also served to define the internal and external relationships, as well as the work structure, for trajectory design as it developed throughout the iterative design process. The six primary segments identified are diagrammed according to the mission architecture in Figure 4.1. While not representative of their design order, the segments will be detailed in their chronological order throughout the following section.

### 4.1.1 Software used for Mission Modeling

Preliminary analysis began in Mathworks MATLAB with the intent for detailed design, modeling, and analysis to be performed with Analytical Graphics, Inc Systems Toolkit (STK). STK is an academically and commercially available modeling and analysis software made for the aerospace, defense and intelligence communities. For the scope of the this project, STK's Astrogator module enabled moderate-fidelity modeling of trajectories spanning from Earth to Mars. Moderate-fidelity was justified given that the model includes, among other aspects, perturbations from other celestial bodies, perturbations induced by atmospheric drag, gravitational zoning (J2), solar pressure, and highly-accurate numerical computation. Lastly, it is important to note that this works presents value to the industry in demonstrating how leveraging an accessible, vetted, commercial software provides a rapid and cost-effective means of preliminary design for missions to and from Mars.

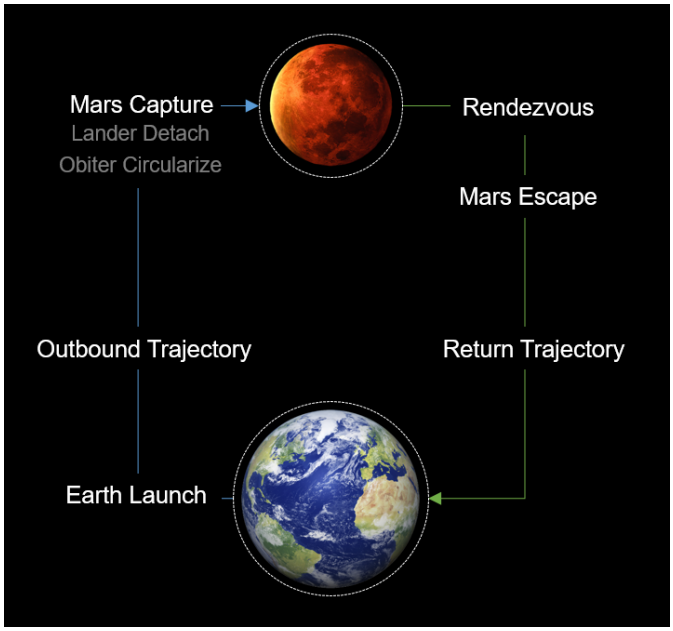


**Figure 4.1:** The six primary trajectory design segments for the proposed mission architecture, diagrammed in sequential and architectural order. These elements were analyzed individually for preliminary analysis, then brought together for further detailed design. Each element will be discussed in detail throughout this section.

## 4.2 Earth Launch

### 4.2.1 Preliminary Analysis

The NASA Ames Trajectory Browser [12] served as a valuable preliminary resource in determining the viability of mission and trajectory concepts by providing visual and high-level information for quick trade-off analyses.The trajectories available with the browser are based off of Lambert's problem applied to interplanetary transfer between Earth and Mars. While the assumptions inherent to Lambert's problem make it an insufficient method of modeling realistic trajectories, it has the most utility in providing the initial estimates the hyperbolic outbound and inbound parameters at Earth and Mars, respectively. At Earth, these translate to capabilities required of the launch vehicle, and at Mars are used to size the ITV propulsion system for capture. The purpose of preliminary analysis was to verify selected trajectories from the trajectory browser and determine the optimal range of departure and arrival dates for outbound trajectory. Optimality was determined by minimizing the hyperbolic excess velocity, or C3, required. In essence, the C3 is amount of energy the launch vehicle must provide the spacecraft by launching it directly into a high-energy interplanetary trajectory. A contour plot of the C3 with respect to the departure and arrival dates is commonly known as an interplanetary "porkchop plot," and provides a clear way of identifying the feasible windows for launch. A porkchop plot for departure and arrival windows between January 2018 and December 2022 is in Figure 4.2.

From the figure, the recurring two-year optimal transfer window between Earth and Mars trend is clearly shown by two distinct contour areas. Since a launch in 2018 was determined infeasible, the best available launch window occurs in the 2020

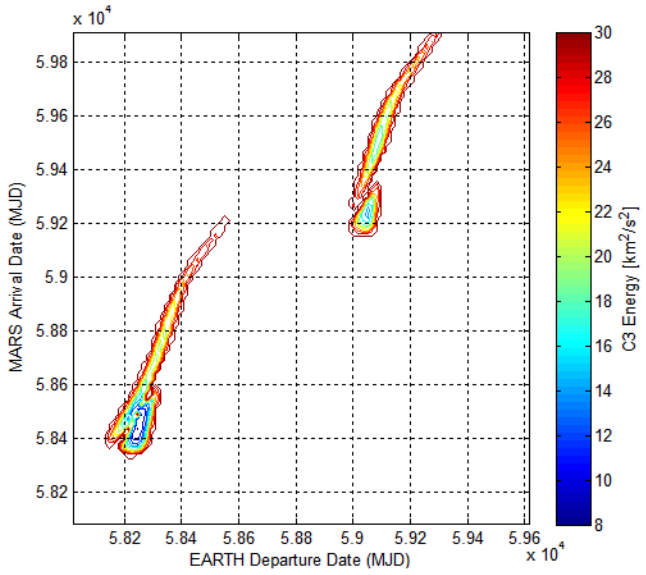


**Figure 4.2:** An interplanetary porkchop plot for Earth to Mars preliminary ballistic trajectory analysis. Lambert's problem is solved to determine the the initial hyperbolic excess velocity (C3), shown in contours, that the launch vehicle must provide for departure and arrival dates spanning Jan 2018 to Dec 2022. A minimum is found for a 2020 launch window departing Earth on Jul 22 2020 and arriving at Mars on Jan 20 2021. While this does not provide a low-thrust trajectory solution, it approximates the range of near optimal dates for Earth launch regardless of propulsion system.

year between June and August. From the plot, a minimum C3 of 13.1 $km^2/s^2$ occurs on a launch date of Jul 22 2020 and arrival date of Jan 20, 2021. The results of this preliminary analysis provided a single best-guess date, as well as a range of acceptable dates for Earth launch independent of the selected propulsion system. The end-design departure date for this mission with electric propulsion is Jun 14 2020, only 38 days difference from the estimate from the preliminary analysis.

### 4.2.2 Launch Vehicle Selection

Two driving numbers for selection of an appropriate launch vehicle were the estimates of the required C3 and launch mass of the complete Mars sample return system. Historical data available through NASA's Launch Services Program Launch Vehicle Performance database provided the capability of existing U.S. launch vehicles as a function of these two variables [13]. For this particular mission, Mars Science Laboratory served as a valuable reference due to its recent flight history, similar launch mass, and shared hardware. MSL launched with an Atlas V 541 configuration vehicle at a launch mass of 3893 kg and C3 of 10.78 $km^2/s^2$. According to the NASA performance database, the maximum mass the Atlas V 541 vehicle can accommodate for a C3 of 10.78 $km^2/s^2$ is 4555 kg, meaning a 17 percent capability margin was provided for MSL. Applying the same margin to the design launch mass of the Mars sample return system, 3300 kg, and C3 of 14.2 $km^2/s^2$, the selected launch vehicle must be able to accommodate a 3860 kg launch mass.

NASA's performance database identifies four launch vehicles that can provide this capability: Atlas V 431, Atlas V 541, Atlas V 551, and Delta IV Heavy. Table 4.1 shows the margins for each launch vehicle at the nominal launch mass, also with a 10 percent mass growth. Considering the performance with the growth factor provides a more realistic estimate and reduces

**Table 4.1:** The first column shows the percent margin for each launch vehicle able to provide a 3300 kg payload a C3 of 14.2 $km^2/s^2$ on an escape trajectory. The second column shows the percent margin if the launch mass grows 10 percent within the four years of development. A baseline acceptable margin of 17 percent is based off of the Mars Science Laboratory mission. An Atlas V 541 satisfies both margins and also has the benefit of having previously flown nearly identical hardware for MSL.

| Launch Vehicle | Maximum Payload [kg] | Margin [%] | Margin with 10% Growth [%] |
|---|---|---|---|
| Atlas V 431 | 3940 | 19.4 | 8.5 |
| Atlas V 541 | 4250 | 28.8 | 17.1 |
| Atlas V 551 | 4665 | 41.4 | 28.5 |
| Delta IV Heavy | 8220 | 149 | 126 |

**Table 4.2:** These are the required hyperbolic excess velocity, right ascension, and declination at burnout for proper transfer from Earth to Mars. It is important to assume that the launch vehicle will not meet these parameters exactly, however small corrections throughout the outbound trajectory can compensate for reasonable errors from the Centaur upper stage.

| | |
|---|---|
| C3 | 14.2 kmˆ2/sˆ2 |
| Right Ascension | 40.0 degrees |
| Declination | -4.0 degrees |

the risk of the selected launch vehicle.

As shown in Table 4.1, the most cost effective launch vehicle that will meet the performance requirements factoring in mass growth is the Atlas V 541, with the next feasible option the Atlas V 551. The 541 configuration also provides the benefit of having flown MSL hardware present in the proposed design, therefore significantly reducing the launch vehicle development and integration costs associated with the Mars sample return mission. Additionally, the Atlas V series has a proven flight history with 100 percent reliability, greatly reducing the associated risk with the mission. Another consideration to risk is that, although the launch mass of the system is not expected to exceed the capability of the Atlas V 541, there is less risk to cost and schedule when upgrading the rocket to an Atlas V 551 due to similarities in payload bay design. The second numeric designation in the Atlas V series is its number of solid rocket stages (four for the Atlas V 541). Upgrading to an Atlas V 551 adds an additional solid stage, however it is likely that the payload bay is negligibly affected and therefore poses less risk to the overall mission.

Therefore, the selected launch vehicle is an Atlas V 541 configuration, an Atlas V series vehicle featuring with four solid stage boosters, a 4.5 meter diameter medium-length fairing, and a single Centaur upper stage launched from Kennedy Space Center in Cape Canaveral, Florida, USA. These specifications were used for designing the ITV structure to withstand launch loads, as well as fit within the payload bay volume.

### 4.2.3 Launch Vehicle Modeling and Validation

Using launch facility, burnout, timing, engine-spec, and hyperbolic escape information from the MSL launch sequence [15], a model of MSL's launch on an Atlas V 541 launch with Centaur upper stage was created STK Astrogator. Since the burn

**Table 4.3:** A targeting routine in STK Astrogator was developed in order to validate the launch sequence for the Mars Science Laboratory mission. Once modeled and verified to a reasonable degree, the model was adapted to the Mars sample return vehicle system. This simulation provided an approximate percent fuel loading for the Centaur upper stage to assess feasibility, as well as an exact launch time given a scheduled escape time from the outbound trajectory. Note that after spacecraft separation the Centaur upper stage does not deorbit - it performs a burn so that it does not contribute to more risk or orbital debris.

| T+ | Event | Duration |
|---|---|---|
| 00:00 | Launch | 04:55 |
| 04:55 | Upper Stage Separation | 00:02 |
| 04:57 | Main Engine Start (MES1) | 07:00 |
| 12:57 | Main Engine Cutoff (MECO1) | 00:02 |
| 12:59 | Coast | 09:49 |
| 22:46 | Main Engine Start (MES2) | 08:22 |
| 33:08 | Main Engine Cutoff (MECO2) | 00:07 |
| 33:15 | ITV Spacecraft Separation | 00:10 |

directions and fuel loading were unknown, a targeting routine was developed that optimized the thrust vector and amount of upper-stage fuel so that the escape parameters successfully matched the real data from MSL. From here, payload launch mass was adjusted to the Mars sample return mission mass of 3300 kg, and the algorithm was run to target the escape parameters developed for the Mars sample return mission outbound trajectory. The result is an estimate of the launch sequence, detailed in Table 4.3, and upper-stage fuel loading that is feasible for the Atlas V 541 configuration launch vehicle and correctly acquires the desired escape parameters for insertion into an interplanetary trajectory to Mars. The Centaur upper stage fueled to 72 percent capacity (3400 kg for MES1, 11320 kg for MES2), which is comparable to the 58 percent MSL fuel loading obtained using the same developed model for MSL.

## 4.3 Outbound Trajectory

With an interplanetary vehicle system that features low-thrust solar electric propulsion, particular attention was focused on the outbound trajectory. Not only is it the critical mass case (thrust-to-mass ratio is the smallest over the entire mission), it is bounded in time by the delivery of the Mars lander to Mars' surface by December 2022 for sample capture as well as optimal launch windows in mid 2020 and development schedules demanding the latest possible launch date. Design of a low-thrust trajectory to Mars under these constraints poses a novel challenge beyond those of existing proposals that use chemical propulsion.

The goal of the outbound trajectory is to place ITV with a relative position and velocity with respect to Mars that will allow it to maneuver for lander release and toward a desired 300 km parking orbit. The nature of the problem is lends itself to three inherently coupled elements, all of which are desired for an efficient, effective transfer: phasing correctly with Mars,

**Table 4.4:** This table provides a breakdown the maneuvers that make up the outbound Earth to Mars trajectory. The ”raise” maneuver has ITV burn tangential to velocity to raise apogee shift the argument of perigee. The phase maneuver is primarily a timing correction maneuver. The ”match” maneuver reduces the relative velocity between the ITV and Mars, and the ”capture” maneuver ensures a stable capture orbit.

| Manuver | $\Delta V$ [km/s] | Fuel Used [kg] | Duration |
|---|---|---|---|
| Coast | 0.0 | 0 | 2.00 months |
| Burn - Raise Orbit | 1.1 | 110 | 4.75 months |
| Burn - Phase | 0.3 | 30 | 1.25 months |
| Burn - Match Orbit | 2.0 | 185 | 8.10 months |
| Burn - Capture | 0.2 | 20 | 0.80 months |
| Total | 3.6 | 345 | 1.40 years |

matching Mars' heliocentric orbit, and maximizing launch vehicle performance. Matching Mars' orbit with correct phasing ensures that the relative position and velocity between the ITV and Mars is small enough that the ITV can be placed into a stable orbit about Mars. In essence, maximizing launch vehicle performance is a direct way of minimizing the required fuel-mass of the ITV propulsion system.

The final outbound trajectory design consists of four discrete burn segments: boost, phase, circularize, and capture. Before the boost phase, 60 days are budgeted after the spacecraft leaves Earth for the ITV to perform system deployment and checks, as well as ensure proper phasing with Mars. After these 60 days, the boost burn augments the nominal ballistic trajectory provided by the launch vehicle with a 1 km/s burn. The spacecraft uses its AC&DS and gimbaled thrusters to orient and keep oriented a thrust vector with components in the velocity and normal directions in order to raise apoapsis to slightly above 1.52 AU and rotate argument of perigee. The burn normal to the orbital plane reduces the radial distance at rendezvous due to relative inclination. The “phase” segment accelerates the spacecraft in its sun velocity direction and serves primarily as a course-correction to ensure correct phasing timing for circularizing. The circularizing involves pointing the thrust in the spacecraft's anti-velocity direction relative to Mars until its C3, or hyperbolic excess velocity, relative to Mars is zero. This maneuver provides an indirect method of matching Mars' orbit by reducing the relative velocity between the two objects. While the end state of the maneuver is theoretically a parabolic orbit, is is realistically unstable and will gain C3 to solar third-body effects and other N-body perturbations. Therefore, the capture burn segment ensures that the ITV captures into a stable, elliptical orbit at the desired 25 degree inclination by burning in the anti-velocity and normal direction until periapsis altitude reaches 50,000 km. The highly elliptical orbit resulting from this maneuver is desired because low-thrust is more effective in adjusting periapsis at high apoapsis, meaning the setup for EDL vehicle drop off requires less fuel. A heliocentric view of the outbound trajectory is shown in Figure 4.3 and the mass and fuel budget is presented in Table 4.4.

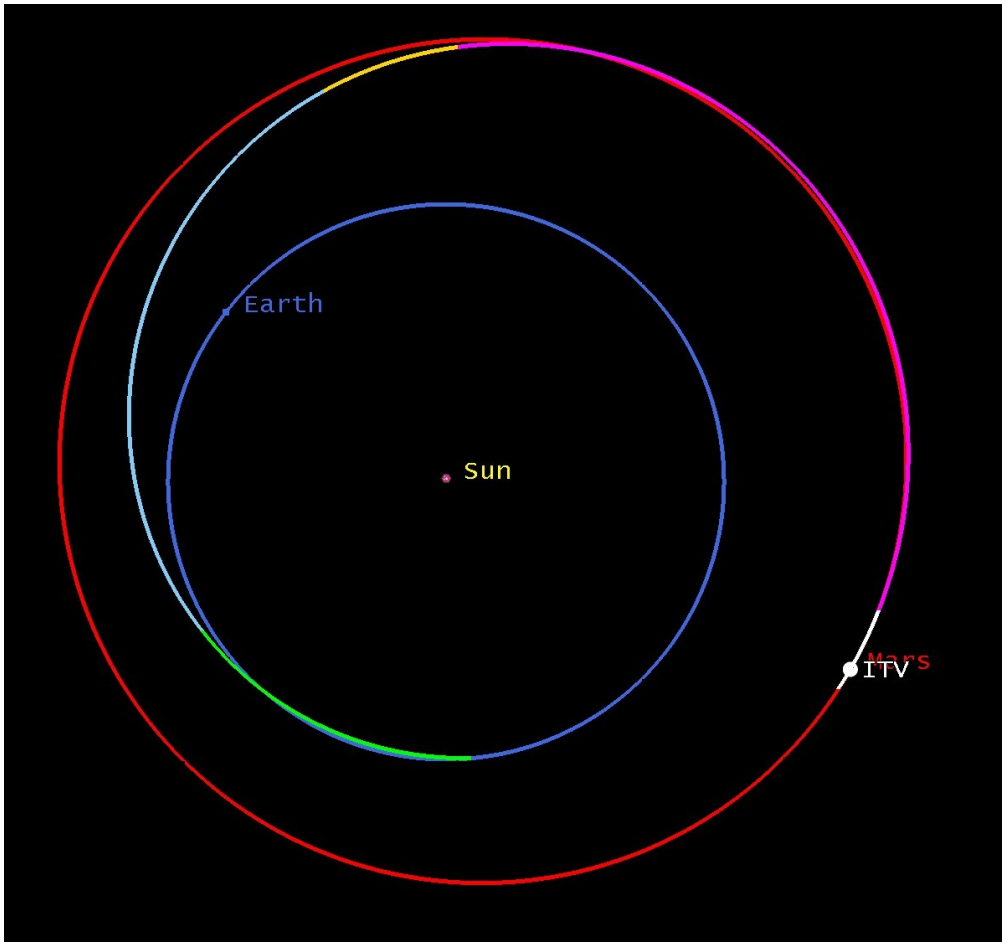


**Figure 4.3:** A two-dimensional view of the Earth to Mars low-thrust trajectory modeled in STK. Initial conditions are the escape parameters of Earth launch, and the final conditions are when the ITV has achieved a stable, highly elliptical orbit about Mars. The total flight time is 1.4 years with a total delta-V of 3.6 km/s and 345 kg of xenon fuel consumed. The trajectory consists of an initial 60-day coast period followed by 4 main burn segments differentiated by color and detailed in the accompanying table.

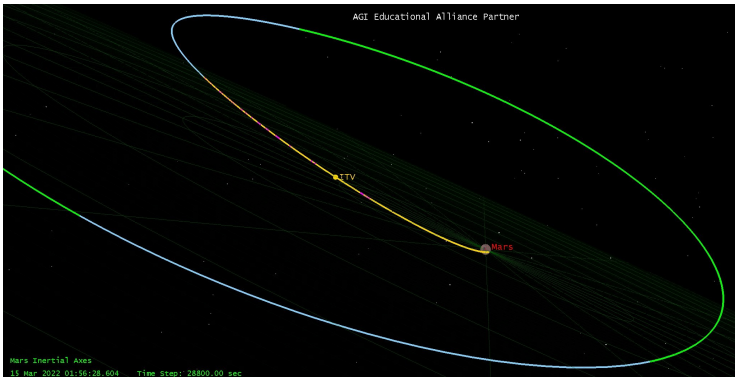


**Figure 4.4:** Maneuvering for EDL vehicle release.

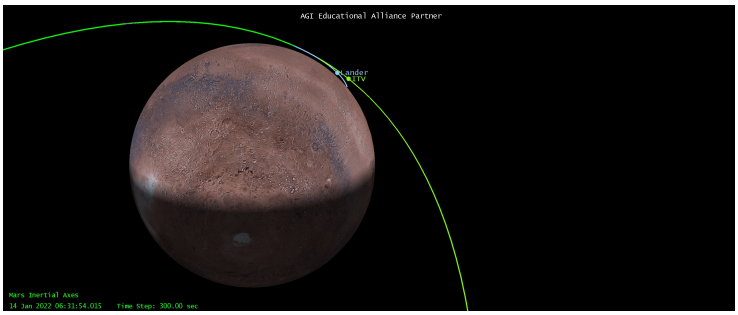


**Figure 4.5:** After successfully executing the targeting maneuver and corrections during coast, the EDL vehicle separates for a precision insertion into Mars' atmosphere at 126 km altitude and entry speed of 4.9 km/s. The ITV continues past periapsis and begins maneuvering to a circular parking orbit.

## 4.4 Mars Capture and EDL Vehicle Release

Once in the stable, highly elliptical orbit about Mars, the ITV maneuvers to provide an accurate release of the EDL vehicle into the Martian atmosphere. Apogee is first lowered to 500,000 km in order to reduce the period of the orbit and ensure that the apoapsis is high enough that periapsis can be moved easily with low-thrust, but low enough that it won't be too sensitive to N-body perturbations. The ITV then performs a burn at this apoapsis to reduce periapsis to the desired 125 km drop off altitude. On the way to periapsis, the ITV is far enough from the center of Mars that solar-third body effects slightly perturb the nominal trajectory. Therefore, an automated sequence is implemented to perform correction burns as necessary so that the periapsis remains within a few kilometers of 125 km altitude.

## 4.5 Maneuver to Parking Orbit

After passing through periapsis and releasing the EDL vehicle, the ITV coasts to apoapsis and performs a burn to change inclination and periapsis. Since low-thrust requires greater time to perform maneuvers, a highly elliptical orbit is neither a mass nor time-efficient method of lowering apoapsis since the time spent burning at periapsis is so short. This is the primary reason for not selecting aerobraking as a more fuel-efficient maneuver. While aerobraking is a proven and highly mass-efficient

**Table 4.5:** This maneuver sequence places the ITV into a highly elliptical orbit at apoapsis, allowing perigee to be easily lowered to the desired insertion altitude. Automated correction burns are performed to counteract pertubations and maintain the periapsis drop off altitude near 125 km. As a result, the EDL vehicle is accurately inserted into Mars' atmosphere at the specified altitude and flight path angle for a precision landing on Mars' surface.

| | Manuver | $\Delta V$ [km/s] | Fuel Used [kg] | Duration |
|---|---|---|---|---|
| | Coast | 0.00 | 0 | 1.0 months |
| | Burn - Set Perigee | 0.25 | 25 | 0.9 months |
| | Coast, Corrections | 0.03 | 2 | 0.5 months |
| | Total | 0.28 | 27 | 2.4 months |

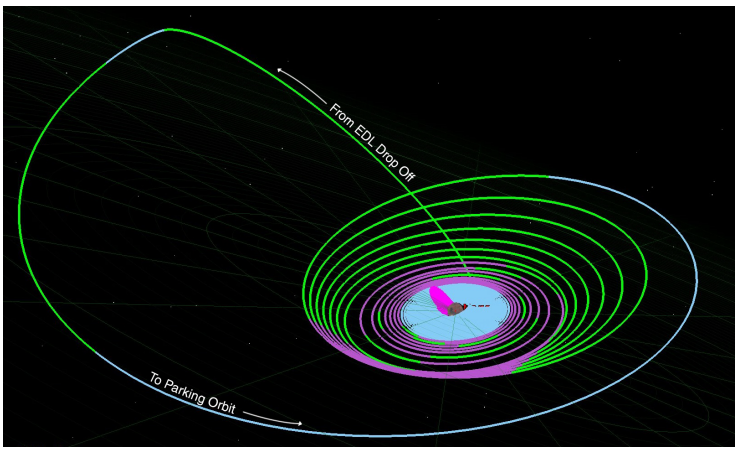


**Figure 4.6:** The center green line is the path the ITV takes after having dropped off the EDL vehicle at Mars periapsis. At apoapsis, the ITV performs a burn to raise periapsis so that it can perform repeated burns at periapsis to lower apoapsis. Eventually the ITV reaches a circular orbit, where it begins to spiral inward (thrusting only in direct sunlight) until it reaches a circular 300 km, 25 degree inclination parking orbit at Mars.

method of reducing energy, the time required to aerobrake did not allow the ITV to be in a parking orbit for rendezvous with the MAV by 2023, due in-part to Mars' minimal atmosphere. Additionally, aerobraking adds risk with atmospheric uncertainty as well as personnel cost to monitor the ITVs progress over a very long period of time.

Instead of aerobraking, the ITV first raises its periapsis so that more time is spent is spent burning to efficiently lower apoapsis. The ITV burns between windows of -45 and +45 degrees true anomaly, and will eventually circularize at its periapsis altitude. From here, an inward spiral maneuver is taken toward the 300 km circular parking orbit. While spiraling, the maneuver has been programmed to shut off burning when not in direct sunlight (eclipsed by Mars). Requiring thrust while out of direct sunlight would put significant requirements on the spacecraft battery and power system, therefore this technique saves mass and complexity in return for negligible added mission time. This process takes 8 months and gives the ITV sufficient time to prepare for rendezvous with the orbiting sample.

**Table 4.6:** This maneuver sequence occurs for the ITV orbiter after dropping off the EDL vehicle. Aerobraking was not considered because the time spent in-atmosphere does not allow sufficient $\Delta V$ to lower apoapsis by the Feb 2023 rendezvous date, although it promises significnat mass savings. Instead, a combination of apogee-lowering maneuvers and a final spiral is used. Note that the spiral does not provide thrust when not in direct sunlight, which introduces eccentricity that must be corrected through thrust vectoring.

| Manuver | $\Delta V$ [km/s] | Fuel Used [kg] | Duration |
|---|---|---|---|
| Coast | 0.00 | 0.0 | 1.0 months |
| Burn - Inclination | 0.15 | 3.5 | 3 days |
| Burn - Set Perigee | 0.20 | 4.5 | 5 days |
| Burn - Lower Apo | 1.60 | 40.0 | 3.5 months |
| Burn - Spiral | 0.80 | 20.0 | 4.0 months |
| Total | 2.80 | 70.0 | 8.7 months |

## 4.6 Orbiting Sample Rendezvous

Once the MAV launches and delivers the OS to orbit, the rendezvous sequence will begin. Nominally, the MAV will deliver the sample to the ITV's 25 degree inclined, 300 km parking orbit, but achieving a perfect insertion is highly unlikely. Analysis on insertion orbit error to inclination and altitude is shown in Section 7 and yields a uncertainty of +/- 1 degree inclination and +/- 10 km altitude. Estimating required $\Delta V$ to rendezvous done by calculating the impulsive $\Delta V$ required to sequentially perform a combined inclination and Right Ascension of the Ascending Node (RAAN) change, and then correct argument of periapsis. Relations from Lagrange's Planetary equations between the impulsive $\Delta V$ and constant thrust (burn angle of 90 degrees) $\Delta V$ are used to scale the impulsive $\Delta V$ to a constant thrust $\Delta V$. Lastly, assuming the OS and ITV are at worst phased 180 degrees apart, a constant thrust spiral is performed to match OS-ITV phase and altitude for rendezvous. However, due to the anticipated insertion orbit errors, the OS and ITV orbits will drift apart with time due to gravitational perturbations from the aspherical nature of Mars. Thus, the described $\Delta V$ calculations were performed while accounting for relative orbital drift. Figure 4.7 shows $\Delta V$ for the rendezvous maneuver as a function of time. Using constant thrust to rendezvous will require approximately 8.5 days which translates to about 400 m/s of $\Delta V$ or about 20 kg of xenon with a 10 percent margin added. The margin is added to reduce the risk of emergent inability to rendezvous with the OS should locating the OS after MAV insertion take longer than anticipated (resulting in more orbital drift and fuel cost). Following rendezvous the linearized equations of relative motion were used to calculate the $\Delta V$ to perform sample intercept. The result is a minimum 0.6 m/s $\Delta V$ and about 80 minutes for intercept - the impulsive RCS thrusters will be used for this maneuver.

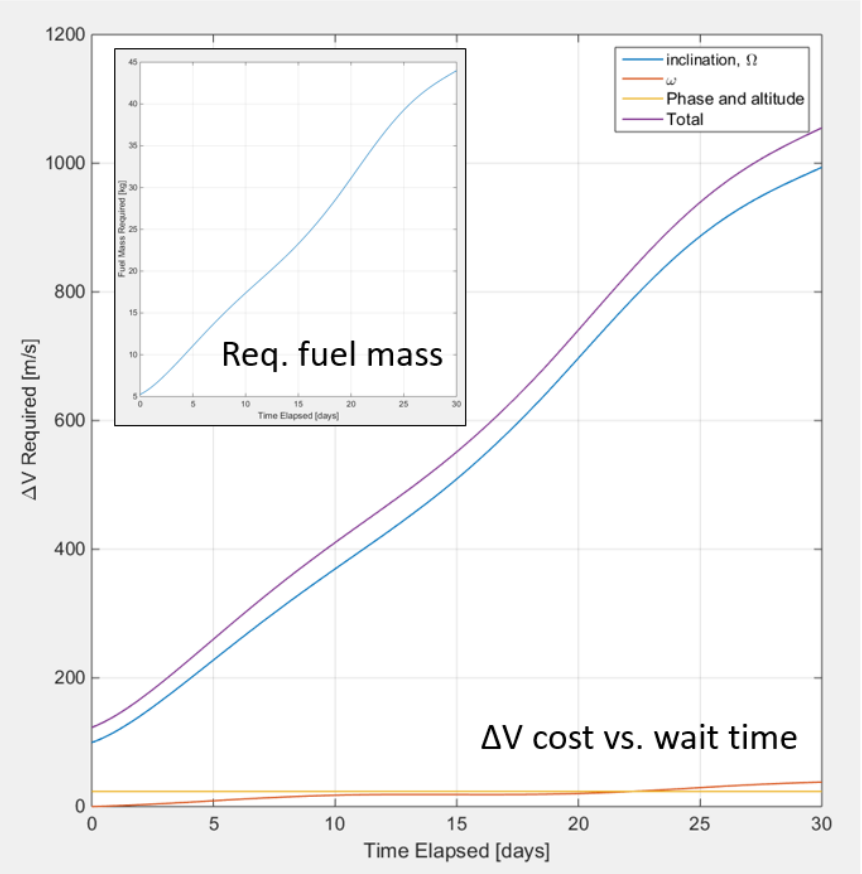


**Figure 4.7:** ITV-OS Rendezvous $\Delta V$ and Xenon Mass Requirements. $\Delta V$ is calculated for a series of sequential burns to correct relative orbital element drift and then phase. Factoring in the time the ITV will need to intercept using constant, low thrust, about 400 m/s of $\Delta V$, 17.5 kg of xenon and 8.5 days will be required to rendezvous.

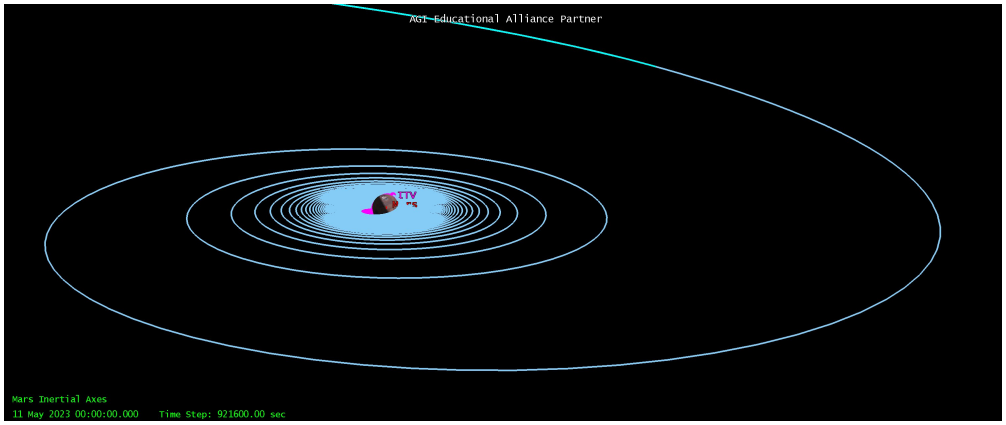


**Figure 4.8:** After successful rendezvous and capture with the orbiting sample, the ITV orbiter performs a spiral escape maneuver by thrusting in its velocity direction relative to Mars (shown in blue). The ITV does not thrust when not in direct sunlight (shown in pink) in order to reduce the mass of the battery. Worth noting is the effect of Mars J2 perturbations on inclination and sun exposure. The spiral trajectory maneuver ends when C3 relative to Mars is zero. The 2.4 month maneuver consumes a total of 60 kg Xenon for 2.8 km/s $\Delta V$.

## 4.7 Mars Escape

The maneuver to Mars escape is a nearly continuous spiral thrust vectored in the spacecraft's velocity direction relative to Mars. The maneuver ends once the ITV achieves a hyperbolic excess velocity, or C3, of zero. For the same reasons as the spiral inward to parking orbit, the escape spiral maneuver does not burn when direct sunlight is eclipsed by Mars. Analysis of burning continuously versus burning only in the sunlight extended the spiral spiral maneuver by approximately one week, a negligible amount of time for significant savings in mass and power. One reason why the difference is negligible is because the ITV is not stationkeeping during this maneuver, and therefore J2 perturbations cause the plane of the orbit to drift toward high inclinations. These high inclinations grant more sunlight and allow the spacecraft to reach continuous sunlight much more quickly than an analysis without J2 effects modeled.

## 4.8 Earth Return Trajectory

It is critical that the return trajectory minimizes fuel as the required fuel is carried throughout the entire mission, thereby affecting all trajectories from launch to Mars escape. In practice, the return trajectory was analyzed first. The return trajectory has the advantage of having the highest initial thrust-to-mass ratio of the mission, no explicit time constraints, and the ability to perform a direct entry descent back into Earth. From simply a trajectory and fuel mass savings standpoint, performing a direct entry descent is the best option because of the additional fuel required for orbital capture at Earth. This decision extends the available trajectory design space because minimum transfer trajectories occur at specific alignments of the two planets, effectively putting constraints on the available times to leave Mars.

In order to piece the elements together, the return trajectory was first analyze to get an estimate of the fuel mass required and departure date. A solution was found using STK Astrogator's differential corrector. An initial burn was set up at Mars escape to lower heliocentric periapsis to 1 AU, followed by a propagation of a single orbit about the sun, a course-correction maneuver, and then propagation until closest approach with Earth. The differential corrector modified the departure date, thrust vector and delta-V for the initial burn, and the delta-V for the correction maneuver using b-plane targeting until the dot product components of the velocity vector and b-plane converged to the desired values. The selected B-plane dot product component were consistent with the latitude and longitude of the EEV landing site, allowing for accurate and efficient targeting from a distance.

The results of the differential corrector are a departure on 2 Aug 2023. With a spiral time of 2.7 months, this means that the spiral start date on Mars would be 11 May 2023. This date allows the MAV to launch as soon as the rover reaches its end of life which reduces risk from time-on-surface, and also grants the orbiter sufficient and additional time to rendezvous with the orbiting sample if needed, helping mitigate risk from inability to find or rendezvous with the orbiting sample. With a spiral escape, or Mars departure date, on 2 Aug 2023, the orbiter will then perform a 2 km/s burn to lower heliocentric periapsis to 1 AU, a 0.5 km/s correction maneuver when the ITV passes periapsis, coast one orbit around the sun so that Earth is in-phase,

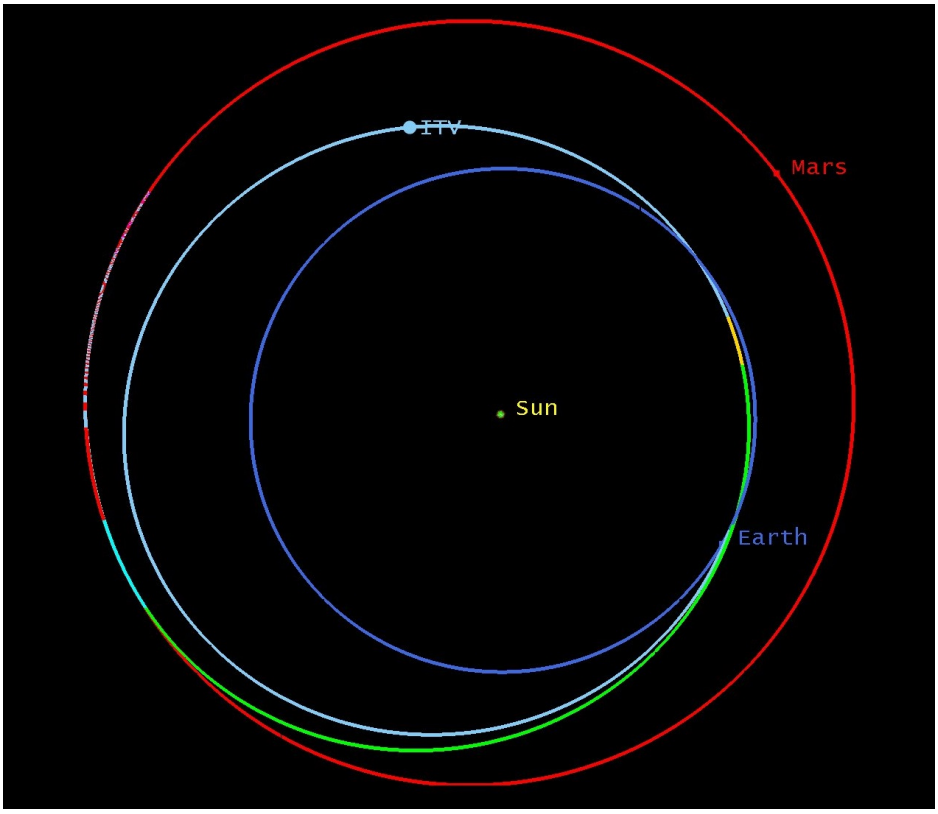


**Figure 4.9:** The Mars to Earth return trajectory significantly reduces its required fuel by performing a direct earth entry instead of orbit capture. Starting August 2, 2023, this means the Mars spiral maneuver starts May 11, 2023. Since the rover end of life is February 2023, this provides a safe margin of time for MAV launch and OS rendezvous while allowing an early departure from Mars to return to Earth. A correction maneuver (yellow) is performed at heliocentric periapsis so that the ITV is able to perform direct entry with Earth on the second pass.

and finally a coast toward an 11.8 km/s entry speed at Earth, landing within a few hundred kilometers of the intended EEV landing site on 26 Aug 2025. Realistically, a few minor course corrections will be necessary for a precision landing in the Utah Test and Training Range, however the amount of fuel required is negligibly small compared to the overall fuel required for this mission.

The return trajectory design is meant to provide an efficient, low-risk method of returning to Earth within a reasonable amount of time. Aligned with the value system design for this mission, the return trajectory provides a solution that minimizes risk, mass, and mission duration. Mission duration and risk are reduced by starting the return trajectory as the sample is captured in orbit around Mars and shortly after the rove end-of-life to reduce the required time on Mars. Mass is minimized by performing a direct Earth entry instead of orbital capture, and also by choosing not to thrust while out of direct sunlight.

## 4.9 Summary

Creative and efficient low-thrust trajectory design enabled the use of solar electric propulsion for the Mars sample return mission interplanetary transfer vehicle and overall mission architecture. The impact is a significantly reduced the mass of the

**Table 4.7:** The return trajectory has been designed to minimize fuel since the mass of the fuel is carred throughout the entire mission all the way back to the Earth launch pad. One potential concern for risk may be the long period of engine shutoff during coast while the engines are near end-of-life. Additional course-correction maneuvers are likely to be occur during the the final coast segment in order to tune the entry parameters of the Earth entry vehicle (EEV) and ensure a more accurate impact landing.

| Manuver | $\Delta V$ [km/s] | Fuel Used [kg] | Duration |
|---|---|---|---|
| Burn - Spiral | 3.25 | 60 | 2.80 months |
| Burn - Lower Peri | 2.40 | 43 | 1.90 months |
| Coast | 0.00 | 0 | 7.60 months |
| Burn - Corrections | 0.50 | 7 | 0.35 months |
| Coast to Impact | 0.00 | 0 | 15.30 months |
| Total | 6.15 | 110 | 2.32 years |

**Table 4.8:** A breakdown of the required Xenon fuel masses for the main trajectory elements of the Mars sample return mission. The outbound trajectory stands out as the most expensive segment of the entire mission; it is critical because it requires the most change in $\Delta V$ to rendezvous with Mars, has the largest ITV mass since the EDL vehicle is attached, and operates under a strict arrival time constraint. Compared to chemical propulsion systems, the fuel required of the NSTAR ion-electric propulsion stands out as it requires only a fraction of the chemical system mass for the same mission capability.

| Trajectory Segment | Xenon Fuel [kg] | Fuel Fraction [%] |
|---|---|---|
| Outbound Trajectory | 342 | 61.3 |
| EDL Drop Off | 24 | 4.3 |
| To Parking Orbit | 52 | 9.3 |
| Rendezvous | 20 | 3.6 |
| Spiral | 59 | 10.6 |
| Return Trajectory | 61 | 10.9 |
| Total | 558 | 100 |

ITV system compared to chemical propulsion alternatives. Moderate-fidelity mission modeling and analysis in STK provided strong support regarding the feasibility and accuracy of the proposed designs. The fuel mass required for the entire mission is 558 kg of pressurized Xenon. A breakdown of the fuel required for primary segments of the Mars sample return mission is shown in Table 4.8. Higher-fidelity mission modeling and analysis, particularly where there is greater control over the spacecraft's thrust vector over time, will drive the required fuel mass below the proposed 558 kg. Therefore, not only does the trajectory design work serve as a novel and competitive facet of the proposed mission, it lays the groundwork for more efficient transportation in future missions between Mars and Earth.

# 5 Interplanetary Transfer Vehicle

The primary function of the Interplanetary Transfer Vehicle (ITV) is to transport the Entry, Descent and Landing (EDL) systems including the nested Lander and Mars Ascent Vehicle (MAV) from Earth to Mars and then return the Martian sample back to Earth nested within the Orbiting Sample (OS) and Earth Entry Vehicle (EEV). As this functionality is central to the RFP, the ITV has a large impact on the overall performance of the MSRS. In turn, two subsystems have a large impact on the design of the ITV: the comparatively massive Mars to Earth payload (EDL, lander and MAV) and the propulsion subsystem comprised of the NSTAR ion electric thrusters. A priority of the ITV design is adoption of designs with flight heritage such that minimal technology development or excessive testing time is required. This will free up the human resources and funds necessary to develop the novel Martian systems discussed in Section 7. This section will discuss the overall configuration of the ITV and its subsystems with analysis supporting the development of subsystems particularly important to the unique needs of a MSRS.

## 5.1 Configuration

Figures 5.1 and 5.2 show spatial representations of the ITV in its stowed configuration at launch and an exploded view of the ITV as it would appear for the remainder of the mission respectively. Given the constrained timeline, and in order to reduce schedule risk and design complexity, the overall shape and configuration of the ITV borrows heavily from heritage spacecraft designs.

The central components of the bus include a 1.2 meter diameter by 1.3 meter tall graphite composite cylinder flanked by aluminum honeycomb panels. This spacecraft geometry would be a derivative of Orbital-ATK's Dawn spacecraft bus, but also shares many similarities with Lockheed Martin's OSIRIS-Rex and MAVEN spacecraft buses. Nested within the cylinder is an oblate spheroidal xenon fuel tank, also a derivative from the Dawn spacecraft xenon tank, while a hydrazine and helium tank attach to aluminum rings around the exterior of the cylinder with the use of struts. The EDL system attaches to the cylinder top via six five-eighths inch bolts coupling the EDL backshell to channel fittings. The coupling mechanisms between the EDL backshell and the cylinder top are to be adapted for use from the mechanisms used for the Mars Science Laboratory (MSL) mission and are shown in Figure 5.3. The bottom of the cylinder couples to an Atlas V Type B1194 payload adaptor which includes a Marmon-type clampband payload separation system [17] to join the ITV to the Centaur Inertial Upper Stage (IUS).

The six aluminum honeycomb panels serve as mounting points for ITV subsystem equipment and as a convenient means to channel away waste heat. The side panels are approximately 1.65 meters wide by 1.2 meters tall and the top and bottom panels are 1.65 meters wide by 1.65 meters long. The positive and negative y-axis faces of the ITV hold panel-mounted, louvred radiators and passive heatpipes built into the aluminum panels. Additionally, the positive and negative y-axis panel faces provide access for two 6.95 meter diameter Orbital-ATK Ultraflex solar arrays which attach to the central cylinder via one degree of freedom gimbals. The interior facing sides of the y-axis panels are mounting points for four Rockwell Collins

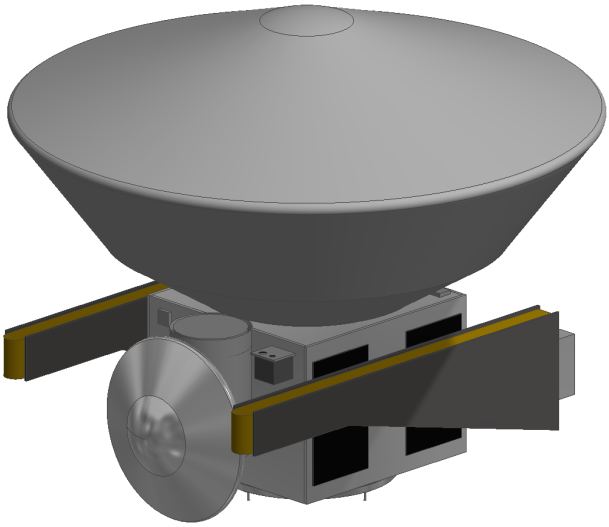

**Figure 5.1:** ITV in its launch configuration with solar panels stowed and the EDL system containing the lander and MAV mounted atop the bus structures. The UltraFlex solar arrays are designed for very compact packing volume

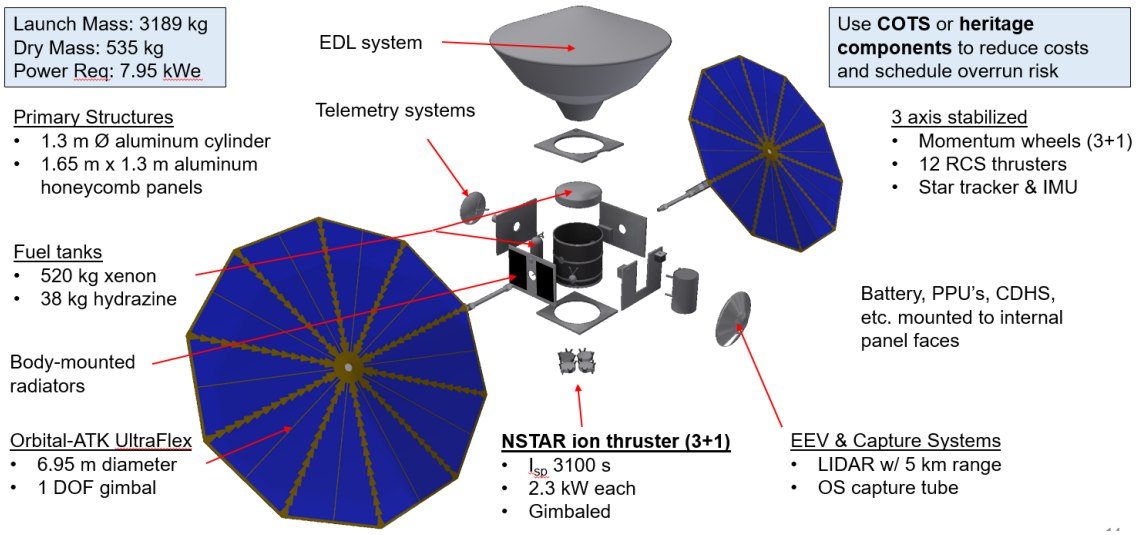


**Figure 5.2:** An exploded view showing the critical components of the ITV. Note the xenon tank stored centrally within the primary cylinder and hydrazine and helium pressurant tanks stored radially. The radiators and solar panels are in the +/- y axis and EEV, sample captures systems and main antennae are in the +/- x axis. The NSTAR thrusters are mounted to the bottom aluminum honeycomb panel right before the interface which will attach to the Atlas V launch vehicle payload adapter.

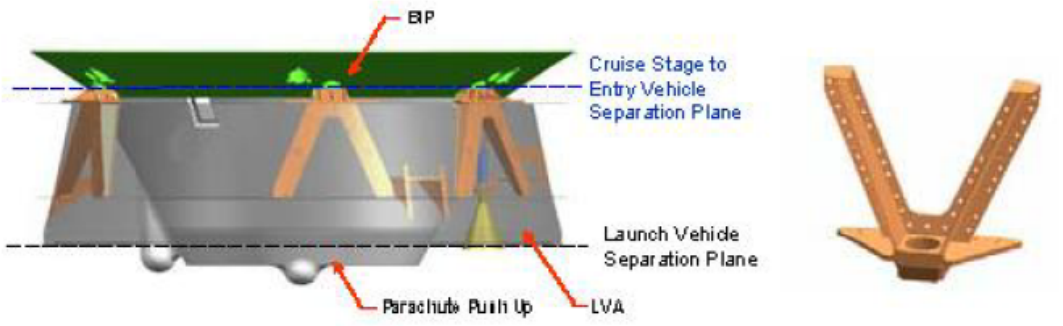


**Figure 5.3:** MSL channel fittings used to link the MSL EDL backshell to the MSL cruise stage. The coupling is achieved through six five-eighths inch bolts. A derivative of these fittings and bolts will be used to join the MSRS EDL backshell and the primary cylinder [16].

reaction wheels and the propulsion subsystem power processing equipment. The exterior of the positive x-axis panel holds a Ball Aerospace CT-602 star tracker and provides access for the 1 meter high gain antenna and mounting points for one of the two low gain antennae. The exterior of the negative x-axis panel is where equipment including a LIDAR sensor, Mars Orbiting Sample Transfer Tube and the EEV is located. The interior of this same panel provides mounting points for the spacecraft battery and C&DHS equipment. The positive z-axis panel houses a Moog coarse sun sensor (three more of which are distributed across the other panel faces) in addition to four 1 N-s thrusters pointing in the positive z-direction for fine translational and attitude control. Lastly, the exterior of the negative z-axis panel is a mounting point for the four gimbaled NSTAR thrusters and eight more RCS thrusters facing in the negative-z and positive and negative x directions.

Table 5.1 shows the ITV mass and power budget at launch from Earth broken down by subsystem. At launch the spacecraft wet mass, including payload, will be approximately 3200 kg of which nearly 560 kg will be fuel. When dry, the ITV itself only masses about 500 kg.

## 5.2 Structures

The critical structures of the ITV bus are derived or adapted from heritage components and include the elements of the primary load path during Earth launch: the channel fittings and bolts linking the EDL backshell to the primary cylinder, the cylinder itself, and the Atlas V Type B1194 payload adaptor. The MSL channel fittings and bolts are already sized for MSL's 3893 kg launch mass which exceeds the anticipated ITV launch mass, and the proposed MSRS will launch in a very similar (though more severe) acceleration environment aboard an Atlas V 541 - the same launch vehicle configuration used by the MSL mission. As the payload adaptor is an off the shell component, structural analysis is only performed to size the primary cylinder in order to ensure the feasibility of mounting the EDL system on top of it.

The most demanding loading case for the primary cylinder is launch. Figure 5.4 from the Atlas V Launch Services User's Guide shows combinations of the maximum expected axial and lateral load factors due to acceleration. The expected axial and lateral vibrational frequencies present in the launch vehicle fairing are 25 Hz and 10 Hz respectively. The primary cylinder

**Table 5.1:** Mass and power budget for the ITV at launch. Note that the payload consists of the EDL vehicle and its contents (the lander and MAV), as well as the EEV and the tube and LIDAR systems required for OS capture. Of particular note is the small propellant mass required by the proposed ITV compared to comparable MSR missions utilizing chemical propulsion systems. Mass and power growth margins have not been explicitly broken out and are instead handled in each subsystem section, though allocated margins are minimal. It is expected that increases in system mass and power requirements will be offset by further reductions in fuel mass required for the trajectories which will result from trajectory optimization. The budget displayed should be considered a current best estimate with small anticipated growth.

| Subsystem | Mass Fraction | Mass (kg) | Power Fraction | Power (kWe) |
|---|---|---|---|---|
| Payload | 0.669 | 2135 | 0.000 | 0.00 |
| Structures | 0.050 | 160 | 0.000 | 0.00 |
| Propulsion | 0.024 | 76 | 0.868 | 6.90 |
| GN&C / ADC | 0.017 | 54 | 0.058 | 0.46 |
| Power | 0.045 | 143 | 0.000 | 0.00 |
| Thermal | 0.009 | 30 | 0.031 | 0.25 |
| C&DH | 0.005 | 15 | 0.006 | 0.05 |
| Telemetry | 0.006 | 19 | 0.036 | 0.29 |
| Dry Spacecraft Total | 0.825 | 2632 | – | – |
| Xenon propellant | 0.163 | 520 | – | – |
| RCS propellant | 0.012 | 38 | – | – |
| Wet Spacecraft Total | 1.000 | 3189 | 1.000 | 7.95 |

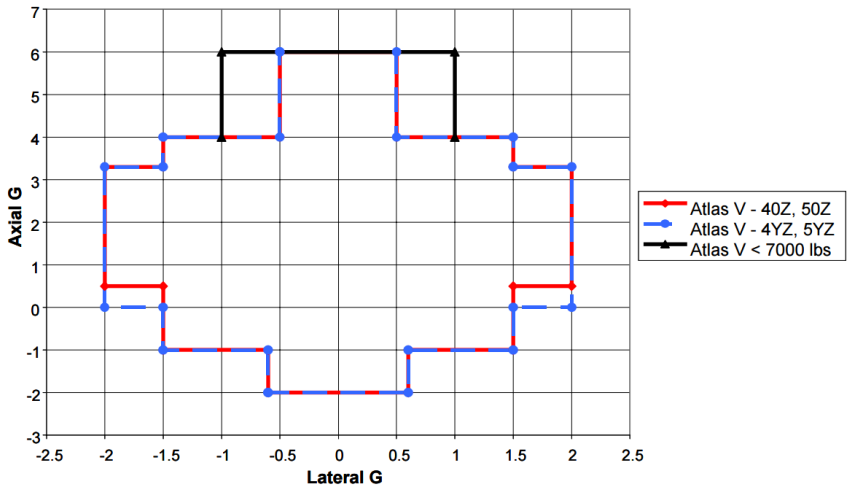


**Figure 5.4:** Atlas V-541 axial and lateral load factors during launch. The MSRS vehicle will weigh nearly 7000 pounds at launch which represents the worst case load factors shown [17].

**Table 5.2:** Results from a primary load-bearing 1.3 meter diameter by 1.3 meter tall cylinder study to ensure that mounting the EDL system on top of the bus was feasible. Results are shown for an Al 7050 cylinder with stresses calculated about the cylinder base just before the launch vehicle adapter interface. Buckling was the limiting case for cylinder wall thickness and the results in the second column correspond to a cylinder with 3.015 mm wall thickness.

| Case | Stress / Frequency (MPa / Hz) | Min. Thickness (mm) |
|---|---|---|
| Axial Stress | 73 | 0.53 |
| Buckling Stress | 91 | **3.015** |
| Axial 1st Mode | 83 | 0.22 |
| Lateral 1st Mode | 52 | 0.09 |

must withstand the combined loading due to the combination of maximum axial and lateral load factors as well as have its first natural frequency in the axial and lateral directions be above 25 Hz and 10 Hz respectively in order to survive the launch sequence. As part of the nearly four year DT&E timeline, primary cylinder testing will occur such that factors of safety of 1.1 to yield strength and 1.25 to ultimate strength or buckling are adopted for structural analysis.

The mass of all the subsystems attached to the bus with the exception of the EDL system and its contents is lumped into a single weight applied at the center of mass of the cylinder. This weight includes a contribution from the cylinder itself, though the final cylinder mass estimate is made iteratively. The center of mass of the EDL system and its contents located above the cylinder top is also considered.The cylinder is then treated as a composite beam experiencing simultaneous axial and lateral loads applied at the center of mass of the cylinder and EDL system. Axial stresses with additional components due to bending are maximum at the cylinder base where the cylinder interfaces with the Atlas V payload adaptor. Cylinder wall thickness is determined by calculating the minimum wall thickness required to meet axial stress requirements, buckling requirements, and first axial and lateral natural frequency requirements. Table 5.2 shows the analysis results. Analysis indicates that a very manageable aluminum cylinder at least 3.015 mm thick and a 1.3 m diameter is sufficient to meet all structural conditions imposed by the launch environment. An aluminum cylinder was used to simplify this feasibility study, but the actual primary cylinder will be a graphite composite derivative from the OSIRIS-Rex or Dawn missions. Primary cylinders from these missions were approximately 1.3 m in diameter. To estimate ITV structural mass including all struts and miscellaneous components, the 160 kg bus mass from OSIRIS-REx is used [18]. This 160 kg estimate is considered a lower bound on structural mass, though no explicit mass margin is accounted for in the ITV mass budget.

## 5.3 Propulsion

After making the decision to use an electric propulsion system as the primary propulsion system for the ITV, an analysis was conducted to determine the optimal thruster specifications. The goal of this analysis was to minimize total mass by optimizing the payload ratio of the ITV. In order to accomplish this, the payload ratio had to be calculated over a range of specific impulse ($I_{sp}$) and burn time. These calculations led to the data shown in 5.5.

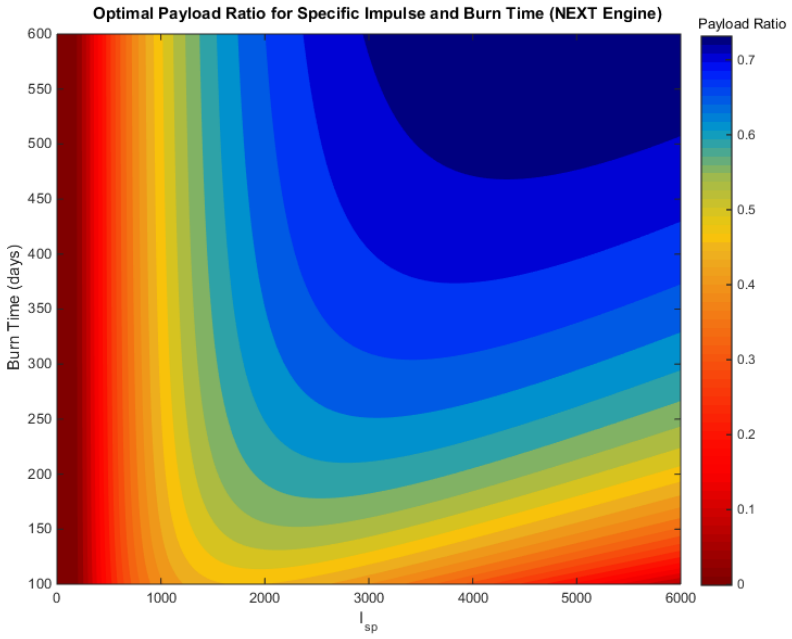


**Figure 5.5:** Optimal payload ratio calculation in relation to burn time and $I_{sp}$.

Because this mission requires the thrusters to burn on both transfers between Earth and Mars, total burn time is such that an $I_{sp}$ of over 3000 s is needed to achieve an optimal payload ratio.

Both ion electric and Hall Effect thrusters were considered for use on the ITV, but ion electric thrusters were revealed to provide a superior payload ratio corresponding with a lower total mass. Hall Effect thrusters provide greater total thrust, but their lower $I_{sp}$ and higher power requirement would necessitate the need for a greater fuel mass and larger power system. This led to the decision to select a configuration of ion thrusters as the primary propulsion system for the ITV, and NSTAR thrusters were selected for this purpose. NSTAR thrusters proved to be optimal for this mission due to their $I_{sp}$ of 3100 s allowing for mass reductions corresponding to the previously calculated optimal payload ratio. Another advantage of these thrusters is that they have a legacy of being used for long range deep space missions in the past, such as Dawn and Deep Space 1. Other heritage thrusters such as NEXT were also analyzed, but NSTAR proved to provide a lower total mass due to a more optimal $I_{sp}$.

The chosen configuration involved using three active NSTAR thrusters with one extra thruster for redundancy. These 8.2 kg, 0.3 m diameter thrusters each provide a thrust output of 92 mN for a total thrust of 276 mN and are gimbaled. Each thruster operates using 2.3 kW of input power, and as previously stated they each have an $I_{sp}$ of 3100 s when operating at max power. A 14.8 kg power processing unit (PPU) is also necessary in order to adjust input power to the necessary voltage level. All mass and power data was obtained from NASA Glenn Research Center. [7]

Table 5.3 shows mass budget of the propulsion system, including fuel mass and all necessary operating equipment. NSTAR thrusters operate using xenon stored in a supercritical state, which allows for a very low fuel mass relative to chemical propulsion and burn times far exceeding that necessary for this mission. Xenon storage requires a 0.9 m diameter tank, the

**Table 5.3:** Mass budget for the propulsion subsystem.

| Component | Mass (kg) |
|---|---|
| 3 + 1 NSTAR Thrusters | 33.3 |
| PPU Assembly | 14.8 |
| DCIU | 2.5 |
| Thruster Cable | 1.0 |
| PPU Cable | 0.8 |
| Xenon Feed System | 1.6 |
| Xenon Storage Tank | 22.2 |
| Xenon Fuel (Outbound) | 502.2 |
| Xenon Fuel (Return) | 121.0 |
| **Total Propulsion Mass** | **699.3** |

dimensions of which have been tested and proven on the Dawn mission. Power for thrusters is provided by two solar panels, explained in the power subsection, and converted into usable energy using the PPU. This analysis has shown that NSTAR thrusters provide the capability and reliability necessary for the mission while greatly reducing cost due to low fuel mass and power requirements.

## 5.4 Electrical Power Subsystem (EPS)

The electrical power subsystem (EPS) consists of power generation capability through the use of two custom sized 6.95 meter diameter Orbital ATK UltraFlex solar arrays and power storage capability through the use of three EaglePicher SAR-10083, 480 W-hr Nickel Hydrogen (NiH2) COTS batteries. Radioisotope thermoelectric generators (RTG) were also considered for power generation capability. However, due to the power requirements of the bus and the three NSTAR thrusters, the mass of an RTG based power generation system would be prohibitive. In addition, due to the mission architecture element of a direct Earth reentry of the sample and burning up the orbiter in Earth's atmosphere, the RTG is not permissible due to the spreading of nuclear material throughout the atmosphere. Other power generation methods, such as nuclear power, are out of the scope of this mission due to their size and ITV power requirements being less than the minimum power needed to realize the benefit of such a large scale power generation system.

When deciding between various types of solar arrays, the UltraFlex stood out because of its advertised savings of one third of the mass and one fourth of the volume of other rigid arrays due to their convenient folding configuration. The UltraFlex panels have flown on many previous missions and can be considered heritage hardware. There is also another version of the UltraFlex called the MegaFlex, however, like with nuclear propulsion, the scale of the system was larger than required by the ITV power generation requirements. The UltraFlex arrays employ 29.5 percent efficient ZTJ solar cells [19]. The limiting

**Table 5.4:** Breakdown of the power needs of the ITV and power generation requirements placed on the two 6.95 meter diameter UltraFlex arrays.

| Subsystem | Total Power Required (W) |
|---|---|
| Propulsion | 6900 |
| AD&CS/GN&CS | 460 |
| C&DHS | 50 |
| Telemetry | 290 |
| TCS | 250 |
| Bus Margin | 160 |
| Total | 8110 |
| With Losses and Battery Charging | 9890 |

case for sizing the two UltraFlex arrays occurs when the ITV is orbiting Mars in a 300 km circular orbit. This case results in eclipse for the largest percentage of any Mars orbit during the mission and also has the shortest period of time during which to charge the NiH2 batteries during each orbital period to maintain normal bus operations. In addition to the battery charging requirement and solar cell degradation losses, a 10 percent margin was added to the power requirements of the bus operations. These additions bring the total power to be generated by the solar array to 9.89 kWe and are reflected in the power budget breakdown shown in Table 5.4. The two UltraFlex arrays are also gimbaled to allow single axis rotation to allow for constant sun pointing to eliminate cosine losses during NSTAR operation at Mars or maintaining a constant sun incidence angle to eliminate waste heat being generated by the arrays when the NSTAR thrusters are not in operation or when the ITV is less than 1.52 AU away from the sun.

The battery has the opposite limiting case as the solar array. The battery requires very large storage capacity, which translates to unreasonably high masses, as the Mars spiral propagates outward from the original 300 km circular orbit. Due to the inclination of the spiral orbit required to begin the interplanetary trajectory back to Earth, the ITV regains full sun exposure at a relatively low orbital altitude of 3077 km, as can be seen in Figure 5.6 where the purple represents time spent in eclipse. However, even using the NSTAR thrusters at this orbital altitude during eclipse would result in a battery mass more than three times that of the battery required only for normal bus operations in eclipse at this circular altitude. Analysis performed in STK showed that shutting the thrusters off during eclipse during the Mars spiral would only add 7 days to the approximately 3 month maneuver and saves more than 100 kg of battery mass. Therefore, only the normal bus power requirements are met with the battery when the ITV is not in full sunlight in Mars orbit.

Power conversion is required for bus and propulsion operations as well. The UltraFlex arrays output power at greater than 100 Volts DC (VDC) [20]. The NSTAR thrusters contain a power processing unit in order to step up the voltage from the UltraFlex arrays to the required NSTAR input voltage and the rest of the components on the bus are converted down from the

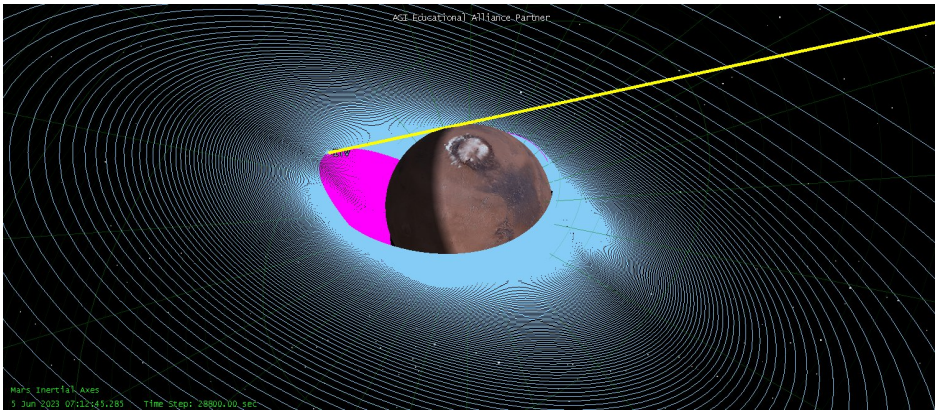


**Figure 5.6:** During the spiral trajectory around Mars to begin the interplanetary trajectory back to Earth, the NSTAR thrusters do not fire in eclipse, shown here in purple, in order to save more than 100 kg of battery mass that would be required for constant thrust through eclipse. The sun vector is shown here explicitly to identify where the spacecraft regains full sun exposure in the spiral trajectory.

**Table 5.5:** Breakdown of the EPS components and their respective masses. [24], [23], [22], [21].

| Component | Total Mass (kg) |
|---|---|
| Custom 6.95 m Diameter Orbital ATK UltraFlex Array x 2 | 102.00 |
| EaglePicher SAR-10083 480 Whr NiH2 Batteries x 3 | 40.14 |
| Vicor Maxi DC DC Converter (Input: 150 VDC, Output: 28 VDC, 500 W) | 0.26 |
| Vicor Maxi DC DC Converter (Input: 150 VDC, Output: 28 VDC, 400 W) x 2 | 0.52 |
| Vicor Mini DC DC Converter (Input: 28 VDC, Output: 3.3 VDC, 75 W) | 0.12 |
| EPS Total | 143.03 |

UltraFlex output voltage to the standard 28 VDC of the bus using Vicor power converters of various sizes. The components requiring 3.3 VDC will receive that voltage through a mini version of the Vicor converters, taking in 28 VDC of converted voltage and outputting 3.3 VDC [21]. The efficiency of the power converters of up to 90 percent is accounted for in the sizing of the solar array with an expected additional 5 percent average reduction in optimal operation [22]. The battery nominally outputs 28 VDC so the only conversion required off battery output is for the lower voltage systems requiring 3.3 VDC [23]. The overall EPS mass breakdown, including power generation, storage, and conversion is shown in Table 5.5.

## 5.5 Thermal Control Subsystem (TCS)

The ITV TCS consists of the following primary components: multi-layer insulation with aluminized silicone oxide coated external surfaces, body-mounted louvered radiators supported by passive heat pipes, and Kapton patch heaters. The multi-layer insulation is approximately 10 layers deep and applied to all bus structure surfaces with the exception of the panels with the radiators in the +/- y axes. The optical absorptivity $\alpha_{solar}$ of the coated MLI was taken as 0.09 and the infrared emissivity

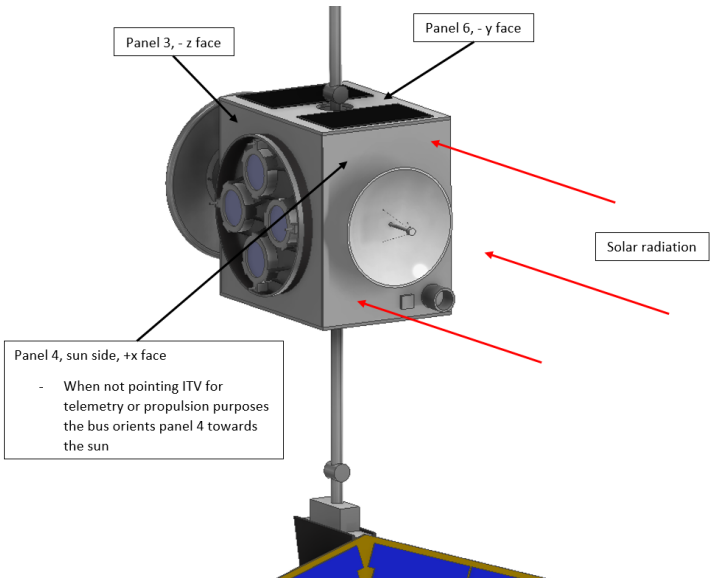


**Figure 5.7:** Illustrations of the attitude the ITV will hold during holding periods in LMO and in solar orbit. The radiator panels on the +/- y faces must be kept normal to the sun and surfaces tuned to act as sun shields with low optical absorptivity and high infrared emissivity pointed towards the sun.

$\epsilon_{IR}$ was taken as 0.15 for all panels except the radiators. The radiators have $\epsilon_{IR}$ of 0.88 [25]. In total, about 3.15 $m^2$ of radiator area is required - these radiators are attached directly onto their respective aluminum honeycomb panels which house passive heat pipes to transfer heat from neighboring panels. Three axis control will be required to point the +/- y axes normal to the direction of direct solar radiation whenever the thrusters are firing at full throttle to prevent ITV overheating. Actively controlled patch heaters with a specific power of 0.8 W / $cm^2$ are distributed across sensitive components including the battery, fuel tanks, and fuel lines. Altogether, about 300 $cm^2$ of patch heater area is used with a combined maximum power output not exceeding 250 W. Figure 5.7 illustrates the TCS required three axis controlled ITV attitude during key stages of the mission.

ITV TCS analysis and component sizing centered on approximating the vehicle as a rectangular prism of dimension equal to the external dimensions given by the ITV aluminum honeycomb panels. Note that the EDL vehicle is mostly a self-contained system and additional EDL vehicle thermal requirements were not considered for this TCS model. The normal directions of the model's six external surfaces were specified and used determine view factors and incidence angles to sources of environmental radiation as a function of time. Note that, since the ITV is three axis stabilized, the spacecraft orientation with respect to the incident solar radiation is fixed for each analysis period. An explicit finite difference code then calculated the temperature of each panel in time as a result of internal and external heat fluxes beginning with pre-specified panel initial temperatures. Equation 5.1 shows the finite difference model used to propagate spacecraft panel temperatures.

$$T_{i+1} = T_i + \frac{\Delta t}{C}\left(Q_{PanelConduction} + Q_{NetRadiation} + Q_{Waste} + Q_{Heater}\right) \tag{5.1}$$

The ITV operates within two thermal regimes for the majority of the mission timeline. The first regime encompasses long

**Table 5.6:** The worst case hot and worst case cold test cases the ITV TCS will need to handle including time in transfer orbits around the Sun and a 300 km parking orbit about Mars. Efficiency loss for calculating propulsion waste heat was taken as fifteen percent for high power modes. All power required for the bus was considered waste heat for high power modes. For low power modes the thrusters are assumed off while CDHS and AD&CS and GN&C are operating in lower power states producing 260 W combined. Assumptions were made that the solar panels could be re-oriented by their gimbals and the bus momentum wheels to ensure only as much power as the bus requires is generated. Waste heat loads were distributed across each panel with the majority loading being transferred via heat pipes to panels 5 and 6 with the radiators.

| Case | Regime | Mode | Propulsion Waste Heat (kW) | Bus Waste Heat (kW) |
|---|---|---|---|---|
| Hot | 1 AU solar | High | 1.04 | 1.05 |
| Hot | 300 km LMO | High | 1.04 | 1.05 |
| Cold | 1.5 AU solar | Low | 0.00 | 0.26 |
| Cold | 300 km LMO | Low | 0.00 | 0.26 |

periods spent in orbit about the sun either transferring to Mars or returning to Earth. The second regime is, nominally, a 300 km altitude, nearly circular low Mars orbit (LMO) in a plane inclined about 25 degrees with respect to Mars' equatorial plane. The external radiation fluxes incident upon the ITV in these two regimes differ considerably. For TCS analysis in solar orbit, the external radiation fluxes considered included only direct sunlight and power radiated to space from the ITV. For TCS analysis in LMO, the external radiation fluxes considered included direct sunlight, sunlight reflected off Mars due to Mars' albedo, infrared radiation emitted by Mars, and power radiated to space out of the ITV. The same sources of internal heat generation were used for both solar orbit and LMO and included waste heat from electronics used for C&DHS, telemetry, and the momentum wheels. Additionally, waste heat resulting from inefficiencies in power conversion from the solar panel output to the input of the three firing NSTAR thrusters (15 percent) was considered for all TCS analyses. Conduction between spacecraft surfaces and analysis of cases with the ITV in low-power mode (thrusters not firing and only essential electronics operating) and high-power mode (thrusters firing and all essential electronics at peak operation) was also considered. Based on external radiation fluxes and ITV power modes, the worst hot environment is expected to occur in solar orbit in a 1 AU orbit with the ITV in high-power mode, and the worst cold environment is expected to occur in a 1.5 AU solar orbit with the ITV in low-power mode. Design of the TCS involved tuning spacecraft orientation, surface optical and infrared absorptivity, and emissivity properties as well as sizing radiators and patch heaters such that the ITV remained functional during both worst case hot and worst case cold environments. Table 5.6 summarizes the analysis cases and relevant important parameters.

Temperature requirements which the ITV must not exceed in order to remain operational are shown in Table 5.7. Based on the placement of ITV subsystem components, these temperature requirements were imposed upon the appropriate panels in the TCS model.

Figure 5.8 shows the estimated transient and steady-state ITV panel temperatures for the worst hot case and worst cold cases after panel properties were tuned to approximate the aforementioned MLI layers, louvered radiators with passive heat pipes, and the dispersed patch heaters. TCS model analysis was propagated long enough for each case to ensure steady-state temperatures were reached. Figure 5.8 shows that the required temperature bounds are achieved for each panel with the

**Table 5.7:** The temperature requirements for nodal panels in the TCS thermal model based on limiting temperature requirements of subsystem components assigned to the node. Note that grouping of subsystems to panels is approximated based on relative subsystem proximity to each panel.

| Components | Min. Temp (C) | Max. Temp (C) | Panel |
|---|---|---|---|
| Thrusters, propellant plumbing | 7 | 55 | 1 |
| OS captures systems, star tracker | 0 | 40 | 2 |
| NiH2 Battery, CDHS | -5 | 20 | 3 |
| Antennae | -95 | 70 | 4 |
| Radiators | -95 | 60 | 5,6 |

specified TCS. As a point of comparison, the Dawn spacecraft required approximately 200 W of heating at a much greater distance of 3 AU which suggests the TCS heater power requirements of 250 W are quite conservative, though the need to cold bias the ITV in order to prevent overheating in 1 AU solar orbit explains the comparatively large power draw estimate [26].

Detailed TCS analysis was required in order to ensure the high ITV power draw due to the NSTAR thrusters would not lead to significant ITV design challenges. Estimates from thermal analysis show that conventional spacecraft TCS systems are sufficient to meet TCS requirements. As a result, an empirically derived 4.5 percent of ITV dry mass is budgeted to account for the mass of all TCS components [27]. While no explicit margin is given for TCS mass growth or TCS power requirements, the power requirements (which will impact ITV mass through power system sizing) are conservative.

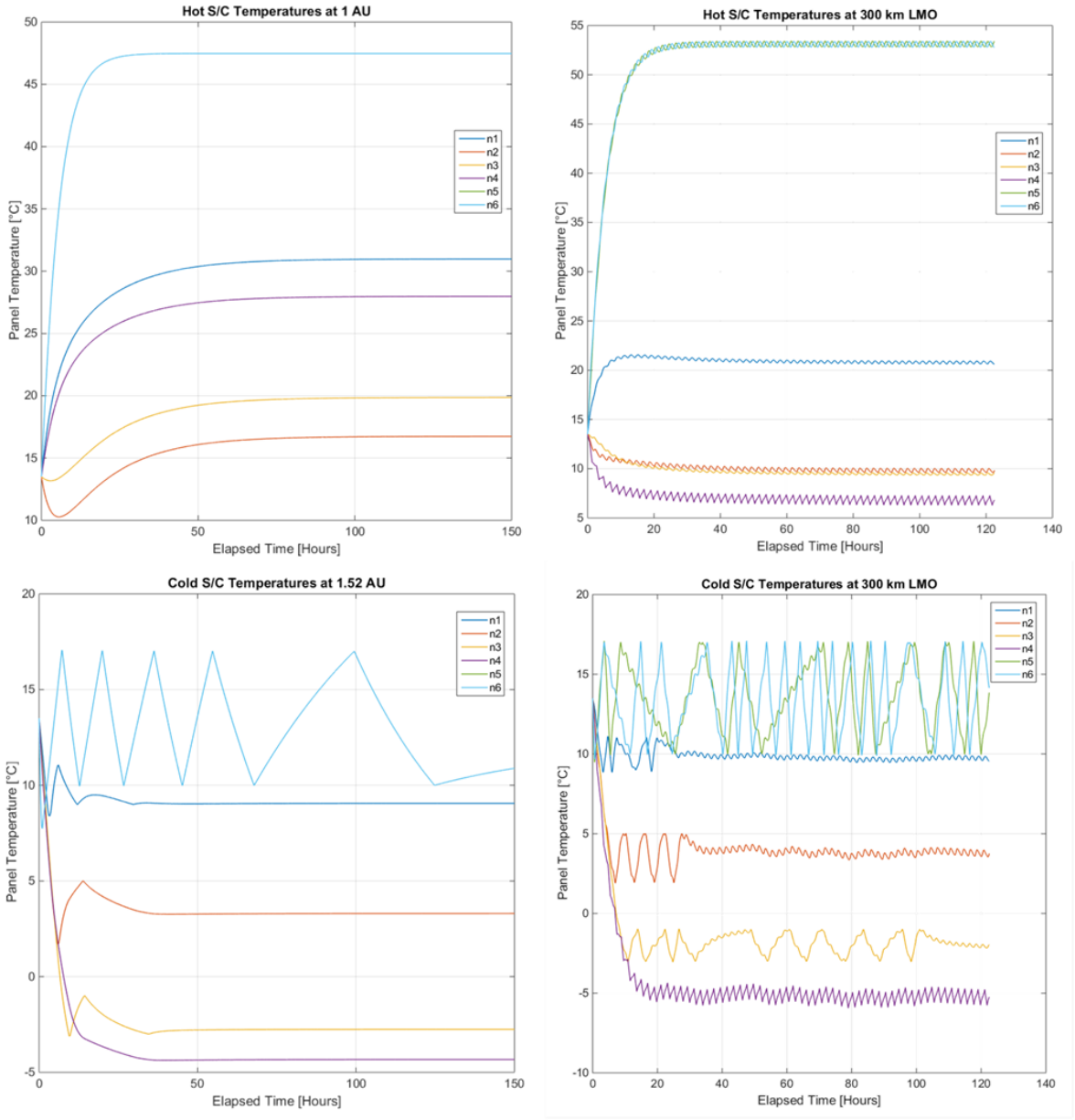


**Figure 5.8:** TCS performance in worst case hot and worst case cold thermal regimes in both 1 AU and 1.5 AU solar orbit and in 300 km LMO.

## 5.6 Attitude Determination and Control and Guidance, Navigation, and Control Subsystems (AD&CS / GN&CS)

The attitude determination and control subsystem (AD&CS) includes the sensor suite to determine the spacecraft attitude as well as the control mechanisms required for spacecraft attitude adjustments throughout the mission. The sensor suite includes a Ball CT-602 star tracker, a Honeywell Miniature Inertial Measurement Unit (MIMU), and four Moog coarse sun sensors. The CT-602 star tracker has an attitude accuracy of 3 arcseconds at the beginning of life (BOL) and 10 arcseconds for angular

rate accuracy at the end of life (EOL) [28]. The most critical use case for the attitude knowledge is the rendezvous of the ITV with the orbiting sample and is satisfied with a 6 arcsecond star tracker as defined by JPL's orbiter concept [10]. Given the mission length of comparable star trackers [29] and assuming constant degradation, the CT-602 tracker will have at least 5.3 arcseconds of angular rate accuracy during the ITV-OS rendezvous maneuver in March 2023. Following that maneuver, the accuracy degradation is no longer of concern as the attitude knowledge requirements can easily be met with the CT-602 EOL performance [10]. The Honeywell MIMU provides redundant attitude knowledge in the case of momentary or briefly extended star tracker loss. The drift in the MIMU is 0.005 degrees per hour and cannot be depended on for accurate attitude knowledge for long periods of time, but is satisfactory for the most common star tracker errors [30]. The Moog sun sensors are present for solar array pointing and emergency mode operations.

The control aspect of the AD&CS includes 12 Aerojet MR-103D 1 Newton minimum impulse thrusters (MIT) and four Rockwell Collins RSI 45-75/60 reaction wheels. The 12, 1 Newton thrusters are arranged to give full three axis control of the spacecraft as well as provide uniform directional thrust in the +/- Z spacecraft axes for the ITV-OS rendezvous. These thrusters are powered by hydrazine in a pressure fed system resized from the internal pressure and hoop stress characteristics of a spherical Airbus 58 Liter bladder tank. The four reaction wheels provide momentum control for the spacecraft in all three rotation axes and one additional wheel is present for redundancy. The reaction wheels were selected based on their suggested spacecraft mass pairing in line with the ITV BOL mass of 3000 kg [31].

The guidance, navigation, and control subsystem (GN&CS) navigates and controls the position of the spacecraft. The guidance and navigation portions of the mission will be achieved through the use of traditional ground tracking methods. With respect to control, the GN&CS simply overlaps the AD&CS's hardware with the 12 thrusters and the pressure fed hydrazine fuel system. The GN&CS generally includes course corrections, station keeping, and any rendezvous procedures, however, due to the use of low thrust throughout interplanetary travel and Mars and Earth approaches, the three NSTAR thrusters will be responsible for planned course corrections and the majority of the spacecraft positioning for the rendezvous procedure. However, the benefits of impulsive thrust cannot be overlooked for station keeping in low Mars orbit, the final precise maneuvers of the ITV-OS rendezvous, and any emergency maneuvers that may be required that are beyond the capability of the constant thrust NSTAR system. These three situations are where the 1 Newton thrusters will be used for the GN&CS in this mission.

Once again, the limiting case of sizing the thrusters comes down to the ITV-OS rendezvous, where the agility requirements are listed as 6.2 arcseconds per second based on the JPL orbiter concept [10]. This requirement drove the selection of the Aerojet MIT configuration. The amount of fuel required for one possible minimum rendezvous maneuver was calculated to be 0.6 m/s for an 80 minute time to intercept once the relative distance between the OS and ITV is 5 km at time equal to zero. The selection of 5 km is due to the range of the LIDAR system used to locate the OS. Rendezvous analysis combined with the estimation that the station keeping requirements for a low Mars orbit of 300 km will be 50 m/s/year and an extra ten percent of reserve $\Delta V$ capability for growth allowance, leads to a total Hydrazine mass of 37.51 kg [32]. This hydrazine mass was calculated using the ideal rocket equation with the Aerojet MIT specific impulse of 221 seconds [33]. The overall AD&CS

**Table 5.8:** Breakdown of the AD&CS and GN&CS components and their respective masses and power requirements. [28], [30], [34], [33], [31], [35], [36]

| Component | Total Mass (kg) | Total Max Power Draw (W) |
|---|---|---|
| Attitude Determination Sensors | | |
| Ball Aerospace CT-602 Star Tracker | 5.49 | 10 |
| Honeywell Miniature IMU | 4.70 | 30 |
| Moog Coarse Sun Sensor x 4 | 0.86 | 0 |
| Attitude / Navigation Control Mechanisms | | |
| Aerojet MR-103D 1N Rocket Engine Assembly x 12 | 1.92 | 130 |
| Rockwell Collins RSI 45-75/60 Reaction Wheels x 4 | 30.80 | 290 |
| Hydrazine Fuel | 37.51 | 0 |
| Hydrazine Fuel Tank | 7.50 | 0 |
| Pressurant (He) | 0.26 | 0 |
| Pressurant Tank | 2.60 | 0 |
| AD&CS / GN&CS Total | 91.64 | 460 |

**Table 5.9:** Breakdown of the C&DHS components and their respective masses and power requirements. [39], [40]

| Component | Total Mass (kg) | Total Max Power Draw (W) |
|---|---|---|
| BAE RAD750 | 0.01 | 5 |
| Airbus 512 Gbit Solid State Recorder | 15 | 45 |
| C&DHS Total | 15.01 | 50 |

and GN&CS mass and power budget for the ITV is shown in Table 5.8.

## 5.7 Command and Data Handling Subsystem (C&DHS)

The command and data handling subsystem (C&DHS) is comprised of a processing unit and solid state recorder (SSR) for storing data that has been received and that is to be transmitted by the spacecraft. The BAE RAD750 processor is identical to the hardware on many previous Mars missions such as Mars Reconnaissance Orbiter and the SSR is a base level recorder [37]. The processor has a lifespan greater than that of the MSRS mission duration, as indicated by its successful operation on MRO for greater than five years [38]. The mass and power budget for the C&DHS can be found in Table 5.9.

**Table 5.10:** Breakdown of the TT&CS components and their respective masses and power requirements. [41], [43]

| Component | Total Mass (kg) | Total Max Power Draw (W) |
|---|---|---|
| 0.3 m Diameter Medium Gain Antenna | 5.00 | 0 |
| Low Gain Omnidirectional Antenna x 2 | 5.00 | 0 |
| Bosch Travelling Wave Tube Amplifier x 2 | 2.20 | 275 |
| General Dynamics Small Deep-Space Transponder x 2 | 6.40 | 15 |
| TT&CS Total | 18.60 | 290 |

## 5.8 Telemetry, Tracking and Command Subsystem (TT&CS)

The telemetry, tracking, and command subsystem (TT&CS) includes the communication system for the spacecraft and ground stations on Earth to transmit and receive signals from one another. All communication to and from Earth for the ITV will go through NASA's Deep Space Network. The ITV TT&CS will also be capable of communicating with the MAV and will serve as a relay for the MAV to communicate with the Deep Space Network on Earth. The signals received by the ITV will be for spacecraft mode toggling, system software updates, and course correction and maneuver specifications. The signals transmitted by the ITV will be system health monitoring, milestone confirmation, and rendezvous verification. Because data transmission is not the purpose of the mission as it is with the majority of spacecraft missions, only X-band communication was selected and data rates on the order of the Mars Science Laboratory cruise stage communication system are acceptable. The spacecraft will transmit and receive signals in the X-band frequency using a General Dynamics Small Deep-Space Transponder (SDST). There is a second SDST on board for redundancy. For sending X-band signals, a Bosch Travelling Wave Tube Amplifier (TWTA) will provide 100 Watts of power to the high and low gain antennas when required [41]. There is also a second TWTA on board for redundancy with a power margin associated with it. Data rates for receiving information will be on par with the Mars Science Laboratory cruise stage communication system, which bottoms out at 0.5 kbits/second uplink rate and 7 kbits/second downlink rate at Mars using a 30 cm medium gain antenna [42]. The mass and power budget for the TT&CS can be found in Table 5.10.

## 5.9 On-Orbit Sample Capture System

Located on the positive x-face of the ITV bus are the two components used in the sample capture system. These components are referred to as the sample capture device and the Next Generation Advanced Video Guidance Sensor (NGAVGS).

There is no heritage system for the system that is the sample capture device. However, a JPL orbiter concept study has proven their basket sample capture to be a TRL of 5 [44]. Using the technology they display, the sample capture device was modified to suit the design of the mission better. The sample capture device is 0.65m in height and 0.6m in diameter. This cylindrical tube contains a cone that is 0.13m in depth from the top of the cylinder where the 0.55m lid is located. Within the

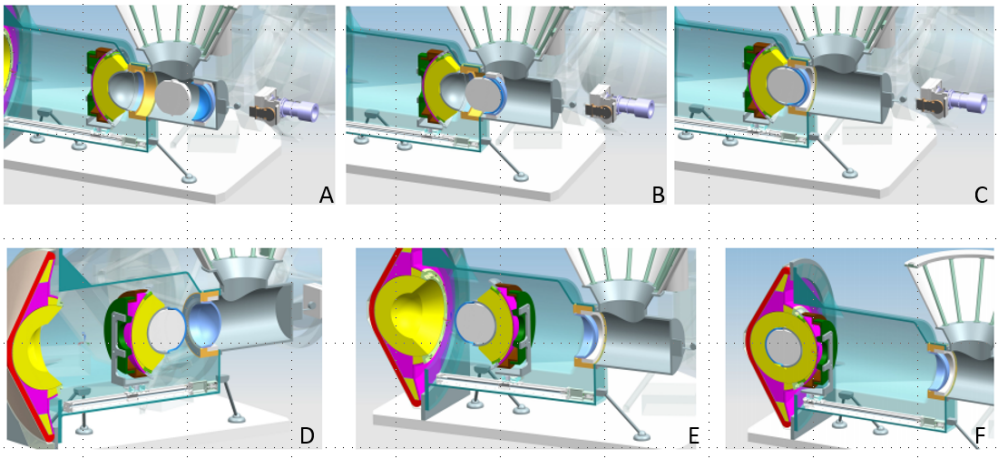


**Figure 5.9:** Above is a different design that shares the core concept of our sample capture device[46]. For this design the orbiting sample enters the cone where it will then travel down to enter the first part of the sample capture device. It will then be enclosed within the top part of the EEV. Once encapsulated it will rotate 180 degrees about the x-axis so that the orbiting sample is facing the EEV. The device will then re-insert the orbiting sample and the top of the EEV into the main body.

cylinder is a device which holds the lid section of the EEV. This device is gimbaled allowing for a 90 degree rotation and has rectilinear motion in the x and y-axis.

The LIDAR system that will be used to perform the maneuver is the NGAVGS. This system is a legacy system used on DARPA's Orbital Express mission and it has a TRL of 9. All of the equipment and software needed for it to work are placed inside a box with the dimensions of 17.78 x 19.05 x 30.48 cm and weighs approximately 8 kg [45]. In addition the LiDAR consumes 20 W in standby mode and when in tracking operations it consumes less than 30 W [45]. The NGAVGS functions in a fashion similar to the legacy system Advanced Video Guidance Sensor. Using image subtraction and manipulation the NGAVGS is able to compute the relative position vector at a maximum range of 5 km and relative attitude information for rendezvous [45].

The rendezvous maneuver begins once the orbiter has located the orbiting sample within the five kilometer range. Two pictures will then be taken sequentially of the orbiting sample illuminated by different wavelengths of laser light. Once the pictures have been completely rendered it will then subtract one picture from the other and create spots from the lit pixel image data [45]. Once the spots have matched the known target geometry, it will then compute the relative position vector and relative attitude to arrive at the target [45].

Once the orbiter is within range of the orbiting sample, it will align itself with the sample capture device and the orbiting sample. Once aligned the orbiter will then approach the orbiting sample and attempt to catch the sample within its capture device. Once the sample has been placed within the device the lid will then begin to close pushing the sample within the device. Once the sample is completely within the device holding the upper section of the EEV with the sample, will rotate 90 degrees and push the sample into the main body of the EEV. Once the upper section of the EEV is connected to the main body, the clamps within will clasp together and seal the EEV.

## 5.10 Earth Entry Vehicle

The EEV model that was selected for use was the NASA chuteless design similar to the EEV in the Stardust mission and the concept design used in the Galahad mission. The EEV designed for the Stardust mission is 0.811 meters in diameter and the forebody heat shield is comprised of phenolic impregnated carbon ablator (PICA) [47]. However unlike the Galahad concept and the EEV design used for this mission, the Stardust EEV contains a parachute that is deployed once it reaches an altitude of 3 km [48]. The Galahad mission uses a chuteless design very similar to the proposed MSRS system. The EEV will use a large number of heritage systems from Stardust and other missions. For the 1.12 meter forebody heat shield it will utilize the same unipiece PICA, the aft body thermal protection system (TPS) will use Acusil II, a heritage system from MSL, and the impact foam will be ROHACELL 200 WF [49]. Through tests that were conducted at NASA Langley, the impact sphere was thoroughly verified and analyzed, resulting in a TRL of 8 for the system [52].

The conceptual design for the proposed MSRS EEV was created using an analysis of past and proposed sample return vehicles. The EEV has an asymmetrical body with a diameter of 1.3 meters and the outer mold line (OML) is a 60 degree sphere-cone with the spherical nose designed to control the maximum stagnation heat rate and provide hypersonic re-orientation capability. The properties of this geometry mean that if there were entry attitude failures, the EEV has the capability to re-orient itself even spin stabilized 180 degrees backwards or tumbling [50]. The heatshield will be comprised of fully dense Carbon Phenolic (CP), while the concave back shell will be comprised of Acusil II [50]. In addition, the interior of the EEV will be comprised of aluminum 2024 honeycomb and an impact sphere that will surround the orbiting sample container [51]. This impact sphere will be comprised of energy-absorbing material (Kevlar/Graphite composite cell walls filled with low density carbon foam) [52]. Lastly, a spin-ring will placed on the back shell surrounding the impact sphere.

The EEV will be bolted onto the sample capture device with four mounting bolts secured in place with four pyrotechnic nuts. Attached upon the mounting bolts will be several springs that will be held in compression for most of the duration of this mission. Before the rendezvous maneuver, a part of the top of the EEV will be detached from the main body and will be shut and sealed once the orbiting sample is within the main body. To seal the top of the EEV, clamps will be placed within the main body and will clasp and interlock the top once it has been reconnected. Once the orbiter has arrived at Earth, the pyrotechnic nuts will be detonated and the springs that were held in compression will push the EEV away from the orbiter. While this is occurring, the spin-ring located upon the body of the EEV will begin to spin stabilize and separate from the EEV once spin stabilization has been achieved.

By performing course corrections, it is possible to achieve an incoming flight path angle of 14 degrees below the horizontal at the atmospheric interface and an entry velocity of 11.5 km/s. The EEV will then crash land at the UTTR and because the likelihood of hitting a sharp rock or one of the many gravel roads that cross the UTTR is not negligible, additional impact protection is needed. Thus, the EEV has an impact sphere incorporated [52]. The impact sphere mitigates this risk by buckling and deforming on impact, reducing the deceleration of the samples below the containment-assurance level of 3500 g's as the sphere crushes [52]. Lastly, using a separate beacon, the samples will be retrieved at the UTTR.

# 6 Mars Entry Descent and Landing

## 6.1 Introduction

The EDL mission segment will begin with detachment from the ITV prior to the ITV entering its highly elliptical orbit. The EDL system serves the crucial purpose of transporting the lander and its science payload safely to the Martian surface. Mars EDL has been completed successfully seven times in the past by NASA missions. However, the Mars Sample Return mission presents new challenges to the EDL system through its connection to the sample capture rover and its guiding requirement of 5 km landing accuracy. Table 6.1 shows a summary of past missions with the MSR mission requirements in the last row.

Examining this table, it becomes evident that both landing accuracy and useful landed mass are increasing over time. Additionally, depending on the chosen site for the MSR mission, it is possible that landing altitude will increase beyond what has been achieved previously. This suggests that the MSR mission will require new capability beyond what has been previously developed.

## 6.2 Landing Challenges

### 6.2.1 Landing Altitude

To date, the United States has had seven successful landings of robotic systems to the Martian surface. Previously landed missions can be grouped in the fact that they have all landed at sites below -1.4 km MOLA [53]. In past missions, this barrier of -1.4 km has been a function of the atmospheric density required by EDL systems to perform their functions [53]. This is significant due to the team's decision to use locations identified by the Mars 2020 Landing Site Steering Committee. The locations called out by the Site Steering Committee can be seen in Table 6.2. In their open letter, the committee identifies one potential location will be above the altitude of -1.4 km MOLA, Nili Fossae Trough.[54] The Nili Fossae Trough North is at an altitude of about -0.5 km MOLA, and would not be accessible with the EDL method used for the Mars Science Laboratory

**Table 6.1:** Examining Pathfinder, Spirit and Opportunity, and Curiosity a trend towards more massive payloads and greater landing accuracy can be seen. This will continue with the 5 km landing accuracy requirement for MSR.

| | Landing Ellipse major, minor axes (km) | Landing Altitude (km) | Entry Mass (kg) | Useful Landed Mass (kg) |
|---|---|---|---|---|
| Pathfinder (1997) | 200, 100 | -2.5 | 584 | 92 |
| Spirit & Opportunity (2004) | 80, 12 | -1.4, -1.9 | 830 | 173 |
| Curiosity (2012) | 20, 7 | -4.4 | 3380 | 899 |
| Mars Sample Return (2022) | 5, 5 | -4.5/ -0.5 | 2300 | 700 |

**Table 6.2:** The sites listed were used to establish bounding cases for EDL. At -500 m Nili Fossae Trough is higher than any past missions have landed [54].

| Landing Location | Altitude (m) |
|---|---|
| Gusev Crater | -1500 |
| Eberswalde Crater | -3000 |
| Holden Crater | -3000 |
| Jezero Crater | -3000 |
| Mawrth Vallis | -2000 |
| NE Syrtis Major | -3000 |
| N Nili Fossae Trough | -500 |
| SW Melas Basin | -4500 |

at the accuracy required by the RFP [54]. As identified in our constraints, successful completion of the MSR mission requires landing within a 5 km radius of the rover.

### 6.2.2 Mars Atmosphere

The driving factor for the difficulty of landing at higher altitudes is the Martian atmosphere. The Martian atmosphere is approximately one percent as dense as the atmosphere that exists on Earth [53]. At this density, the atmosphere has the detriment of spacecraft heating without the benefit of significant speed reduction early in the re-entry trajectory. This has the effect of reducing time for EDL events and adds difficulty to the problem of decelerating from hypersonic entry speed to non-damaging subsonic landing speed. Two ballistic re-entry trajectories can be seen in Figure 6.1, where one trajectory is an Earth entry, and the other is a Mars entry. Note that the Mars trajectory begins decelerating at a much lower altitude. Despite significant differences in size and mass between Earth and Mars, the greatest differentiator between Earth and Mars EDL is the slight Martian atmosphere [53].

## 6.3 EDL Trades

### 6.3.1 EDL Trades Introduction

During the preliminary research for the EDL system, one key decision point emerged that guided the design going forward. This decision point was whether to develop a new EDL system around an inflatable aerodynamic decelerator, or to augment a previous system in order to improve landing accuracy. With a required useful landed mass of 700 kg, approximately 200 kg less than Mars Science Laboratory, this opened the design space to make both options feasible for consideration. More detail supported the approximation of 700 kg is given in the section “Mars Systems”. This useful landed mass also had the effect of ruling out supersonic retro propulsion systems such as the “Red Dragon” concept. The Red Dragon which was considered in

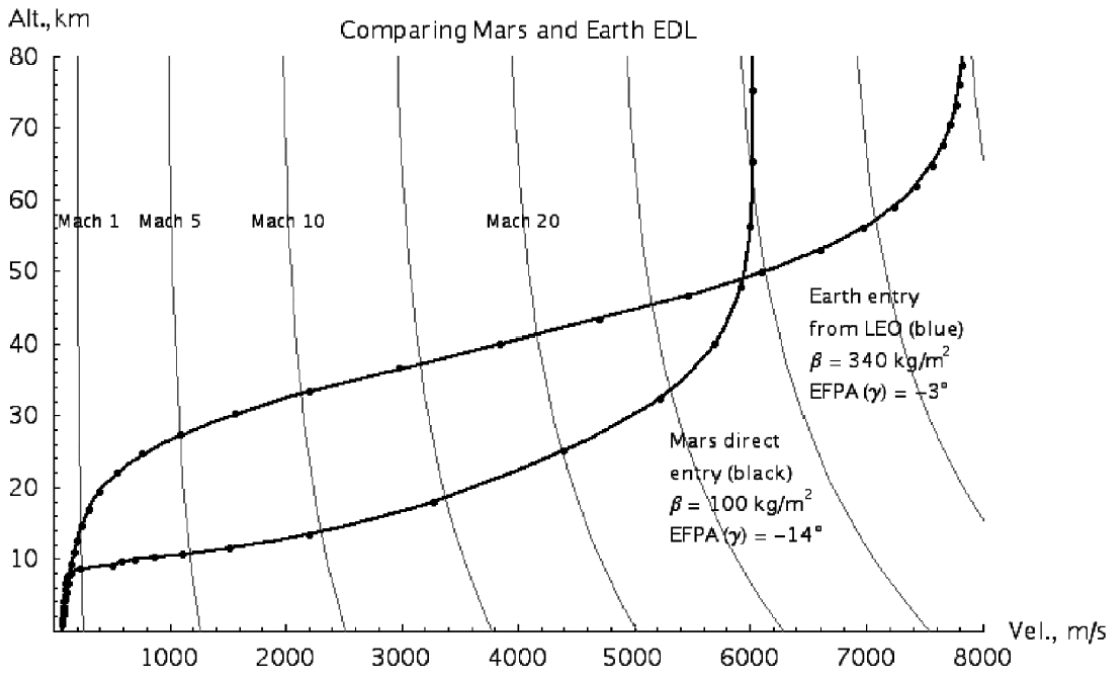


**Figure 6.1:** Altitude-velocity comparison of a typical ballistic EDL at Earth and Mars[53]

the preliminary design phase would require significantly greater launch costs to send a 7-10 mt landing system with potential for 2 mt useful landed mass. Where our useful landed mass is only 35 percent of the Red Dragon capability, the system was thought to be infeasible [55].

### 6.3.2 Inflatable Aerodynamic Decelerators

Looking first at the inflatable aerodynamic decelerators, the benefit was quickly apparent. In the paper entitled "Entry, Descent, and Landing for Human Mars Missions" NASA Langley Entry, Descent and Landing Principal Investigator for the Space Technology Mission Directorate, Michelle Munk estimates the benefit resulting from hypersonic inflatable aerodynamic decelerator (HIAD) can be quantified as a mass savings of 20 percent compared to rigid vehicles [56]. Evidence of the prominence of IAD's as emerging technologies can be seen in the 2015 NASA Technology Roadmaps Entry, Descent, and Landing Publication. In the 2015 roadmaps, deployable hypersonic decelerators are listed as an enhancing technology for several missions in the 2026 timeframe and as an enabling technology for the Crewed Mars Surface Mission [57]. Further evidence of investment in IAD technology can be seen through the 2012 Inflatable Reentry Vehicle Experiment 3 (IRVE-3) test program and the ground-based testing in National Full-Scale Aerodynamic Complex (NFAC) of 6 meter inflatable structure [57].

However, despite recent advancements there has been no demonstration of flight-relevant-scale deployable hypersonic decelerators to date. According the NASA's Technology Roadmaps, "Major technical challenges include scalability, reliable deployment, aeroelastic and aerothermal effects advanced guidance algorithms ... and aerodynamic stability and controllability

**Table 6.3:** The components identified represent key components needed to achieve a landing accuracy of 100 m. Maximum use of heritage components is desired to minimize cost.[58]

| System Components | Heritage | Comments |
|---|---|---|
| Entry Guidance | MSL, Apollo | Bank-only control |
| Mach 2 Parachute | Viking | Non-steerable |
| IMU | MSL | |
| Radar Altimeter / Velocimeter | MSL | |
| Descent Imager | New | Need faster frame xfer than MER DIMES |
| Image Processing Algorithms | New | Match detected features to stored onboard map |
| Onboard Nav Filter Algorithm | New | Process IMU, radar alt / vel, and imaging data types |
| Powered Descent Guidance | New | delta V- optimal or nearly so |

of large deployable or flexible structures" [57]. Finally, it should be noted that while IAD's have advantages for reduced heating and g loads for all size payloads, they are considered to be of particular relevance to missions with large-mass payloads such as future crewed missions [57]. With a smaller useful landed mass than Mars Science laboratory, MSR is not in the category of large-mass payloads.

### 6.3.3 Augmenting Past Landing Architecture

Alternatively, looking at the other side of the trade, researchers working with JPL have proposed system advancements that will allow pinpoint landing architectures with minimal technology development. Improvement of the system lies within reducing uncertainty at strategic points in the EDL process. Currently, the main sources landing error come from uncertainty in navigating the spacecraft to a desired entry point, uncertainty in the Mars atmosphere model, uncertainty in the ability to measure vehicle aerodynamic coefficients, map-tie error, and wind drift [58]. In "Performance Trades for Mars Pinpoint Landing," Dr. Aron Wolf and team outline a reference system architecture capable of achieving a pinpoint landing on Mars with a useful landed mass of 725 kg [58]. At the ITV mass estimate of 700 kg, this reference architecture is a good fit to deliver the system. The reference system design leverages heritage flight technologies wherever possible in order to minimize development cost. The breakdown of this system can be seen in Table 6.3. Note that within the table, technologies are used from the MSL mission as well as from older missions as part of the Viking and Apollo programs. While this cost savings is a benefit to our mission, there are also additional risks anticipated due to added difficulty of integrating high TRL items.

**Table 6.4:** Masses are given for the entry and powered descent phases for several main components.

| **Mass Parameter** | **[kg]** |
|---|---|
| **Entry Mass** | **2300** |
| Supersonic Chute Mass | 40 |
| Heat Shield Mass | 516 |
| **Mass at Powered Descent** | **1650** |
| Lander Mass | 700 |
| Loaded Propellant | 276 |
| Nominal Descent Propellant | 89 |
| Divert and Hover Propellant | 71 |

### 6.3.4 Technology Readiness Level Evaluation

Before making a final decision, the overall technology readiness level was evaluated for both systems considered. According to the 2015 NASA Technology Roadmap, inflatable entry systems were rated a TRL 5 with a five year maturation program. This was based on the current state of the art technology, IRVE-3 as well as the results of ground based testing and thermal testing of a flexible TPS [57].

The same process was repeated for the augmented architecture, again using the 2015 NASA Technology roadmaps. Advanced Sensors for real-time three dimensional terrain mapping were given a TRL 5 with 3 year maturation program [57]. This readiness level was based on current state of the art scanning/flash lidar, stereo vision and phased array radar systems. High fidelity sensor modeling and simulation tools were given a TRL 9 based on MSL terminal descent system and the physics based dust accumulation modeling for small body navigation. Additionally, convex optimization problem solving for real-time fuel optimal solution for use in large diverts was given a TRL 5 with 3 year maturation plan [57]. This level is given based on demonstration in small-scale rocket free flyers in the (ADAPT) program. The guidance for large divert on flight computer was given a TRL of 5 with 3 year maturation program. Finally, the testbed, used to demonstrate the large divert guidance was also given a TRL 5 with 3 year maturation plan [57].

When this information is compared against our mission timeline, significant risk begins to emerge with respect to inflatable entry systems. With our technology development period starting in May 2016 and our launch date set in June 2020, the acceleration of the maturation program, at best adds great cost and schedule risk and at worst is impossible to accomplish. The three year maturation program for all TRL 5 items related to TRN is feasible within our four year technology development timeframe. For this reason the decision was made to use the augmented heritage system.

The augmented heritage system will use the reference system identified in “Performance Trades for Mars Pinpoint Landing”. A breakdown of the mass of key elements can be seen in Table 6.4. The EDL system mass is broken into an entering phase and a landing phase.

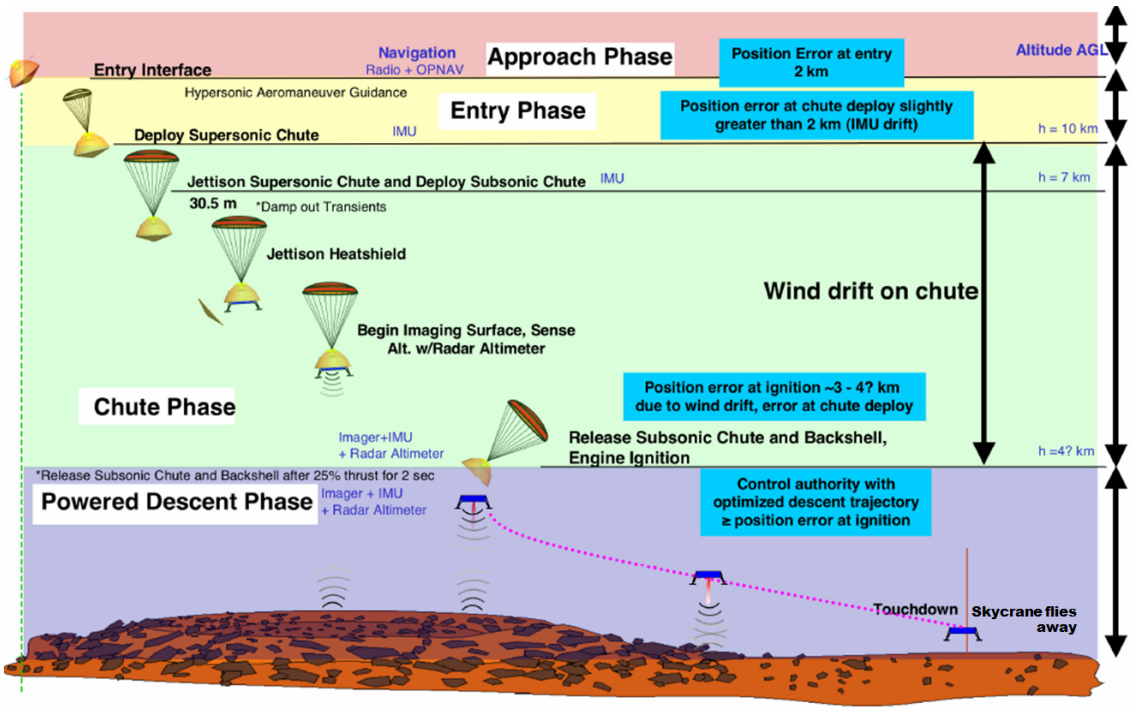


**Figure 6.2:** The four phases of EDL are shown with key elements and their altitudes identified [58].

## 6.4 Entry Descent and Landing Timeline of Events

Figure 6.2 from "Performance Trades for Mars Pinpoint landing" shows the timeline for EDL events.

The four phases of EDL can be seen in 6.2, separated by color. The approach phase will deliver the EDL system to make contact with Mars atmosphere with anticipated velocity of 4.9 km/s and flight path angle of 14 degrees. During the approach phase, position and velocity knowledge will be maintained from Earth ground stations and transmitted to the ITV spacecraft bus. After crossing the 125 km altitude point, the entry phase will begin where the system will use MSL heritage hypersonic guidance and C.G. offset to fly a lifting trajectory. State of the art guidance will direct the vehicle toward the landing site, rolling the vehicle about the offset C.G to change the lift vector [58]. In the entry phase, position and velocity information will be given by the IMU. During this phase, the system will be protected from heat loads using a 4.5 m diameter heat shield. The heat shield is a legacy PICA ablative material developed for MSL. Additionally, the system will be encapsulated by the aeroshell used in the MSL mission.

This segment of the EDL mission is also important for some milestone moments it contains. Using "Atmospheric Environments for Entry, Descent, and Landing," the team performed calculations to identify the maximum deceleration, max heating rate and to identify the location these events would occur. The results of the calculations, corresponding to our entry conditions, ballistic coefficient and a scale height calculated from a simple Mars atmosphere model were that the vehicle would experience max deceleration of 9.8 g's at an altitude of 28 km MOLA and a maximum heating of 36 W/cm2 at approximately 40 km MOLA [59].

When the IMU senses a specific velocity condition, the supersonic parachute will be deployed, beginning the chute phase. In this phase, the main means of deceleration will be in the form of a supersonic DGB parachute. During the chute phase, the heat shield will be jettisoned to allow imaging of the surface and to initialize the radar altimeter. Wind drift error will also accumulate during this segment that will need to be adjusted for in the final phase.

Finally, the powered descent phase will begin upon firing of the engines on the Skycrane system (Skycrane was used in the MSL mission). The anticipated 3-4 km of error that have accumulated from the various sources of uncertainty will be attenuated during this phase with the assistance of the new TRN system and newly developed fuel optimal guidance system. The fuel optimal guidance system represents an improvement upon Apollo heritage guidance, and allows for large divert maneuvers for hazard avoidance. When the propulsive system has completed its error reduction trajectory, the Skycrane will perform a brief hover to lower the system onto Mars surface before flying away a safe distance [57].

Because this system is designed for a pinpoint landing, the EDL system presented is capable of achieving a 5 km landing accuracy with a factor of safety exceeding 10. In this system, mass growth will be offset by a reduction in propellant available for error correction, while still allowing a safe margin for large divert, hover, and soft landing. Additionally by leveraging heritage capabilities and pairing with mid TRL TRN technologies already in development, this system will reduce cost and reduce risk. The greatest risk currently anticipated is in integrating high TRL items together with a new lander. The risk is partially mitigated by the successful integration of the aeroshell, heat shield, DGB parachute, C.G offset guidance, and Skycrane on the MSL mission. The technology development cost is described more in section 8 but is deemed to be within acceptable bounds judging from past missions.

# 7 Mars Systems

## 7.1 Martian Ground Systems

### 7.1.1 Lander Configuration

The useful landed mass that the EDL system delivers to the surface of Mars is 700 kg, with a 10 percent margin for mass growth included, and consists of a lander base with six deployable legs, a contamination area seal off from the Martian atmosphere and the Martian Ascent Vehicle (MAV). The lander base is 60 kg and made up of an aluminum box beam platform measuring 1.2 meters in width and 2.75 meters in length. These dimensions were driven purely by the length of the MAV and the clearance needed in the contamination area to load the sample into the second stage of the MAV. The box beam platform was chosen in order to reduce weight while at the same time managing the loads applied by the MAV and its support structure.

Obstacle clearance was also a concern when designing the platform; therefore the height was determined by analyzing the cumulative fractional area covered by rocks versus diameter. This data was taken at the Pathfinder lander site and a model was made to predict rock distribution. This data, in Figure 7.2, shows a sharp decrease in abundance of rocks with increasing diameter [60]. This was then used, along with the rock abundance data map from Viking IRTm [61], to analyze all of the potential landing sites identified by the Mars 2020 rover landing site committee. Since this data indicates there is low likelihood of encountering a rock larger than half a meter the platform height was chosen as 0.5 meters from the Martian surface. This height is consistent with the height to landing platforms used in past missions.

The legs of the lander are linear actuators fitted with springs in order to absorb the landing loads when deposited on the surface by the EDL system. The linear actuators on the legs allow for the platform to adjust for slight surface inclinations and orient itself to level horizontal position. The legs are also are distributed asymmetrically to accommodate the shifting of the center of mass when the MAV is tilted from horizontal to its vertical launch position. The material thicknesses of the lander base were determined using parametric FEA structural analysis to not only make sure that they could survive the landing loads and support the weight of all the ground subsystems in Martian gravity, but also ensure that the structure wasn't over designed.

For powering the lander both solar panels and radioisotope thermoelectric generators (RTG) were considered. The primary considerations for sizing a solar powered system on Mars include the latitude of the landing site, Mars' position relative to the Sun, and the local dust conditions. Additional, technology-specific considerations include the panel efficiency, the size of the solar array and the arrays specific mass or mass per unit array area.

The latitude of the landing site, Mars' position, and the local dust conditions are the major factors in determining the average solar insolation on the Martian surface, $\overline{F}_{tot}$. The latitude and Martian time of year impact the local solar zenith angle, $\mu_{SZA}$, and radial distance from the Sun, $r$, which in turn affects solar insolation incident upon the top of the atmosphere. The Martian atmosphere is thick with dust and, occasionally, planet-encompassing dust storms. The amount of dust in the atmosphere was measured by the Viking Landers and is quantified in terms of optical depth, $\tau$. If a constant optical depth

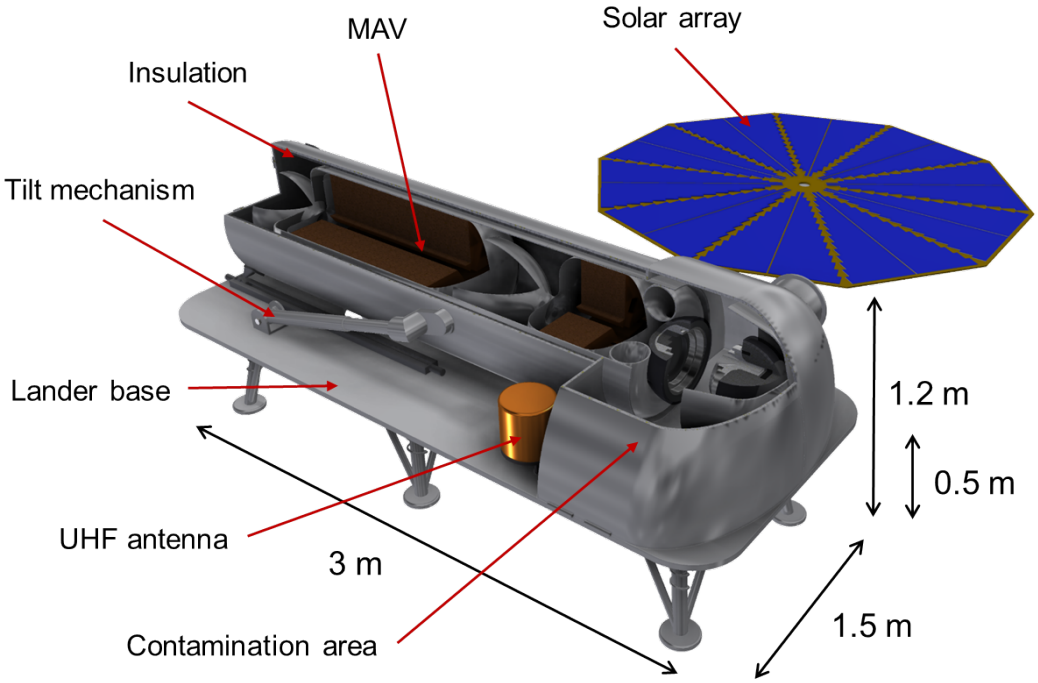


**Figure 7.1:** Useful landed mass including lander base, contamination area, MAV, and MAV tilt system.

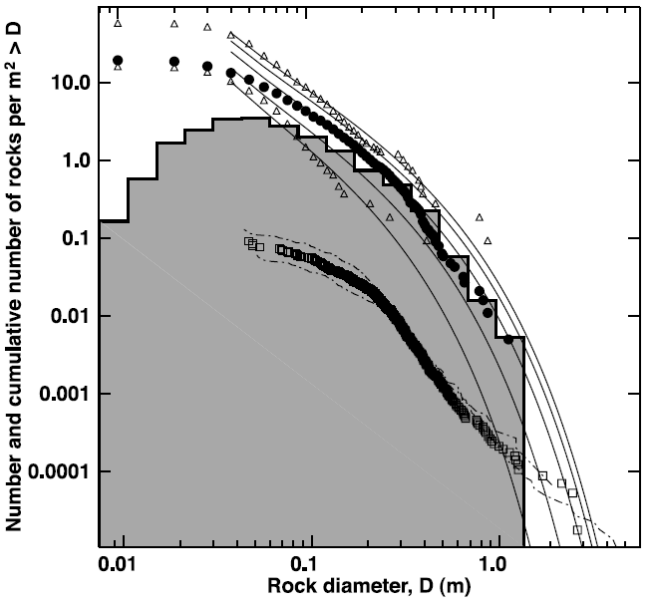


**Figure 7.2:** Cumulative number of rocks per $m^2$ greater than diameter D at the Pathfinder landing site. The histogram plotted along with these exponential functions shows a steep drop in number of rocks per $m^2$ greater than 0.5 m.[60]

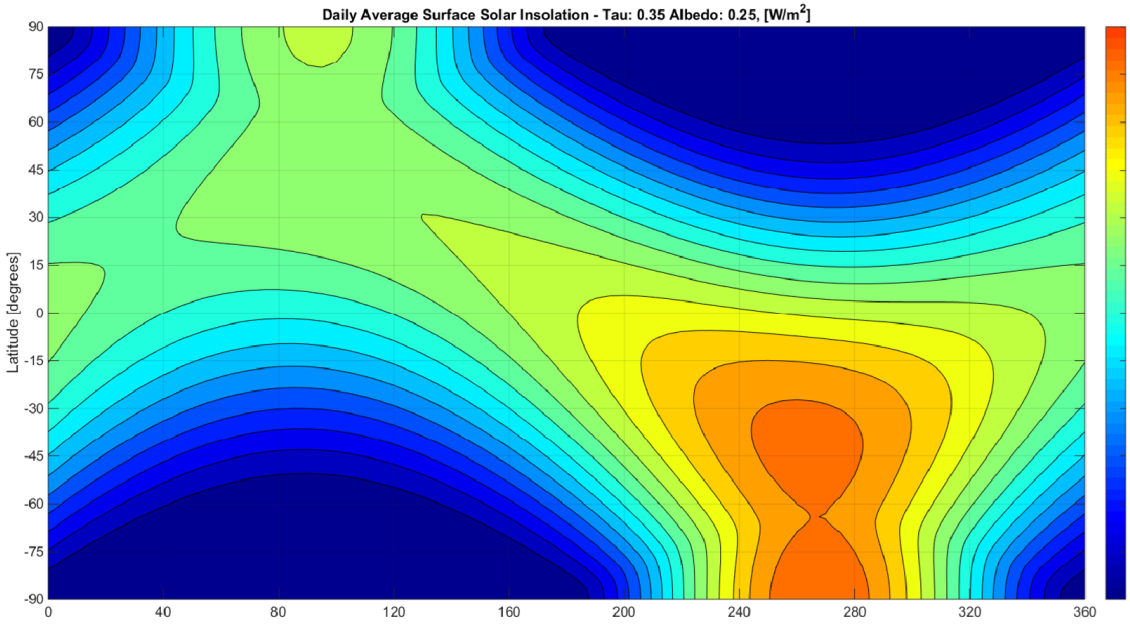


**Figure 7.3:** A heat map of how much sunlight hits the Martian surface as a function of time of year, measured in Areocentric longitude, and latitude of surface location. These results include a model for the Martian atmosphere diffusing and absorbing sunlight and surface albedo. The optical depth is assumed constant at 0.35, and albedo assumed uniformly constant at 0.25. Note that the optical depth will vary throughout the Martian year and can increase to as much as 6 during heavy dust storms.

of 0.35 is assumed, which matches Viking Lander data but assumes no dust storms, then a model for the impact of optical depth on scattering or absorbing sunlight can be applied to the solar insolation model shown in Equation 7.1 [62]. In Equation 7.1, $S_0$ is the average solar insolation hitting Mars's atmosphere, $\overline{r}$ is the average distance between Mars and the Sun, $H$ is the half-day length in radians, and $A_{Mars}$ is the Martian albedo. The $NNIF$ is the normalized net irradiance function; a numerical fit applied to an empirical dust model extracted from Viking Lander data and itself a function of $\mu_{SZA}$, $\tau$, and $A_{Mars}$ [62].

$$\overline{F}_{tot} = \frac{S_0}{\pi}\left(\frac{\overline{r}}{r}\right)^2 \int_0^H \mu_{SZA}\frac{NNIF}{1-A_{Mars}}dh \tag{7.1}$$

The results for the solar insolation incident upon the Martian surface after optical depth effects are considered is shown in Figure 7.3.

The other alternative for powering the ground systems is a radioisotope thermoelectric generator (RTG). RTGs operate by turning heat from the radioactive decay of an element, commonly Plutonium-238, into electricity via an array of thermocouples. RTGs are desirable for space missions as they output a near constant electric power as well as thermal power which can be used to heat electronics or fuel systems. RTGs also have an extensive flight heritage. On Mars, RTGs were used in the Viking Landers and Curiosity rover.

NASA's current generation RTG is the Multi-Mission RTG (MMRTG) most recently used on the MSL Curiosity rover.

**Table 7.1:** Breakdown of estimated power consumption for all of the subsystems on the lander. These power estimates are used in the sizing of the solar array and batteries.

| Lander Subsystem: | Power Required (W): |
|---|---|
| MAV Tilt | 35 |
| Sample Capture | 4 |
| Heat/Thermal Control | 40 |
| Attitude Control | 1 |
| Command & Data Handling | 5 |
| Communication | 25 |
| Solid State Memory | 10 |
| Computer | 5 |
| Total | 125 |

One of the next generation RTGs is known as the Advanced Stirling RTG (ASRTG) and converts the heat into a mechanical motion to achieve nearly four times the efficiency of the MMRTG. Each ASTRG is slated to output 130 Watts of electric power and 500 Watts of thermal power with a nominal dimension of 76 cm by 46 cm by 39 cm and a mass of 32 kg per unit [63].

A power breakdown of the components on the lander can be seen in Table 7.1. The 125 W total is a current best estimate of what these subsystems require calculating in efficiencies and mechanical losses. It is important to note that the thermal power required for the lander is 40 W, far less than what is output by the RTG mentioned above. The use of an RTG would require radiators on the lander to adequately manage the excess thermal power. Additionally while the output electric power of the RTG is almost exactly what is needed for this mission, solar panels provided increased mass savings.

The power used to size the solar panels for the lander included nomial lander operations, while excluding the power required by the tilt mechanism and the sample capture system. This nominal operation is estimated to require 86 W of power, which will be provided by an Orbital ATK UltraFlex solar array. The UltraFlex solar array was chosen for its high packing density and low weight [64], and will be fitted with triple-junction (ZTJ) Gallium Arsenide (GaAs) cells with a minimum average efficiency of 29.5 percent.[65] Using this efficiency, the predicted arrival date on Mars, the solar irradiance on the Martian surface for the worst case latitude and a mission life of two years the solar array is estimated to be 2.75 square meters. To reduce complexity the solar array is also sized to provide the required power without needing to track the sun as it moves across the sky. The area corresponds to a 2 meter diameter which is estimated to be 3 kg based on scaling off of the Phoenix lander solar panels.[64] These solar panels offer a significant mass savings over the 32 kg RTG.

The batteries carried on the lander are Lithium-ion, which offer a much better energy density than batteries used for space missions in the past and greatly reduce the required battery mass. The batteries were sized using the data in NASA's guidelines on the use of Lithium-ion batteries.[66] They are able to handle the heating and mechanical power requirements of the lander,

coming out to a mass of 17.5 kg each. Even though one battery can handle the power requirements of the thermal and MAV tilt system, there are two batteries on the lander for redundancy.

Heating requirements come from the electronics on board the lander and the solid rocket grains in the MAV. The Martian surface experiences temperature swings between -133 and 27 degrees Celsius.[67] While the electronics are space rated the computer is able operate at temperatures between -55 and 125 degrees Celsius [68], the solid state recorder can operate at temperatures between -25 and 60 degrees Celsius [40] and the rocket grains can only handle thermal cycling between about -50 and 60 degrees Celsius [69]. To ensure that each of the components are within their operating temperature a combination of patch heaters and insulation are used. As for communication the lander is equipped with a Ultra High Frequency (UHF) antenna for communication with the orbiter as it pass overhead and an omnidirectional low gain antenna for receiving data directly from Earth through the Deep Space Network (DSN). These are the only antenna because the needs of the lander are very low since it is not directly performing scientific analysis itself and does not need to transmit that data. The only information transfer that is needed is health data updates, sample capture confirmation and general software updates for the lander. The low gain antenna, due to the fact that it is omnidirectional, does to need to be reoriented so that it receives data from Earth. However, due to this feature it is not optimal for data transmission back to Earth. The UHF antenna is a shorter range communication device and allows the lander to send health data to the orbiter, which can then be sent back to Earth if needed.

### 7.1.2 Mars Ascent Vehicle Tilt / Support System

When the lander makes it to the surface of Mars the MAV it is positioned horizontally on top of the lander base. This is so that the sample container can be easily taken from the rover and placed on top of the second stage of the rocket. This means that a mechanism is needed to tilt the MAV up to its vertical launch configuration. The tilt mechanism is 141 kg and consists of two aluminum pistons and linear actuators that work together to bring the MAV from horizontal to vertical in 5 minutes. This requires about 35 W to power, with losses, which can easily be handled by the batteries on the lander. Once the tilt mechanism has oriented the MAV upright, the nozzle of the first stage will be aligned with the exhaust port located in the platform of the lander base. Like the lander base, the tilt mechanism is comprised of aluminum and the thicknesses and dimensions of the individual components are size to handle the loads that are imparted by the act of lifting the MAV.

### 7.1.3 Sample Capture Mechanisms

Planetary considerations ended up having a large influence on the design of the lander and to an extent the MAV, which will be discussed in the following MAV Design section. Contamination of Mars by Earth is handled by assembling the spacecraft on Earth in a clean room. However, preventing contamination of Mars to Earth requires some design considerations. Before the sample returns to Earth the chain of contact must be broken. This system is designed to break the chain of contact on the surface of Mars and has preventative measures to ensure that there isn't any recontamination of the system before it deposits the sample at Earth. On Mars, the lander is equipped with a contamination area which is sealed off from the Martian

**Figure 7.4:** MAV is tilt to its vertical launch position with OS in payload bay and nose cone sealed to second stage.

atmosphere. This means that the inside of it remains Earth clean throughout the journey to Mars, EDL and taking the sample cache from the rover. The 114 kg contamination area is a portion of the lander design that is novel and thus where a majority of the technology development for this mission would focus. A Mars sample containment system which would break the chain of contact on the surface of Mars has not been designed or built before. Therefor the current TRL of 1 for this system is the lowest of any in this mission architecture. The one advantage this could provide is in system integrate further down the line. Since the EDL system is an augmented sky crane design lander could be designed to work with the constraints of that system.

The contamination area contains all of the lander electrics, batteries and sample containment systems. The inside of this contained area is pressurized to the same pressure as the Martian atmosphere. The side of the contamination area has a port on the side oriented so that the rover's arm can easily insert the sample container. The port opening is covered by a Kevlar

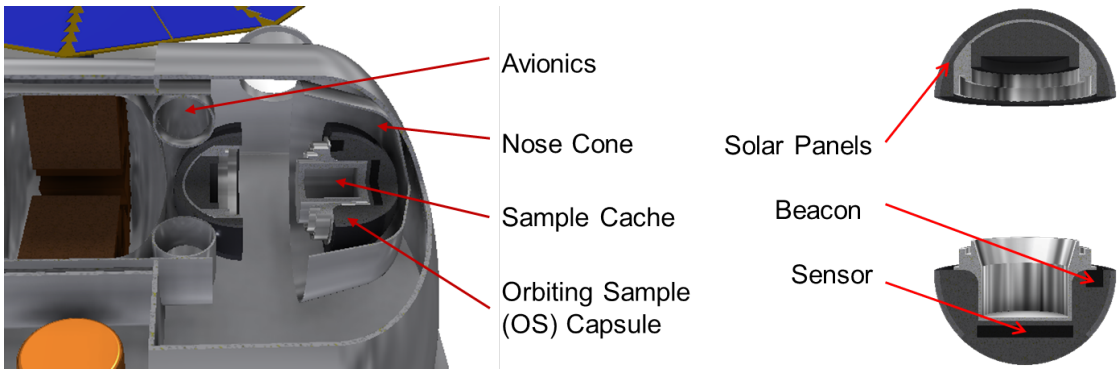


**Figure 7.5:** On the left is the contamination area meant to receive the sample cache fromt eh rover and break the chain of contact on Mars by first coating it in a Kevlar membrane and then placing it into the OS encasement. On the right is the OS in its open configuration ready to receive sample. These halves will be sealed together once sample is placed inside.

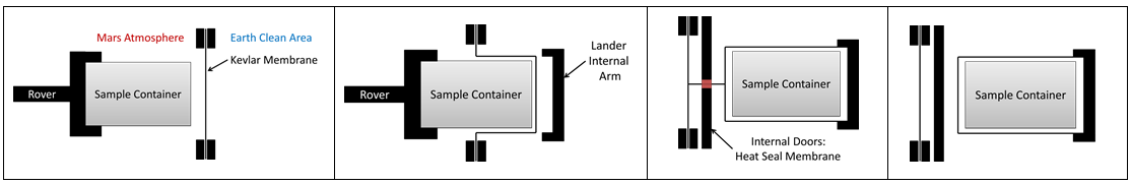


**Figure 7.6:** Sequence of events of sample container being received by the lander through the port on the side of the contamination area. The figure above steps through the sequence from when the lander pushes the sample container through the Kevlar membrane and to when it is fully coated with the Kevlar membrane.

barrier that the rover must push the sample slowly through. As the sample is pushed through the barrier the Kevlar deforms to envelope the sample container. Once the rover has pushed the sample far enough through the port, a robotic mechanism on the inside of the contamination area will grasp the sample container with its Kevlar coating and pull it the rest of the way through the port. Once the sample container has cleared the port a set of doors internal to the port will come down, pinch the Kevlar and heat seal it together while at the same time cutting so that it is no longer attached to the port. The doors will serve as the new barrier to the Martian atmosphere and the sample will be in the Earth clean area with a Kevlar membrane encasing it. An internal mechanism will then move then maneuver the sample to the open payload bay in the nose cone of the MAV.

In the nose cone is another encasement called the Orbiting Sample (OS) which contains beacons, sensors and solar panels which will help the orbit locate it in Martian orbit. The OS is a design borrowed and scaled form the NASA JPL Orbiter Mission Concept Study.[70] When the lander is deposited on the surface the OS is split into two halve, Figure 7.5, one being attached to the second stage of the MAV and the other attached to the nose cone. Between the two halve is enough room for the containment area's internal mechanism to orient and deposit the 15 cm by 15 cylindrical sample container. Once the sample has been placed in the half attached to the nose cone, the nose cone is moved so that the other half of the OS is locked into place and then the nose cone is seal to the second stage.

Once the nose cone has been sealed the contamination area breaches along the length of the MAV and hinges away from the MAV to allow it to tilt into its launch configuration. This leaves the payload bay of the second stage and the OS Earth clean and means that an Earth clean OS is delivered to the orbiter. The OS contains solar panels, a sensor and a backup UHF low duty cycle beacon to assist the orbiter in finding its position.[70]

## 7.2 Mars Ascent Vehicle Design (MAV)

The MAV is designed to transport the sample, once captured, from the surface of Mars into Mars orbit to rendezvous with the orbiter at an altitude of 300km. This part of the mission has never been attempted before and thus entails new design considerations and opportunity for innovation. Ensuring an optimum MAV design requires investigation into the staging, structure, MAV configuration, fuel selection and fuel source. The solution found was a two stage composite propellant solid rocket, which was selected on a basis of its low complexity, its storability, and its low mass. The final design is a 410 kg rocket which achieves insertion accuracies of 10 kilometers and 1 degree of inclination using a liquid injection thrust vectoring

system.

### 7.2.1 MAV Design Parameters

The first design parameter is payload for the MAV. The payload will be the orbiting sample (OS), and the avionics required to perform the orbital insertion. The sample container weighs 3 kg and the remaining components of OS weigh a total of 7 kg. For the rendezvous-based system, an estimate of 15 kg for avionics per the RFP was made to bring the total payload to 32 kg [4].

The second orbital parameter is the altitude at which the payload is to be placed. A study was performed to study the effects of adjusting the altitude of this orbit on both the mass of the MAV and the mass of the orbiter. It was found that increasing the altitude for the orbital insertion would increase the mass of the MAV by 0.13 kg/km but would only reduce the mass of the orbiter by 0.007 kg/km. Due to the MAV mass being more sensitive to altitude this trade drove the desired insertion orbit to occur as low as possible. The lower limit of 300 km was selected based on concerns about the stability of the orbit for the ITV.

### 7.2.2 MAV Fuel Selection

Investigation into fuels that could be used in the MAV focused on those that were most mass efficient, storable, and scalable as well as whether they can be produced on the surface of Mars or need to be brought from Earth. A mass efficient fuel directly reduces the mass of the MAV propulsion system, which has benefits for reducing the required landing mass for the EDL system and ultimately the cost of the entire mission.

With regard to the attainment of fuel that will be used by the MAV, there were two methods considered: In-situ Resource Utilization (ISRU) or storable fuel brought from earth. ISRU is dependent on the time spent on the Martian surface, and will be limited to 50 days for the sake of maximizing the amount of time available to perform an orbital rendezvous. The goal of ISRU would be to reduce the total mass of the system by utilizing resources on the surface of mars to produce fuel. The costs incurred by this method are the equipment to produce the fuel, and the additional mass of the power systems required to run the equipment. Because the landing site is not specified, mining resources cannot be reliably depended on for propellant production, so the ISRU process will be restricted to the use of the Martian atmosphere.

In the event that the propellant is not produced on the Martian surface, storability of the fuel is crucial. The MAV will not launch until 21 months after earth departure, so any fuel that is brought from earth must be stored for that period. Considerations must include fuel degradation as well as storage tank corrosion. Both present risk to the mission that should be avoided by selecting the fuel and storage methods appropriately.

The next consideration and design trend of interest is scalability. With a payload mass of 32 kg the MAV will be much smaller than conventional launch systems. This means that the launch system needs to scale down well in order to be a good candidate. Systems with low density liquid propellants are only efficient on large launch systems and will incur structural mass penalties on smaller launch systems. Alternatively, simple solid rocket systems incur fewer structural mass penalties for

smaller systems.

### 7.2.3 Preliminary MAV Modeling

In order to select a fuel, a model for the MAV propulsion system must be established by which the fuel options can be compared. The model used for the purposes of fuel selection is based off of the ideal rocket equation. This equation requires a known $\Delta V$, specific impulse ($I_{sp}$) of the fuel and payload mass to predict the initial mass of the rocket. Because the dry mass of each upper stages serves as the payload for its lower stage, the dry mass must know in order to proceed. The dry mass fraction of each stage was determined using empirical fits based on data of existing rockets. These empirical fits are specific to each system type. For the preliminary design, $I_{sp}$ of the rocket is determined by the fuel alone. Multiple stages and can be incorporated by applying the equation iteratively with the payload of the first stage being the second stage and so on. In order to determine the mass of the rocket a value must be determined for $\Delta V$.

To select preliminary value for $\Delta V$, the insertion orbit is used. By using the orbital velocity at this altitude, and a correction for the potential energy between the surface and this orbit, the target $\Delta V$ was determined to be $4.6km/s$. A Matlab function was written to determine the optimum fuel distribution between a multiple stages of a rocket. In general, increasing the number of stages on a rocket will lower the required mass of the rocket to achieve a given $\Delta V$. However, with the empirical fits used to determine the structural fraction of each stage, this is not always the case. Because each stage has a fixed amount of mass associated with it that is not dependent on fuel, there exists an optimum number of stages to achieve a given $\Delta V$. This effect can be seen in the Figure 7.7.

### 7.2.4 ISRU Options

ISRU and ISPP were explored as alternatives to bringing the MAV fuel from Earth in order to reduce the mass delivered to the surface of Mars by the EDL system. With these methods, the mass of the stored fuel is replaced with equipment and ingredients to produce a desired fuel. Because the ISRU is restricted to using the Martian atmosphere, the reactions used to produce the propellant are limited to three primary methods. The first possibility is carbon dioxide electrolysis which uses the mechanism in Equation 7.2.

$$CO_2 \rightarrow CO + \frac{1}{2}O_2 \qquad \Delta H = 282.98kJ \tag{7.2}$$

This reaction produces carbon monoxide and oxygen from carbon dioxide, a plentiful resource in the Martian atmosphere. This reaction is endothermic and requires a large amount of electrical power to be supplied in order for the reaction to proceed. The next option for fuel production on Mars is through the Sabatier reaction. The stoichiometric formula is given in Equation 7.3.

$$CO_2 + 4H_2 \rightarrow 2H_2O + CH_4 \qquad \Delta H = -165.0kJ \tag{7.3}$$

This reaction produces methane and water from hydrogen and carbon dioxide. Hydrogen is not a resource that is readily available on Mars and would be brought from Earth. This reaction has the advantage of being endothermic, and would only require power to initiate the reaction. The next possible reaction considered was the electrolysis of water. The stoichiometric formula is given in Equation 7.4.

$$H_2O \rightarrow H_2 + \frac{1}{2}O_2 \qquad \Delta H = 285.83kJ \tag{7.4}$$

This equation produces hydrogen and oxygen from water. Due to the flexibility in the rover location, a location cannot be chosen for water content, and access to water cannot be guaranteed. Therefor this method would be limited to the products of the Sabatier reaction. This reaction is also endothermic and has higher power requirements than carbon dioxide electrolysis. These primary reactions allow for the direct production of hydrogen, methane or carbon monoxide as potential fuels.

### 7.2.5 ISRU Equipment

One significant consideration for ISRU is power generation. For both carbon dioxide and water electrolysis the reactions are highly endothermic. The power systems discussed in the ground systems could be sized to run these reactions, but the mass penalties imposed on the lander are significant. These masses can be seen in the ISRU summary table. It is important to note that even though the methane fuel option can be created by the exothermic sabatier reaction, either water or carbon dioxide electrolysis would be required to produce the oxygen. In addition to additional power requirements, ISRU and ISPP require specialized equipment. By using hydrogen as the primary ingredient, the primary options for ISRU are zirconia electrolysis, used for carbon monoxide electrolysis, and the sabatier reaction, for water electrolysis, existing as a potential to recycle the water produced by the sabatier reaction. The mass for systems to produce fuels using these methods, was found to scale linearly with the required rate of fuel production [71]. As the duration on Mars is assumed to be 50 days, the mass and power requirements of these systems can be found using a linear fit. Combining this information with the power systems and ingredient requirements described above yields the following table which summarizes the requirements of ISRU. The values in this table are all in kilograms and the equipment masses are derived from the amount of fuel needed to launch the minimum 32 kilogram payload.

**Table 7.2:** Mass requirements to perform ISRU on the Martian surface for the given fuels. Here the hydrogen option with solar panels is a significant frontrunner in terms of mass, but the solar panel area of 95.4 kg of solar panels is nearly 400m2, and the other fuel options have larger requirements for their power systems. With the EDL vehicle constraining the volume of the Martian lander, using RTGs for power could be required.

| Fuel | H2 Mass | Power System Mass [kg] | | Equipment | Total Mass [kg] | |
|---|---|---|---|---|---|---|
| | [kg] | Solar | RTG | Mass [kg] | Solar | RTG |
| H2 | 18.4 | 115 | 678 | 550 | 683 | 1246 |
| CO | 0.0 | 257 | 1510 | 620 | 877 | 2130 |
| CH4 | 55.4 | 517 | 2751 | 1590 | 2163 | 4396 |

**Table 7.3:** This table compares the mass of a MAV required to achieve the predicted $\Delta V$ of 4.6km/s. Here it can be seen that the optimum solid system has two stages, the optimum monopropellant and bipropellant systems have three stages. Of these systems the solid rocket has the lightest mass.

| System | Solid | | | Monopropellant | | | Bipropellant | | |
|---|---|---|---|---|---|---|---|---|---|
| Fuel | Al+AP | | | MMH | | | MMH+NTO | | |
| Stages | 1 | 2 | 3 | 1 | 2 | 3 | 1 | 2 | 3 |
| Mass [kg] | 517.9 | 508.5 | 526.0 | 1513.0 | 967.8 | 914.4 | 4696.0 | 802.9 | 795.3 |

### 7.2.6 Storable Propellant Design

For storable fuel options, the primary divide is between liquid and solid fuels. Hydrazine is a standard choice for a highly storable and relatively high performance liquid fuel. It can be decomposed as a monopropellant or it can be burned with nitrogen tetroxide as a bipropellant. Burning it as a bipropellant results in higher $I_{sp}$ but also extra complexity. Green fuels are currently being considered as a replacement to hydrazine, with comparable performance and a lower toxicity. In the event that hydrazine is chosen these would also be considered. The alternative to a liquid system would be a solid system. Solid rocket systems have the advantage of being very simple, but the disadvantage of not being throttleable. The solid rocket propellant considered was a high performance composite propellant using aluminum as a fuel, ammonium perchlorate as an oxidizer, and hydroxyl terminated polybutadiene (HTPB) as a binder. To determine the structural masses of these rockets, the specifications of required components were investigated, and empirical fits were performed on data made available by TU Delft [83]. From these investigations it was found that the solid rockets scaled down more efficiently than the monopropellant or bipropellant rockets. On the other hand, the bipropellant systems outperform the solid rockets in terms of $I_{sp}$. To determine the optimum system for the MAV the total performance of the rockets was compared over a range of $\Delta Vs$ to observe the trends in the data.

It can be seen from Figure 7.7 that a two stage solid rocket is the most efficient rocket to achieve the required $\Delta V$ of 4.6km/s and is the optimum number of staged in this range. This is convenient because while solids are unable to be throttled, the first stage can be used primarily for gaining altitude, and the second stage can be used to circularize. Additionally, the

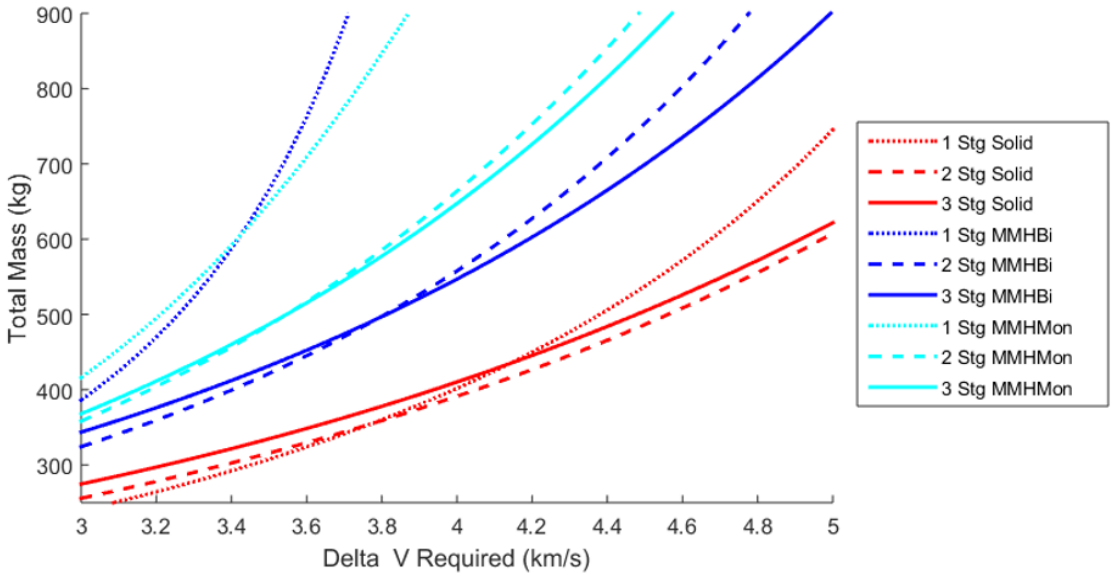


**Figure 7.7:** This figure compares the mass required on the MAV to deliver the OS to orbit based on preliminary analysis. In general each the system mass increases as the required $\Delta V$ increases. Additionally, the optimum number of stages for each system increases with increasing $\Delta V$.

mass of the solid rocket required to perform the maneuver is preliminarily found to be 506kg, which is lighter than the more complicates liquid systems, and the very complicated ISRU systems. For these reasons the solid rocket was investigated further.

### 7.2.7 Solid Rocket Detailed Design

In order to further design the solid rocket, the analysis performed on the rocket must move beyond a single Isp and a rough $\Delta V$ estimate. First more accurate model of the rocket must be constructed. In order to model the combustion within the solid rocket, NASA's Chemical Equilibrium with Applications (CEA) was used [82]. This program models the combustion and dissociation of the solid propellant with a given starting temperature and pressure. The outputs of this are the flame temperature, the specific gas constant and the ratio of specific heats. Frozen flow is assumed and isentropic flow equations are utilized to compute the mass flow rate through the throat of the nozzle. This mass flow rate is balanced with the mass flow rate computed from the regression rate and the surface area of the propellant to determine a new chamber pressure. From the nozzle geometry and the chamber conditions the thrust of the rocket is computed. This process is iteratively repeated to compute the burn profile of a given grain. In order for the rocket to achieve positive acceleration, a high surface area grain surface area is required. In order to achieve this high initial surface area while still having a space efficient propellant grain, a star grain configuration was chosen. The acceleration curve for the final grain design can be seen in Figure 7.8.

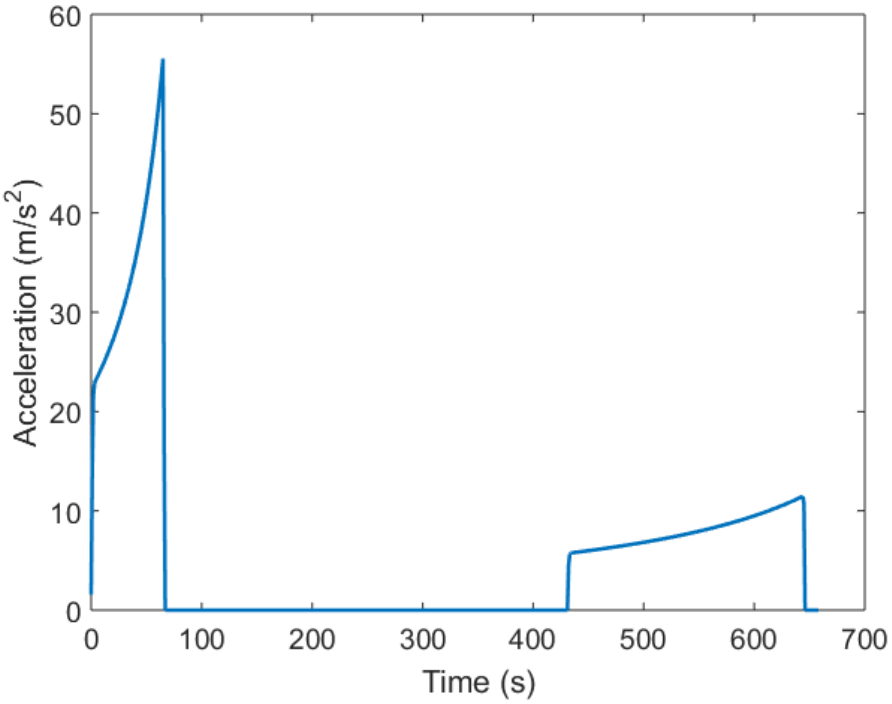


**Figure 7.8:** This is the acceleration of the solid rocket over time for the final design of the MAV. It can be seen that the peak acceleration occurs at the burnout of the first stage of the rocket at a value over $55m/s^2$.

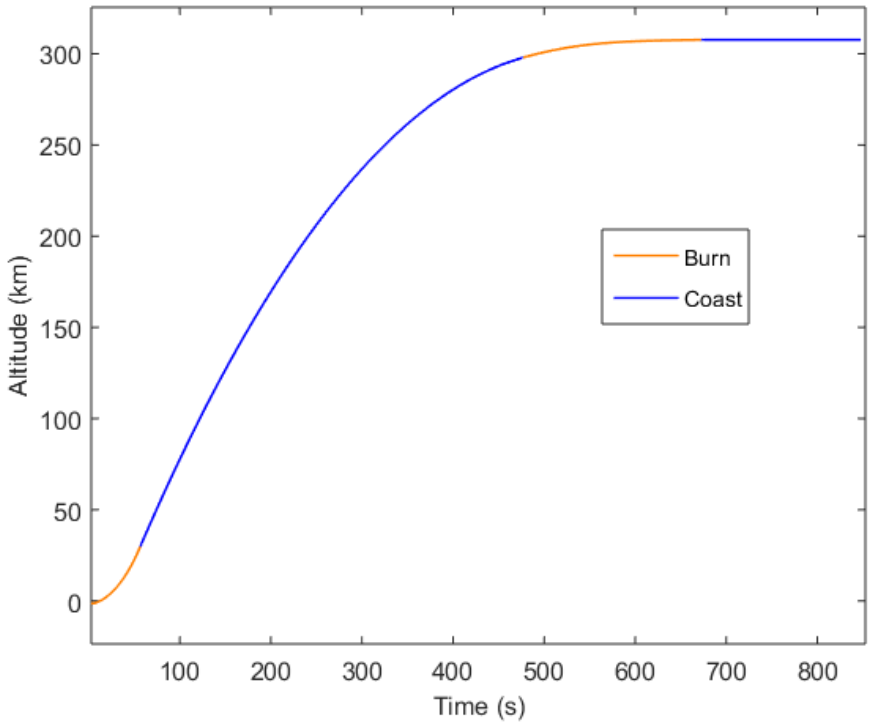


**Figure 7.9:** This figure shows the altitude of the solid rocket with respect to time. This shows that the first stage burn gives the rocket the majority of its altitude raising. The second stage of the rocket is primarily used for circularizing the orbit.

Next modeling of the forces that act on the rocket is required. These are gravity and atmospheric drag. The gravity model comes from the simple Newtonian gravitation equation seen in Equation 7.5.

$$F_{Gravity} = \frac{GMm}{\|r\|^3}\overline{r} \tag{7.5}$$

$$F_{Drag} = \frac{1}{2}\rho C_D S \|V\| V \tag{7.6}$$

The drag model from mars uses Equation 7.6 where the density is a function of altitude. The value of $C_D$ is assumed to be 0.3 for a bullet shaped body, and s is the cross sectional area of the rocket. The $v$ is the velocity of the rocket relative to the local atmosphere. The density of mars was modeled as an exponential function of the scale height. These forces and the thrust of the rocket are iteratively integrates through a symplectic integration scheme to determine the final state of the rocket payload. The kinematic model prevents energy drift by using a forwards step to compute velocity and a backwards step to compute position.

The maneuver the rocket performs to achieve orbit is a gravity turn. In this maneuver, the rocket burns in the direction of its velocity and uses gravity to eliminate its radial velocity. With this maneuver the rocket begins by burning radially away from Mars, but due to the rotation of Mars, it has a tangential component to its velocity. After a variable amount of time the rocket turns so that it is burning in the direction of its velocity instead of radially. After the first stage burns out, the rocket separates and coasts until it is nearing the apoapsis of its trajectory. The second stage then ignites to circularize its orbit. This maneuver is a very efficient way to enter orbit on a planet with low atmospheric density like mars. Numerical optimization is used to determine the turn time and the coast time for a given rocket configuration. The fuel mass is adjusted by hand until the desired orbit of 300 km is achieved with grain masses of 224 and 56 kg for the first and second stage respectively. In Figure 7.9 the insertion trajectory of the final rocket can be seen.

It is important to note that this rocket engine design is novel, and while the solid rocket system is simple compared to others considered, this total system is at a TRL of 2. The development of this rocket would be expected to require significant resources in terms of time, budget and personnel. This rocket would be one of the biggest concerns for causing development overruns in terms of cost or time, and would require careful management and an aggressive schedule. It could be advantageous to adapt an existing solid rocket to perform this orbital insertion as this could save significant developmental expenditures.

### 7.2.8 Attitude Determination and Control

For a rocket that only thrusts in the direction that it is moving, the accuracy of its insertion is determined by the accuracy in its predicted thrust profile, and the accuracy of its ability to point towards its intended flight path. For the first source of error, the thrust can be augmented by another system to cope with uncertainty. For the second type, a Monte Carlo simulation was run where the direction of the thrust of the rocket was offset from its velocity in a normally distributed angle. This error angle

is set to be normally distributed and is analogous to a pointing error either in the attitude control or the attitude determination system. The target accuracy was set above to be within 10 km and within 1 degree of inclination. This requires a 2 sigma pointing accuracy of 0.5 degrees. The results from the Monte Carlo simulation can be seen in Figure 7.10. From these figures it can be seen that the avionics of the rocket must be able to determine its velocity with a minimum 2 sigma accuracy of 0.5 degrees.

The attitude control system on the rocket was selected to be liquid injection after the nozzle. This has the benefit of augmenting the thrust in addition to providing a pitching moment. Strontium perchlorate mixed with water was selected to be the injectant due to its reasonable performance, high density and its stability [72]. For preliminary design work, the thrust vectoring required is assumed to be 2 percent of the impulse for the first stage and 1 percent of the impulse for the second stage [72]. Because the injectant also augments the thrust, an additional 5 percent was included due to the uncertainty in the thrust profile of the solid rocket grain. Using a conservative side specific impulse of strontium perchlorate results in 25 kg of strontium injectant for the first stage and 5 kg of injectant for the second stage. This works out to 13 and 2 liters of injectant respectively. When this injectant is included, the total mass of the rocket to deliver the OS to an altitude of 300km becomes 410 kg.

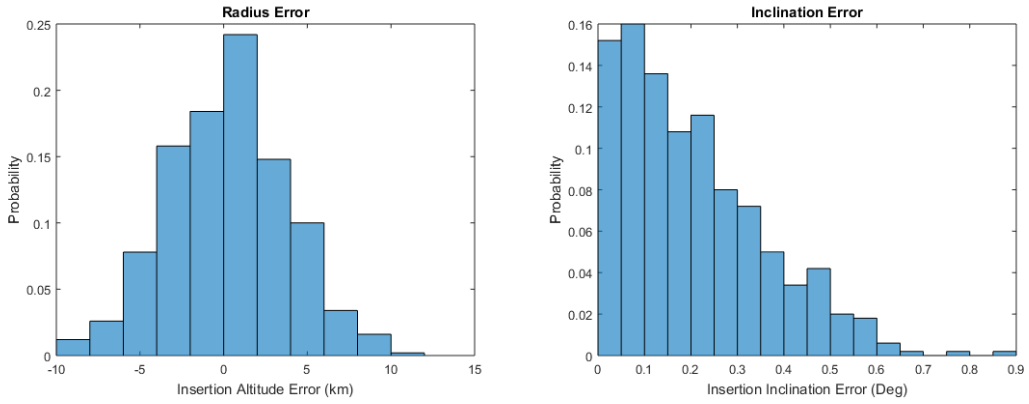


**Figure 7.10:** This shows the altitude results of a Monte Carlo Simulation using a 2 sigma rocket pointing error of 0.5 degrees. On the left, it can be seen that the rocket insertion altitude is normally distributed, and that this has an accuracy of 10 km. On the right, it can be seen that the insertion error is less than 1 degree.

### 7.2.9 Contamination Design Considerations for the MAV

While the chain of contact for the sample is broken on the surface, a few design modifications were made to the MAV design to prevent recontamination of the OS. This is because the MAV will be exposed to and traveling through the Martian atmosphere after the contamination area opens. Dust could cling to the skin of the rocket which may present a challenge when in orbit. Thus, the skin of the second stage were designed as detachable fairings. These fairings would break away from the second stage of the rocket after the vehicle is out of the Martian atmosphere. This would prevent any lingering dust from following the second stage, and thus the OS, as it approached the orbiter. This would guarantee that an Earth clean OS is delivered to the orbiter and allow the orbiter more flexibility when returning to Earth's sphere of influence.

# 8 Risk Mitigation and Cost Evaluation

## 8.1 Risk

As with every spacecraft mission, there is risk involved from the first day of development through the final moments of system operation. The majority of the risks that are identified here are specific to the MSRS mission development rather than general risks associated with spacecraft missions. Considering the identified risks, a risk matrix was created in order to visually display and plot the likelihood and severity of each risk. This matrix is shown in Figure 8.1.

The first risk describes the scenario where the orbiting sample cannot be found either due to a hardware malfunction or anomalous MAV insertion parameters resulting in the OS being out of ITV detection range. To mitigate this risk, 10 percent fuel margin on top of a conservative rendezvous analysis was included such that extra fuel is available for the ITV to use to locate the OS. In a similar vein, the second risk is the scenario where the OS if found, but has been inserted at an inclination or altitude which makes rendezvous impossible. To mitigate this risk the MAV design included a thrust vectoring system which, with Monte Carlo analysis, was shown to limit 2-sigma inclination and altitude error to within bounds achievable by the ITV and its fuel mass. Furthermore, the ITV rendezvous fuel calculation was performed with the anticipated worst-case error considered. The third risk that was taken into account considers the thermal environment on the Martian surface that could cause MAV engine failure due to severe cracking of the solid rocket propellant grain. This would result in a total rocket failure during MAV lift-off and was mitigated by inclusion of an active thermal control subsystem on the lander designed for the worst case landing location temperature swings. The fourth risk identifies the possibility that the landing site terrain could be incompatible with the rover sample deposit or MAV launch configuration. The outcome of this risk occurring would result in changes to the MAV launch configuration procedures and is mitigated by including actuated lander feet and additional rotation in the MAV tilt system.

Two additional risks include a failure of the lander and MAV contamination systems to completely break chain of contact with Mars and an off-nominal OS reentry trajectory at Earth. The resulting consequences with respect to both of these Earth-centered risks would be that either the ITV is not allowed to enter the Earth's atmosphere or that the OS burns up in the Earth's atmosphere inadvertently. Mitigation of likelihood of contamination system failure is achieved through the Earth-clean barrier system and MAV fairing designs described in Section 7. In the event that the ITV still remains contaminated after capturing the OS in orbit, then fuel is present onboard the orbiter to slow down before Earth and enter a lunar trailing orbit such that another vehicle could be sent from Earth to recover the samples from the ITV in a controlled fashion.

The most critical mission risk is a development schedule overrun. This risk is both specific to MSRS because of the systems being developed but is also common for space programs in general. The consequence is a missed launch window, which could translate to mission failure. To address the likelihood of encountering a development schedule overrun, the use of modular COTS components, heritage systems, and components at a moderate TRL at the start of development were

preferred during component selection. Development of the project budget also considered reserves which could be used to accelerate technology development. In addition, using the money saved on development of standard and semi-standard hardware to develop the new, low TRL systems for the MSRS mission can reduce the likelihood of development overruns in these systems. The risk matrix after the implementation of these mitigation strategies is shown in Figure 8.2.

| Number | Risk |
|---|---|
| 1 | Orbiter cannot find OS (lost) |
| 2 | Orbiter cannot reach the OS (unreachable) |
| 3 | Environmental conditions cause unexpected engine behavior (ie grain cracking) |
| 4 | Landing site terrain incompatible with sample deposit or launch configuration |
| 5 | Failure of comtamination systems to completely break chain of contact with Mars |
| 6 | Off-nominal OS reentry trajectory at Earth |
| 7 | Development Schedule Overuns |

| Number | Consequence |
|---|---|
| 1 | Extra fuel expenditure, possible mission failure |
| 2 | Extra fuel expenditure, possible mission failure |
| 3 | Total rocket failure |
| 4 | Redesign of sample deposit or launch configuration procedure |
| 5 | Not allowed to enter Earth's atmosphere |
| 6 | OS burns up in Earth's atmosphere (worst consequence) |
| 7 | Miss launch window |

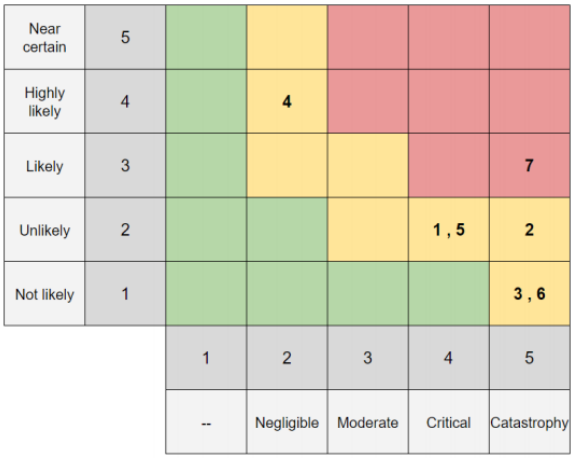


Likelihood Key (%)

| 1 | 2 | 3 | 4 | 5 |
|---|---|---|---|---|
| 0 – 20 | 20 - 40 | 40 - 60 | 60 - 80 | 80 - 100 |

**Figure 8.1:** Identification of key risks and consequences that are particular to a Mars Sample Return Mission.

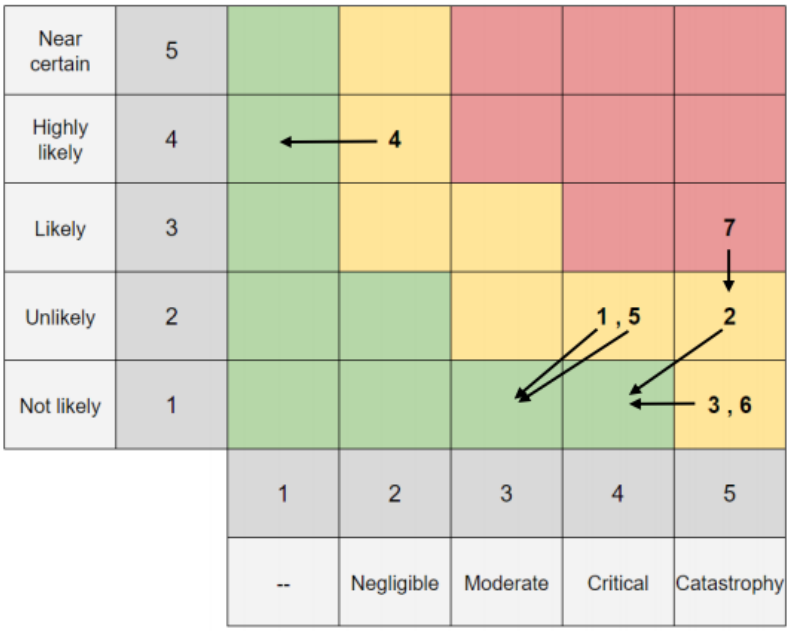


**Figure 8.2:** Post Burndown risk matrix. The anticipated new likelihood and severity of each of the identified risks after actions implemented in the proposed design such as extra budget reserves and fuel margins are accounted for.

## 8.2 Cost

The costing methodology developed estimates the project will cost, including reserves, approximately $1.61 billion USD (FY16) of which $1.38 billion will come from four years of a development, test and evaluation (DT&E) phase and the remaining $229 million will come from five years of an operations phase. The costing methodology is based on estimating the complexity of the proposed MSRS relative to other sample return missions or missions with similar critical technologies such as solar electric propulsion or Martian EDL systems. Estimating relative complexity lead to determining average yearly DT&E and operations rates which were then used to estimate total mission costs. The spread of project expenditures over time for each phase was estimated using empirical models derived from a body of other spacecraft missions.

Figure 8.3 shows the trend in operations cost per year and development cost per year for selected missions with linkages that can be extended to the proposed MSRS. Stardust was a highly cost-effective Discovery-class sample return mission which sent a lightweight 300 kg vehicle to collect samples from the coma of a comet, OSIRIS-REx is an asteroid sample return mission scheduled for launch in 2016 with a spacecraft launch mass near 2000 kg [73][74]. The Dawn mission involved sending a robotic probe using ion electric propulsion to Ceres and Vesta in the asteroid belt and at launch the spacecraft massed 1217 kg [75]. Of notable relevance, the proposed MSRS will use the same NSTAR thrusters from Dawn, a similar bus configuration, a similar quantity of xenon, and a xenon tank design derived from Dawn. Lastly, the Mars Pathfinder (274 kg launch mass), Mars Reconnaissance Orbiter (MRO)(2180 kg launch mass), and Mars Science Laboratory (MSL)(3893 kg launch mass) missions were included to ensure that costs associated with the additional burden of design, travel, and operations at Mars were considered in developing the MSRS cost model [76][77][78]. The selected missions trend nearly linearly in operations rates versus development rates.

Considering design complexity, a projected launch mass of approximately 3200 kg, and the four year timeframe available for MSRS DT&E, the MSRS is bracketed by OSIRIS-REx on the lower end and MSL on the higher end. The Stardust, Dawn and Pathfinder missions involved smaller spacecraft which and did not require significant vehicle configuration changes throughout the span of their respective missions so the lower region of the curve in Figure 8.3 was deemed unattainable for the proposed MSRS. The MRO mission had substantial heritage supporting it in the form of the Mars Odyssey and Global Surveyor orbiters thus the added cost associated with designing significantly novel systems was not present. The OSIRIS-REx mission has a similar 46 month DT&E timeframe and has a significantly novel system development in the instruments, capture mechanism and dynamics required to collect a sample from its target asteroid. However, the much lower launch mass suggests the MSR mission will not be lower cost than OSIRIS-REx. The proposed MSRS is very similar to MSL in that the design requires two major vehicle configurations and the need to land on Mars. However, the cost of the MSRS will be greatly reduced relative to MSL due to lower launch mass and, with the exception of the MAV and lander, adoption of many TRL 6-9 systems including using an augmented version of MSL's EDL system. Thus, operations costs were estimated at about $35 million per year and development costs were estimated at about $220 million per year. Note that extending these rates to the projected mission schedule resulted in the $920 million DT&E phase cost and $183 million operations phase cost.

To accommodate anticipated challenges with MAV motor and guidance and lander BPP technology development reserves were added to these cost estimates. Per recommendations in NASA's Decadal Survey, a 50 percent reserve for DT&E and a 25 percent reserve for operations were included bringing total project cost to $1.61 billion [81]. Notably, this is near the approximately $1.3 billion MSR project cost quoted by the JPL proposal discussed in Section 3. However, the JPL MSR proposal only includes funds for the ITV portion of the proposed MSRS but not the lander or MAV [10].

Figure 8.4 models how these costs will be distributed over time using an empirical fit derived from a number of other spacecraft missions as a base, but adjusted for the peculiarities of the proposed MSRS timeline [80]. Rate of DT&E spending is expected to increase rapidly following the beginning of the DT&E phase and approaching the required Earth launch date. Operations spending is expected to increase as more man hours are needed during the complex sequences required for Mars capture, MAV launch, and OS intercept before tapering off as the ITV returns to Earth.

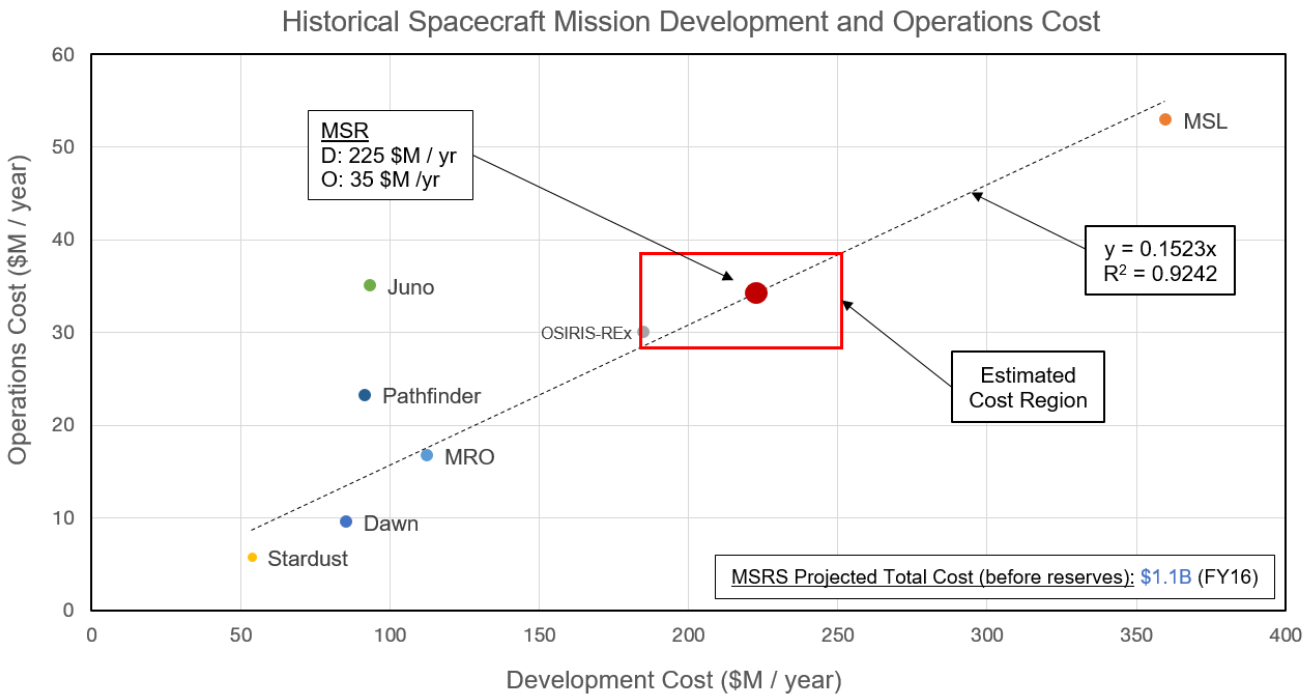


**Figure 8.3:** A cost estimating relationship built by surveying relevant spacecraft missions and estimating the relative complexity of the proposed MSRS [73][74][75][76][77][78][79].

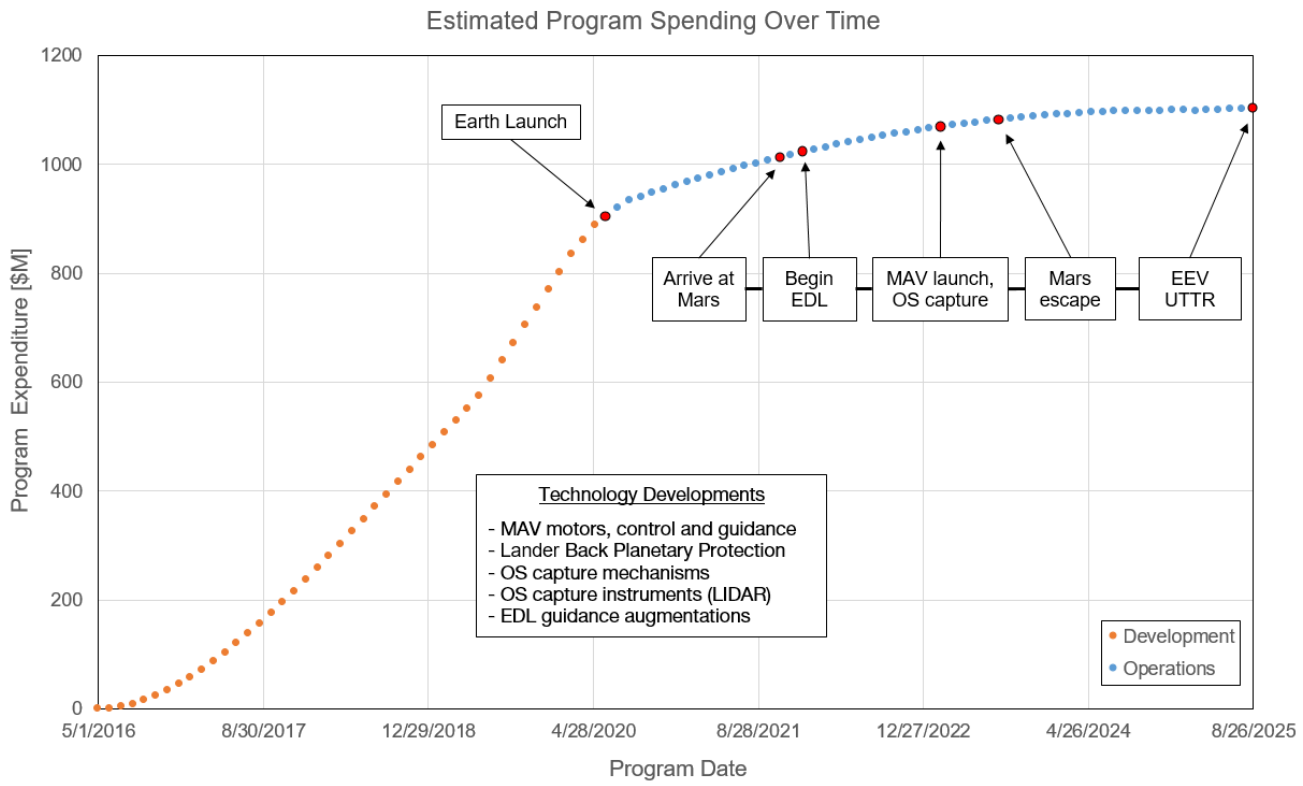


**Figure 8.4:** Anticipated project cumulative spending based on empirical fits to typical spacecraft mission spending curves.

# 9 Design Summary and Conclusions

A mission architecture has been defined in line with the strategy defined in the value system design. This architecture proves that a solution exists that can be further optimized and has a moderate fidelity for a Mars Sample Return mission. There were several key decisions that affected the choice of the architecture. These key decisions that affect the architectural level design include the number of Earth launches, the decision to perform an ITV-OS rendezvous in low Mars orbit, how the sample was to be retrieved at Earth, the fuel to be used by the MAV, and the propulsion system to be used by the ITV. Upon further analysis it was shown that the chosen architecture has reduced cost, mass, and risk in all of these key decisions. It is especially important to note how competitive the proposed MSRS is relative to an existing MSR concepts which utilize chemical propulsion. The JPL MSR concept discussed in the key trade section has an estimated cost around $1.3 billion and those costs only include a mission to send an orbiter to collect the sample in Mars orbit and return it to Earth [10]. By comparison, though marginally more expensive, the proposed MSRS includes capabilities to perform the entire MSR mission.

For the chosen architecture, some of the technology chosen will mostly consist of legacy systems such as the NSTAR thrusters, the EEV, the skycrane, a disc-gap band parachute, and the Ultraflex solar arrays. While other technology will be more innovative such as the contamination procedures used on the Martian surface, the Orbiting Sample, the MAV, and the sample capture device used in the Mars orbit rendezvous.

A significant aspect of the mission design involves the trajectories taken to get to Mars and back. The entire payload is launched from Earth on June 14, 2020 by an Atlas V 541 rocket. The final trajectory design from Earth to Mars consists of four main burn segments: boost, phase, circularize, and capture. Once the ITV has been captured at Mars, the EDL payload will detach and enter the Martian atmosphere. The ITV will then be kept in a station keeping orbit until the MAV has launched. Once the MAV has launched and has ejected the Orbiting Sample, the ITV will then execute a rendezvous maneuver to capture the orbiting sample. The ITV will then spiral out of the Mars sphere of influence and begin its next phase of the Mars to Earth trajectory. The ITV will perform an orbit about the Sun in order for Earth to properly phase and allow the ITV to perform a direct descent entry within the constraints of the EEV system.

The primary risk in the presented architecture is a development schedule overrun which would result in mission failure due to the missed June, 2020 launch window. To mitigate this risk, the proposed MSRS uses COTS hardware, heritage systems and components of at least moderate TRL for all possible systems such that systems that must be very novel, the MAV and BPP systems aboard the lander, will have access to as much time, funding, and personnel for their respective technology developments. Furthermore, budget reserves suggested by NASA's Planetary Science Decadal Survey are implemented to account for development and operations cost overruns and assist with meeting the prescribed mission timeline. For the entire mission design, it is estimated the project will cost, with reserves, approximately $1.61 billion USD of which $1.38 billion will come from four years of a Development, Test and Evaluation phase and the remaining $229 million will come from five years of an Operations phase.

One key area of advancement that this mission architecture and analysis has provided is the validation of the feasibility of a MSRS centered about a low-thrust solar electric propulsion system. There was significant effort put into understanding the limiting cases and changes in efficiency associated with an electric MSRS architecture that are very different than the challenges associated with a conventional chemical MSRS architecture. A single point trajectory solution was found for each mission segment using low thrust that can each be further optimized for an even greater mass reduction given additional time and manpower resources. The mass savings gained from an electric MSRS architecture come with little additional risk added due to the use of space-flight proven NSTAR thrusters and enable a very competitive MSRS in comparison to existing MSRS concepts heavily reliant on chemical propulsion.

THIS PAGE INTENTIONALLY LEFT BLANK

# References


[1] "NASA Announces Mars 2020 Rover Payload to Explore the Red Planet as Never Before", *NASA* [online], 31 July 2014, http://www.nasa.gov/press/2014/july/nasa-announces-mars-2020-rover-payload-to-explore-the-red-planet-as-never-before.

[2] "NASA's Management of the Mars Laboratory Project", *NASA Office of the Inspector General* [online], 8 June 2011, https://oig.nasa.gov/audits/reports/FY11/IG-11-019.pdf, [retrieved 2 October 2015].

[3] "NPD 8020.12D: Planetary Protection Provisions for Robotic Extraterrestrial Missions", *NASA Procedural Requirements* [online], http://nodis3.gsfc.nasa.gov/npg_img/N_PR_8020_012D_/N_PR_8020_012D_.pdf, [retrieved 10 October 2015].

[4] "Request For Proposal: Mars Sample Return System", *AIAA Foundation Student Design Competition 2015/2016: Undergraduate Team-Space Transportation* [online], [retrieved 4 May 2016].

[5] "Atlas V 551." *Spaceflight101* [online], 2016, http://spaceflight101.com/spacerockets/atlas-v-551/, [retrieved 23 March 2016].

[6] Camey, Mike. "Launch Vehicle Performance Website." *NASA* [online], 20 July 2015, http://elvperf.ksc.nasa.gov/Pages/Query.aspx, [retrieved 6 April 2016].

[7] Sovey, J. S., Rawlin, V. K., and Patterson, M. J.: "Ion Propulsion Development Projects in U. S.: Space Electric Rocket Test 1 to Deep Space 1." *Journal of Propulsion and Power*, Vol. 17, No. 3, pp. 517-526, May 2001.

[8] "Atlas V Launch Services User's Guide." *United Launch Alliance* [online], March 2010, http://www.ulalaunch.com/uploads/docs/AtlasVUsersGuide2010.pdf, [retrieved 24 March 2016].

[9] Sklyanskiy, E., Grover, M. R., Steltzner, A. D., Sherwood, "RED DRAGON-MSL HYBRID LANDING ARCHITECTURE FOR 2018" (PDF), February 2012, *NASA Jet Propulsion Laboratory*, [retrieved 7 Dec 2015].

[10] Christensen, P., May, L., "Planetary Science Decadal Survey Planetary Science Decadal Survey MSR Orbiter Mission MSR Orbiter Mission", March 2010, http://sites.nationalacademies.org/cs/groups/ssbsite/documents/webpage/ssb_059308.pdf, [retrieved 29 January 2016]

[11] Parker, J., “Low Thrust Orbit Propagation Software”, 2001, http://ccar.colorado.edu/asen5050/projects/projects_2001/parker/Software.html, [retrieved 3 November 2015]

[12] Foster, C., “NASA Ames Research Center Trajectory Browser”, *NASA Ames Reasearch Center*, 30 March 2016, http://trajbrowser.arc.nasa.gov/

[13] Carney, M., “Launch Vehicle Performance Website”, *NASA Launch Services Program*, 13 April 2016, http://elvperf.ksc.nasa.gov/

[14] “Launch Vehicle”, *Jet Propulsion Laboratory*, http://mars.nasa.gov/msl/mission/launchvehicle/

[15] “Trajectory Data”, *NASA JPL*, Aug 2011, https://mars.jpl.nasa.gov/images/launch_sequence_diagram-full.jpg

[16] Dahya N., and Roberts E. T., "Design and Fabrication of the Cruise Stage Spacecraft for MSL", IEEEAC paper #1168, December 2007, http://dx.doi.org/10.1109/AERO.2008.4526539

[17] "Atlas V Launch Services User's Guide", *United Launch Alliance*, March 2010, http://www.ulalaunch.com/uploads/docs/AtlasVUsersGuide2010.pdf [retrieved 15 February 2016]

[18] Lauretta D. S., "Spacecraft Structure - The Bones of OSIRIS-REx", https://dslauretta.com/2014/06/04/spacecraft-structure-the-bones-of-osiris-rex/ [retrieved 21 March 2016]

[19] UltraFlex Solar Array Systems, *Orbital ATK*, 2015, https://www.orbitalatk.com/space-systems/space-components/solar-arrays/docs/FS007_15_OA_3862 UltraFlex.pdf, [retrieved 2016]

[20] “ST8 (Space Technology 8)”, *eo Portal Directory*, https://directory.eoportal.org/web/eoportal/satellite-missions/s/st8, [retrieved 2016]

[21] “Vicor Mini Family 28 V Wide Input”, *Vicor*, 2016, February, http://www.vicorpower.com/documents/datasheets/ds_28vin-mini-family.pdf, [retrieved Spring 2016]

[22] “Vicor Maxi Family 150 V Input”, *VICOR*, September 2015, http://cdn.vicorpower.com/documents/datasheets/ds_150vin-maxi-family.pdf [retrieved March 2016]

[23] Nickel Hydrogen System Technical Data Sheet, 6 February 2003, http://www.eaglepicher.com/images/aerospace/datasheets/Batteries/PS_P_S_2.6.1.1a_battery_sar10083_pg13.pdf, [retrieved March 2016]

[24] White, S., Spence, B., Trautt, T., & Cronin, P. (n.d.). “ULTRAFLEX-175 ON SPACE TECHNOLOGY 8 (ST8) – VALIDATING THE NEXTGENERATION IN LIGHTWEIGHT” SOLAR ARRAYS, *NASA*,

https://esto.nasa.gov/conferences/nstc2007/papers/Banicevich_D1P3_NSTC-07-0048.pdf, [retrieved Spring 2016]

[25] Gilmore D., "Surface Optical Property Data," *Spacecraft Thermal Control Handbook Volume 1: Fundamental Technologies,"* The Aerospace Corporation, doi: 10.2514/4.989117

[26] "Dawn," *NASA Space Science Data Coordinated Archive*, NSSDCA/COSPAR ID: 2007-0431, http://nssdc.gsfc.nasa.gov/nmc/spacecraftDisplay.do?id=2007-043A [retrieved 3 March 2016]

[27] Wertz J. R., Larson W. J., "Spacecraft Subsystems: Thermal," *Space Mission Analysis and Design*, 3rd Ed., Microcosm Press, Torrance, CA, 1999

[28] "Ball Aerospace CT-602", *Ball Aerospace & Techonologies Corporation*, http://www.ballaerospace.com/file/media/D0540_CT-602.pdf, [retrieved Spring 2016]

[29] "CT-601 High Accuracy Star Tracker", *Ball Aerospace & Techonologies Corporation*, https://engineering.purdue.edu/~bethel/ct601.pdf, [retrieved Spring 2016]

[30] "Honeywell MIMU", *Honeywell*, September 2003, http://www51.honeywell.com/aero/common/documents/myaerospacecatalog-documents/MIMU.pdf, [retrieved Spring 2016]

[31] "RSI 45 Momentum and Reaction Wheels", *Rockwell Collins*, https://www.rockwellcollins.com/Data/Products/Space_Components/Satellite_Stabilization_Wheels/RSI_45_Momentum_and_Reaction_Wheels.aspx, [retrieved Spring 2016]

[32] Strizzi, J., Kutrieb, J., Damphousse, P., & Carrico, J., "Sun-Mars Libration Points and Mars Mission Simulations", *The Astrogator's Guild*, http://astrogatorsguild.com/wp-content/papers/0201_sun_mars_lib_pts.pdf, [retrieved Spring 2016]

[33] "Monopropellant Data Sheet", *Aerojet Rocketdyne*, 23 May 2006, https://www.rocket.com/files/aerojet/documents/Capabilities/PDFs/Monopropellant Data Sheets.pdf, [retrieved Spring 2016]

[34] "Coarse Sun Sensor", *MOOG*, 2014, http://www.moog.com/literature/Space_Defense/Spacecraft/AOCS-GNC/Coarse_Sun_Sensor.pdf, [retrieved 2016]

[35] "EPDM - Bladder Tank BT 01/0", *Airbus Defence & Space*, http://www.space-propulsion.com/brochures/propellant-tanks/58lt-n2h4-bladder-tank-bt01-0.pdf, [retrieved 2016]

[36] "ATK Part Number 80345-1", *Orbital ATK*, http://www.psi-pci.com/Data_Sheets_Library/DS345.pdf, [retrieved 2016]

[37] "Command and Data-handling Systems", *NASA*, http://mars.nasa.gov/mro/mission/spacecraft/parts/command/, [retrieved 2016]

[38] "Mission Overview", *NASA*, http://mars.nasa.gov/mro/mission/overview/, [retrieved 2016]

[39] Cady, A. "RAD750 System Flight Computer", *Caxapa*, 13 February 2002, from http://caxapa.ru/thumbs/440955/02-0576.pdf, [retrieved 2016]

[40] "Solid State Recorders for space applications", *Airbus*, 2014, http://www.space-airbusds.com/media/document/ens_5_ssr_2014_bd.pdf, [retrieved 2016]

[41] "Travelling Wave Tube Amplifiers (TWTAs) for Space Application", *Bosch*, http://www.electronicnote.com/site/PDF/TWTA Brochure.pdf, [retrieved Spring 2016]

[42] Makovsky, A., Ilott, P., & Taylor, J., "Mars Science Laboratory Mission and Spacecraft Summary", *NASA JPL*, http://descanso.jpl.nasa.gov/monograph/series13/DeepCommo_Chapter8--141029.pdf, [retrieved Spring 2016]

[43] "Small Deep-Space Transponder (SDST)", https://gdmissionsystems.com/wp-content/uploads/2015/07/SDST_-_DS5-813-12.pdf, [retrieved Spring 2016]

[44] May, L., & Christensen, P., "Planetary Science Decadal Survey MSR Orbiter Mission (Including Mars Returned Sample Handling)*", NASA JPL,* 2010

[45] Howard, R., Bryan, T., Lee, J., & Robertson, B., "*NEXT GENERATION ADVANCED VIDEO GUIDANCE SENSOR DEVELOPMENT AND TEST", NASA Marshall Space Flight Center*, http://ntrs.nasa.gov/archive/nasa/casi.ntrs.nasa.gov/20090017766.pdf, [retrieved March 2016]

[46] Gershman, B., "Sample Containment Technology for Mars Sample Return*", NASA JPL*, 25 March 2015, [retrieved February 2016]

[47] Martin, A., & Weng, H., "Numerical Investigation on Charring Ablator Geometric Effects: Study of Stardust Sample Return Capsule Heat Shield", January 2015, *University of Kentucky*, http://uknowledge.uky.edu/cgi/viewcontent.cgi?article=1024&context=me_facpub, [retrieved March 2016]

[48] "Stardust | JPL | NASA", *NASA JPL* ,26 November 2003, http://stardust.jpl.nasa.gov/mission/capsule.html, [Retrieved 6 May 2016]

[49] Arnold, J., Milos, F., Tang, C., Baker, A., Cassell, A., Scola, S., Winski, R., "An Application of the Multi-Mission Earth Entry Vehicle : Galahad – An Asteroid Sample Return Mission", *NASA,* 14 June 2010, http://solarsystem.nasa.gov/docs/po505.pdf, [retrieved March 2016]

[50] Samareh, J., Maddock, R., Winksi, R., "*An Integrated Tool for System Analysis of Sample Return Vehicles", NASA, Langley Research Center,* United States, NASA Langley Research Center, 2012

[51] Maddock, R. W., Abston, H., Samareh, J., Arnold, J., Baker, A., Sepka, S., . . . Winski, R. "Multi-Mission Earth Entry Vehicle: Design Trade Space and Concept Development Status", *NASA,*14 June 2010, https://solarsystem.nasa.gov/docs/pr407.pdf, [retrieved March 2016]

[52] Gershman, R., Adams, M., Dillman, R., Fragola, J.,"Planetary protection technology for Mars Sample Return", *IEEE*, http://ieeexplore.ieee.org/stamp/stamp.jsp?arnumber=1559390, [retrieved 03 May 2016]

[53] Braun, Robert D., and Robert M. Manning, "Mars Exploration Entry, Descent, and Landing Challenges." *Journal of Spacecraft and Rockets* 44.2 (2007): 310-23. Web.

[54] Ken Farley, Ken Williford, John Grant, Matt Golombek, and Allen Chen, "2020 Landing Site for Mars Rover Mission", *2020 Landing Site for Mars Rover Mission* [online]. NASA Jet Propulsion Laboratory, http://marsnext.jpl.nasa.gov/, [01 Dec 2015]

[55] Lemke, L. G., L. C. Huynh, and A. A Gonzales, "Mars Sample Return Using Commercial Capabilities: Propulsive Entry, Descent, and Landing of a Capsule Form Vehicle", *2014 IEEE Big Sky Aerospace Conference* [submitted for publication].

[56] Munk, M.M., Cianciolo, A.D., "Entry, Descent, and Landing for Human Mars Missions", *Global Space Exploration Conference,* 22-24 May 2012; Washington, DC; United States. NASA Langley Research Center; Hampton, VA, United States.

[57] "2015 NASA Technology Roadmaps TA 9: Entry, Descent, and Landing Systems", *NASA,* July 2015, http://www.nasa.gov/offices/oct/home/roadmaps/index.html, [retrieved 6 May 2016]

[58] Wolf, A., Tooley, J., Ploen, S., Ivanov, M., Acikmese, B., & Gromov, K. (n.d.). "Performance Trades for Mars Pinpoint Landing", *2006 IEEE Aerospace Conference,* doi:10.1109/aero.2006.1655793

[59] Justus, C.G., Braun, R.D., "Atmospheric Environments for Entry, Descent, and Landing", *5th International Planetary Probes Workshop and Short Course,* 23-29 June 2007, Bordeaux; France, NASA Marshall Space Flight Center; Huntsville, AL, United States,

[60] Golombek, M. P., A. F. C. Haldemann, N. K. Forsberg-Taylor, E. N. Dimaggio, R. D. Schroeder, B. M. Jakosky, M. T. Mellon, and J. R. Matijevic, "Rock Size-frequency Distributions on Mars and Implications for Mars Exploration Rover Landing Safety and Operations", *J.-Geophys.-Res. Journal of Geophysical Research: Planets 108.E12* [online], [retrieved 2003]

[61] "Mars Space Flight Facility - Mars Data Sets", *Java Mission-planning and Analysis for Remote Sensing (JMARS)* [online], [retrieved Spring 2016] <http://jmars.mars.asu.edu/maps/?layer=MOLA_Color>. Viking IRTm Rock Abundance

[62] Haberle, R., Gwynne, O., Atkinson, D., et al, "Atmospheric Effects on the Utility of Solar Power on Mars," *Resources of Near Earth Space*, U. Arizona Press Space Science Series, 1993, [retrieved 5 October 2015]

[63] "Viking Mission to Mars, NASA Facts", *NASA Jet Propulsion Laboratory* [online], http://www.jpl.nasa.gov/news/fact_sheets/radioisotope-power-systems.pdf, [retrieved 1 October 2015]

[64] "UltraFlex™ Solar Array Systems", *Orbital ATK* [online], 2015, https://www.orbitalatk.com/space-systems/space-components/solar-arrays/docs/FS007_15_OA_3862 UltraFlex.pdf, [retrieved 2016]

[65] "ZTJ Space Solar Cell", *SolAero Technologies* [online], 2015, http://solaerotech.com/wp-content/uploads/2015/03/ZTJ-Datasheet.pdf, [retrieved 2016]

[66] "Guidelines on Lithium-ion Battery Use in Space Applications", *NASA Glenn Research Center* [online], May 2009, http://ntrs.nasa.gov/archive/nasa/casi.ntrs.nasa.gov/20090023862.pdf, [retrieved 2016]

[67] "Mars Facts",http://nineplanets.org/mars.html, [retrieved 2016]

[68] "RAD750 System Flight Computer", *BAE Systems* [online], 13 Feb 2002, http://caxapa.ru/thumbs/440955/02-0576.pdf, [retrieved 2016]

[69] Huggett, C., "Solid Propellant Rockets", Princeton, NJ: Princeton UP, 1960, [online]

[70] Christensen, P., & May, L. "Planetary Science Decadal Survey Planetary Science Decadal Survey MSR Orbiter Mission MSR Orbiter Mission", March 2010, http://sites.nationalacademies.org/cs/groups/ssbsite/documents/webpage/ssb_059308.pdf, [retrieved Fall, 2016 ]

[71] Zubrin, R., Frankie, B., & Kito, T. (1997). "Mars In-Situ Resource Utilization Based on the Reverse Water Gas Shift: Experiments and Mission Applications", *Pioneer Astronautics*, [retrieved December 5, 2015]

[72] "Solid Rocket Thrust Vector Control", NASA SP-8114, 1974

[73] "NASA Assessments of Selected Large-Scale Projects," United States Government Accountability Office, GAO-15-320SP, 26 March 2015, http://www.gao.gov/assets/670/669205.pdf [retrieved 8 January 2016]

[74] "Stardust/NExT," NASA Space Science Data Coordinated Archive, NSSDCA/COSPAR ID: 1999-003A, http://nssdc.gsfc.nasa.gov/nmc/spacecraftDisplay.do?id=1999-003A [retrieved 8 January 2016]

[75] "Dawn Launch, Mission to Vesta and Ceres," NASA Press Kit, September 2007, https://www.nasa.gov/pdf/189670main_dawn-launch.pdf [retrieved 8 January 2016]

[76] "Mars Exploration," NASA Mars Exploration Program, https://www.nasa.gov/pdf/55390main_07%20MEP.pdf [retrieved 8 January 2016]

[77] "NASA's Management of the Mars Science Laboratory Project," NASA Office of Inspector General, Report No. IG-11-019, https://oig.nasa.gov/audits/reports/FY11/IG-11-019.pdf [retrieved 4 January 2016]

[78] Spear A. J., "Low Cost Approach to Mars Pathfinder and Small Landers," IAA-L-0505, NASA Jet Propulsion Laboratory, Pasadena, CA, 14 April 1994, http://trs-new.jpl.nasa.gov/dspace/bitstream/2014/33871/1/94-0603.pdf [retrieved 8 January 2016]

[79] "Mars Exploration Rover Launches," NASA Press Kit, June 2003, http://mars.nasa.gov/mer/newsroom/merlaunch.pdf [retrieved 8 January 2016]

[80] Wertz J. R., Larson W. J., "Cost Modeling," *Space Mission Analysis and Design*, 3rd Ed., Microcosm Press, Torrance, CA, 1999

[81] "Vision and Voyages for Planetary Science in the Decade 2013-2022," National Research Council Committee on the Planetary Science Decadal Survey, The National Academies Press, Washington, D.C., https://solarsystem.nasa.gov/docs/131171.pdf [retrieved March 20 2016]

[82] McBride, B., Sanford G., *CEA*, Glenn Research Center: NASA, 1971

[83] Zandbergen B.T.C., "Chemical system dry mass estimation", Faculty of Aerospace Engineering, TU-Delft, 2005, http://www.lr.tudelft.nl/en/organisation/departments/space-engineering/space-systems-engineering/expertise-areas/space-propulsion/system-design/analyze-candidates/dry-mass-estimation/chemical-systems/, [retrieved on 15 March 2016]